DECIPHERING SEX-SPECIFIC PATHOLOGIES IN CAVD THROUGH DISEASE-INSPIRED ENGINEERED VALVE MODELS

By

Lysmarie Figueroa Rios

A dissertation submitted in partial fulfillment of

the requirements for the degree of

Doctor of Philosophy

(Biomedical Engineering)

at the

UNIVERSITY OF WISCONSIN-MADISON

2024

Date of final oral examination: 08/01/2024

The dissertation is approved by the following members of the Final Oral Committee:
Kristyn Masters, Professor, Biomedical Engineering
William Murphy, Professor, Biomedical Engineering
Sean Palecek, Professor, Chemical and Biological Engineering
Wendy Crone, Professor, Engineering Physics
Wan-Ju Li, Associate Professor, Biomedical Engineering

Dedicated to the women who crafted my path and are no longer here;
Maria (Mery) M. Irizarry
Heroilda (Lolin) Irizarry
Ivonne de Lourdes Figueroa-Rodriguez

&

To my parents, Maria E. Rios and Hector S. Figueroa

Acknowledgements

I always knew I wanted to become a scientist. I draw inspiration from my mom who as a Science teacher always came home with demos and experiments that explained simple but fundamental concepts. Throughout my childhood both my mom and my dad encouraged me to participate in any activity that was of my interest; Girl Scouts, Tae Kwon Do, Choir, Guitar, Swimming and of course Science. Growing up I had great science role models, my biology, chemistry and math middle and high school teachers kept igniting this light in me, through their encouragement I participated in what felt like a million science fairs, right there and then I solidify my conviction to purse science as my career. When I joined college, I encountered people passionate about science that welcomed me in their world. Dr. Edu Suarez, Dr. Wilfredo Ayala, Lenin Godoy, Nelly Arroyo & Dr. Carmen M. Ortiz. All these individuals played a pivotal role in my academic formation and for that, I am forever grateful.

With their blessing I embarked my journey to Grad School. I came to Wisconsin, Madison for my third internship and immediately knew this is where I wanted to pursue my graduate education. I had incredible experiences as an intern in Dr. Ray Vandeby's Lab which give me a place in his lab even though I had no prior biomedical engineering experience and who even after my acceptance at UW Madison as a BME student continued to support me. Being part of this experience

was not possible without the unconditional support from GERS director, Kelly Burton. Kelly was truly remarkable and helped me navigate my graduate school journey through the years; from finding a lab, to checking with each of us on a personal level. Although I was far from home, I felt like she cared for each of the GERS members as our families would.

Thanks to her, I met my advisor Dr. Kristyn Masters. I still remember the first interview I had with her and the moment I received her email asking if I would like to join her lab. I was over the moon that day! I was finally able to work on something that I really, really liked and that never in a million years thought I'd had the opportunity to do. I want to express my gratitude for encouraging me to keep going even in the toughest times of this Ph.D. You gave me a space to reflect and grow, both personally and professionally. Coming from a biology background I was unsure about how I would fit in with the rest of the lab, but I quickly felt the support from the lab members present during that time and the ones that came after.

I am deeply thankful to all the Masters Lab, LaTonya Simon who was the most amazing peer mentor, to my lab friends Vaidehi Patil and Ashley Scott-Patterson with whom I shared struggles and joy and overall unconditional support, to my undergraduate students, specifically to Noah Pollard for always being there willing to take charge and assist in this very difficult project and the rest of our peer students and staff, specially Ali Absbapour for making our days lighter with jokes,

Ning Yang for her incredible scientific resourcefulness as well as her advice. I also want to thank my committee for all the feedback I gained through these years in our committee meetings and for your disposition.

However, life goes beyond our career goals and dreams. In my personal life I have really wonderful people that showed me support in a million different ways. I want to thank you all for being so understanding and supportive during this journey. First, I want to express thanks to my parents who were always supporting and encouraging me from the distance and for letting me know every day how much they love me; to my brother and my sister-in-law who were always there to listen to my frustrations and joys, to my partner and my step kids for giving me their unconditional love and support, and to all my friends kept in contact through the years, and kept supporting to achieve my dreams. And last, but not least I want to thank myself for not giving up, for being resilient, for allowing myself to find help when needed and continue going until I achieving my young self's dream.

Abstract

Calcific Aortic Valve Disease (CAVD) is one of the most common valvular ailments, affecting over 10 million Americans each year over the age of 65. Despite its similarities with atherosclerosis, no treatments have been successfully developed to stop or halt disease progression, making total valve replacement the only course of treatment. Risk factors for CAVD include age, biological sex, hyperlipidemia, diabetes mellitus, and smoking, with males being twice as likely to suffer from the disease. Although hallmarks of CAVD such as valve sclerosis (valve thickening) and stenosis (valve stiffening) are present in all diseased valves, males and females exhibit different clinical outcomes. For the same severity of aortic stenosis, males have highly calcified valves, while females have more fibrotic valves. The mechanisms underlying these divergent clinical outcomes are not yet fully understood.

There is very limited literature considering sex as a biological variable in CAVD research, as most past studies have used mixed cell cultures, often resulting in conflicting results. Only in recent years have cellular-scale sex differences been considered. To understand why females and males present different clinical outcomes, we need to study the etiology of CAVD in both sexes. However, this has been challenging since most human valve specimens used in studies come from cadaveric sources or patients undergoing transcatheter aortic valve replacement (TAVR).

CAVD hallmarks are characterized by valve leaflet thickening and stiffening as a consequence of extracellular matrix (ECM) remodeling mechanisms. Because of the role

of the ECM in contributing to disease progression, it is necessary to consider cell-ECM interactions in CAVD studies. Three-dimensional (3D) culture platforms provide a valuable tool to combine these aspects. Many researchers have implemented the use of 3D scaffolds that mimic characteristics cells experience in vivo.

In this thesis, we focus on creating disease-inspired tissue-engineered models that mimic changes in the ECM present during CAVD progression to understand the differential fibrotic expression in females and males. Chapter 4 describes the creation of disease-inspired hydrogel models that mimic the transition of collagen enrichment as observed during disease progression. Motivated by the results in Chapter 4, Chapter 5 focuses on understanding how the biological and architectural properties of collagen affect the fibrotic behavior of females and males VICs. VICs cultured in these disease-inspired scaffolds were then exposed to TGF-β1 to elucidate the combinatorial effects of ECM changes and exposure to pathological stimuli on VICs' fibrotic responses. Chapter 6 discusses the observed results, study limitations, and future considerations.

Table of Contents

Chapter 1: Introduction

1.1 CAVD Progression

Calcific aortic valve disease (CAVD) is one the most common valve ailments in the US affecting the aging population. Despite sharing similarities to atherosclerosis, the development of effective treatments to halt or eradicate disease progression has not been successful. Unfortunately to this date, total valve replacement remains the only therapeutic alternative. Our inability to develop effective therapeutic options is in part due to our incomplete understanding of the events that occur during disease progression. Current theories on disease development propose that CAVD is initiated by the infiltration of lipids through the disrupted endothelial layer of the valve leaflets[1,2]. The integrity of the valve endothelial layer can be compromised by improper blood flow causing oscillatory shear stress of the aortic valve leaflet causing lipid infiltration and triggering an inflammatory response[3,4]. Biochemical cues from this inflammatory response such as the release of cytokines, chemokines, and growth factors then activate fibrotic and calcific processes within the aortic valve. This affects the tissue homeostasis and its ability to properly regulate the ECM remodeling and the native tissue's cell behaviors. Ultimately, this results in heavily fibrotic/calcified valves with impaired valve mechanics which could result in death if not timely intervened.

Limitations in how CAVD has been studied over the years have hindered our capacity to understand how these events develop. Understanding disease etiology has been hampered due to our inability to access specimens at diverse stages of disease

progression. Most tissue specimens are sourced from cadavers or individuals undergoing valve replacement which only provide snapshots of the late stages of disease. Information

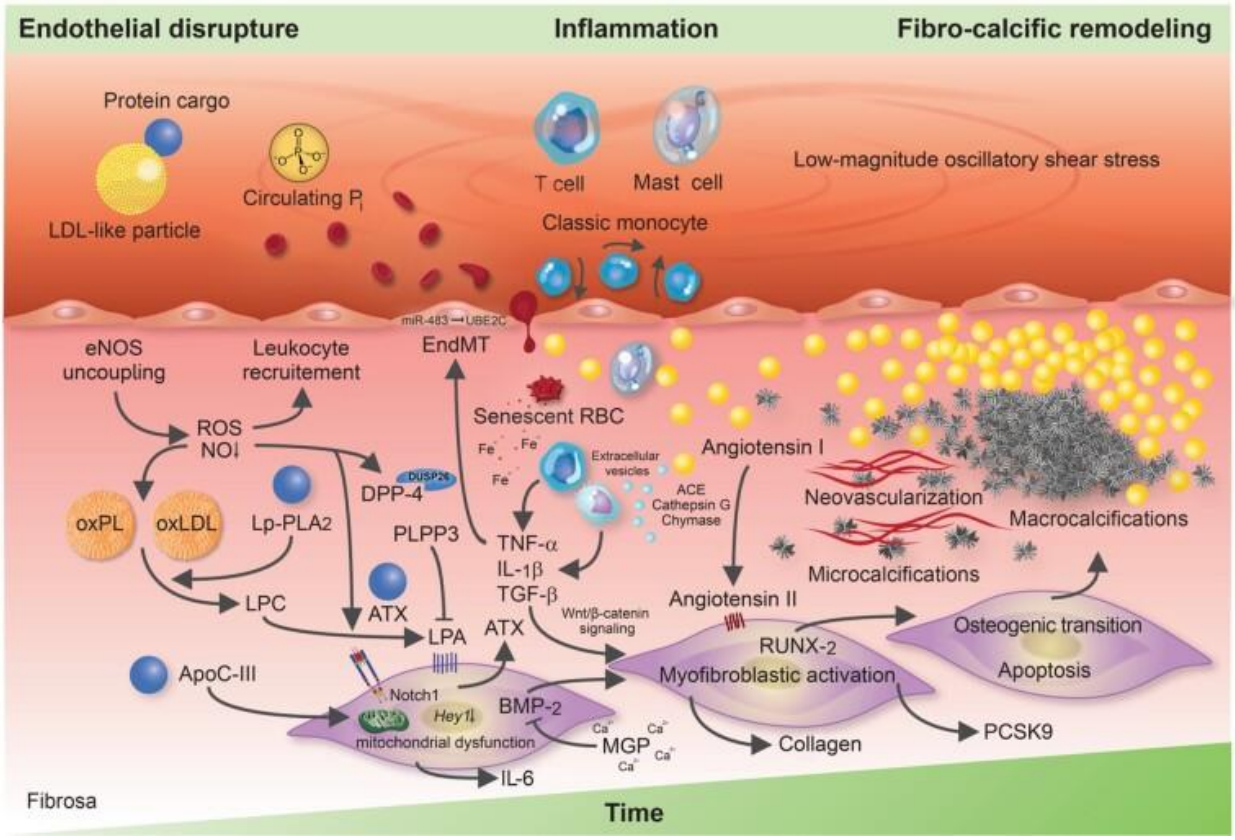

Figure 1.1 Molecular and cellular mechanisms that occur during CAVD progression.[2]

obtained from these specimens also vary depending on the individuals' biological sex as females reach the late stages of valve stenosis with highly fibrotic valves while males exhibit highly calcific valves. Thus, consideration of sex as a biological variable is necessary to understand why females and males present with different clinical outcomes. We could achieve this by particularly by looking at how diverse events of disease progression affect females and males differently to better understand disease progression

and hence develop better therapeutic approached to stop or halt onset of CAVD progression.

Additionally, due to the complex interactions that occur within the valve leaflet structure, the development of culture systems that mimic the changes that occur at different stages of disease is needed. 3D culture platforms provide us with a great tool to tackle these constraints as they offer great tunability to adjust for the mechanical, biological, and biochemical cues that are known to contribute to cellular-scale sex dependent behavior and maintenance of tissue homeostasis in CAVD.

This thesis is aimed developing and implementing the use of 3D models as a tool to better understanding sex-dependent fibrotic responses of VICs in CAVD. In the following sections, we will discuss in more detail elements of the valve architecture and composition, the diverse culture platforms currently used in CAVD research, and the pathobiology of CAVD focusing primarily on valve fibrosis. In addition, we will highlight the importance of the consideration of biomaterials to study the hallmarks of CAVD through the lenses of recent research findings in CAVD using biomaterials.

1.2 The native aortic valve: A look into the native tissues' structure and composition

The aortic valve (AV) is composed of three semilunar leaflets that allow unidirectional blood flow from the left side of our hearts into the aorta. Despite how thin the aortic valve leaflets are, they are a fascinating, complex, and sophisticated tissue. The AV leaflets are lined on both sides by a monolayer of valvular endothelial cells (VECs). VECs help

regulate the valve's mechanical integrity properly for a tissue under constant hemodynamic forces, aid in the modulation of the tissue's mechanical properties, and regulation of the ECM[5–7]. Within the leaflets, we can find another cell population known as valvular interstitial cells (VICs) whose main role is to maintain tissue homeostasis by regulating their extracellular environment.

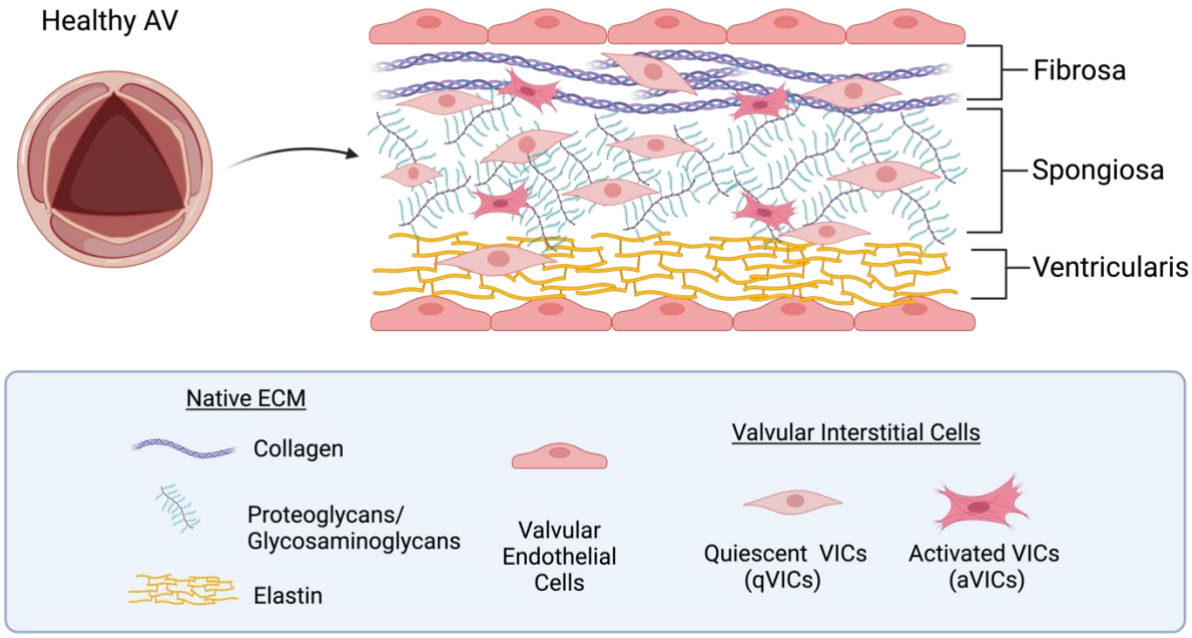

Figure 1.2 Schematic representation of the aortic valve architecture and composition in its native state.

VICs come in various subtypes. Quiescent valvular interstitial cells (qVICs) are the main cell population in the healthy valve[8]. However, when exposed to pathological factors, whether mechanical or biological, they could differentiate into activated valvular interstitial cells (aVICs). aVICs adopt a myofibroblast phenotype in an attempt to maintain ECM homeostasis. During disease, they can subsequently differentiate into osteoblastic valvular interstitial cells (obVICs) which contribute to aortic valve calcification[7,9,10].

The ECM of the AV is comprised of a distinct trilaminar structure with unique biological and mechanical features. On the aortic side lies the fibrosa layer. The fibrosa is mainly composed of circumferentially oriented Collagen I and III conferring the leaflet great mechanical support and tensile strength to support the extreme hemodynamic forces[11]. Between the fibrosa and ventricularis lies the spongiosa whose main components are proteoglycans and glycosaminoglycans which provide great lubricity and mechanical cushion to the leaflet. On the ventricular side lies the ventricularis which main component is elastin providing the valve with mechanical elasticity during the valve opening and closing[11,12]. This tri-laminar architecture and the distribution of the ECM components and cells within the valve leaflet are necessary to maintain proper valve function.

1.3 CAVD Fibrosis Explored through Biomaterials

The development of fibrosis within the aortic valve leaflet happens as a product of diverse interactions within the populating cells and between the cells and their environment. Due to the many contributors of fibrosis in CAVD a clear mechanism of how it starts within the AV leaflet is not well understood. In addition, CAVD outcomes present differently in females versus male individuals with females having more fibrotic valves and males having more calcific valves for the same degree of stenosis making it more challenging to decipher the underpinnings of fibrosis etiology. During the early stages of the disease, increased production of proteoglycans (PGs) and glycosaminoglycans (GAGs) is observed, a known early hallmark of CAVD[13]. During the late stages, GAGs can be found concentrated around the calcific lesions in the fibrosa layer[14] and spread across the valve. Collagen production also increases but Collagen fiber deposition is disorganized within

the leaflet[15]. This ECM remodeling process during disease results in the loss of the trilaminar structure hence affecting the tissue homeostasis.

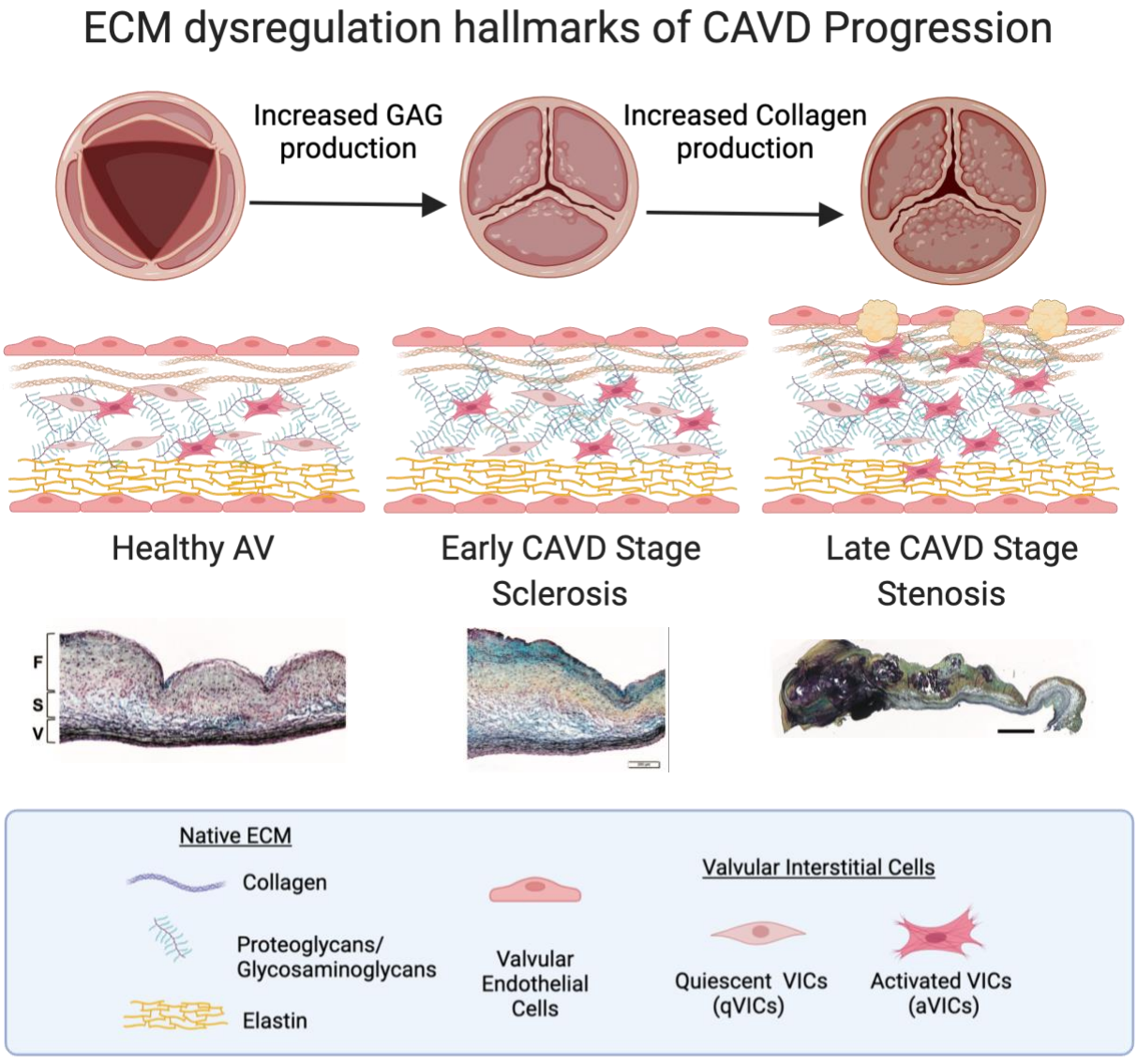

Figure 1.3 Schematic representation of hallmarks of ECM dysregulation in CAVD *Adapted from*[11]

In this section we will discuss how ECM mechanics and biological cues work to drive fibrosis in the valve. In the last decade, more attention has been directed towards

understanding how ECM composition and alterations influence cell behavior in the context of CAVD. A study by Mahler et al.[14] showed that VECs seeded in a 3D GAG-Collagen (CS-Coll, HA-Coll, Dermatan Sulfate (DS)-Coll) scaffold underwent endothelial to mesenchymal transformation (EndMT) noted by the expression of ACTA2 gene and a-SMA protein expression. However, VECs particularly seeded in CS-Collagen 3D hydrogels showed increased expression in Collagen and GAG production. In addition to alterations to the ECM, VECs can undergo EndMT through exposure to paracrine signaling of molecules such as TGFB-1, TNF-a, and IL6[16,17].

Mechanical cues such as shear stress also play a role in VEC EndMT. A study by Zaffran et al.[18] demonstrated how VEC EndMT is dependent on the source of origin VECs (aortic vs ventricular side). VECs obtained from the aortic side showed upregulation of pro EndMT markers such as ACTA2, Snail and TGFB-1 and down regulation PECAM-1, an endothelial marker. Conversely, VECs obtained from the ventricular side showed no activation of pro EndMT markers however, PECAM-1 expression was highly upregulated. Another study by Lacerda et al.[19] showed VECs under prolonged pulsatile shear exposure underwent EndMT demonstrated by upregulation of aSMA and TGFB-1 compared to VECs exposed to laminar flow. In essence, VECs significant contribution to fibrosis lies in its ability to adopt a fibroblast-like phenotype and behavior.

During disease, ECM remodeling results in the loss of the trilaminar structure affecting the valve homeostasis. VICs in the leaflet, can perceive the mechanical or biological changes that occur in the ECM and in turn adopt a myofibroblastic phenotype. AVICs are

characterized for their main role in ECM repair during disease. When VIC activation is prolonged, their repair abilities adversely affect the leaflet homeostasis by inducing an imbalance between matrix repair and matrix dysfunction. VIC activation can occur as a result of mechanical cues such as substrate stiffness, scaffold mechanics, and/or composition. Recent data showed that adult human and porcine VICs cultures in 3D poly(lactic-co-glycolic) acid (PLGA) and poly(aspartic acid) (PASP) hydrogels exhibiting anisotropic features similar to those found in the native heart valve had increased production of Collagen and GAGs compared to PLGA hydrogels alone[20]. Substrate stiffness has been widely investigated and corroborated to be one of the drivers of VIC differentiation. A study by Anseth et al. used a photodegradable hydrogel to tune topographical stiffness and look at the effects stiffness has on VICs myofibroblastic differentiation. The data showed that VICs on higher modulus substrates (15 Kpa) had a 70% of myofibroblastic activation compared to VICs on a soft modulus substrate (3 Kpa) which had about 20% myofibroblastic activation. The data also showed that activation could be reversed by decreasing the topographic stiffness[21]. Other studies show that in vitro VIC differentiation (and reversal) via substrate stiffness modulation is correlated to VIC morphology[22].

Scaffold composition mimicking the native or disease AV provides us with the tools to study how particular ECM-Cell interactions occur in the native and disease valves. A study by our lab[13], highlighted the importance of isolating the roles of ECM molecules such as HA and CS in disease progression. In this study, quiescent VICs (qVICs) were cultured on gelatin methacrylate (GelMa) + hyaluronic acid (HA) or GelMa + chondroitin

sulfate (CS) substrate mimicking native and pathological enrichment of GAGs (1X GAGs vs 4X GAGs respectively). Results showed that GAG enrichment did not promote the production of inflammatory or VIC activation markers which have a subsequent role in initiating tissue fibrosis through the recruitment of immune cells within the leaflet and production of pro-fibrotic markets through VIC activation. However, the presence of pathological amounts of CS in these hydrogel substrates proves to be essential in retaining and regulating the availability of oxidized low-density lipoprotein (oxLDL), a molecule important in the initiation of inflammation and fibrosis, to VICs. VICs exposed to oxLDL in the pathological GelMA - 4X CS model had increased levels of inflammatory cytokines, myofibroblastic markers and GAG production, hence promoting disease progression through a positive feedback loop. These results coincide with a study by Khademhosseini et al.[23], in which culture of VICs in a 3D GelMA-HA scaffold did promote VICa myofibroblastic differentiation, but when treated with a profibrotic TGFB-1-1 VIC myofibroblastic differentiation was induced. This is particularly important since the type of ECM alteration can affect VICs types in very distinct manners. Additionally, 2D and 3D cultures may elicit completely different responses in cultured VICs. Grande-Allen[24], used 3D heterogenous multi-laminar tissue construct to evaluate VIC pathogenicity in a matrix-dependent manner. Tissue constructs were designed to have varying ratios of Collagen to hyaluran while maintaining similar mechanics. This allowed the cells to have a localized matrix signal similar to what is seen in the native valve. VICs in construct with increased Collagen layers exhibited a more pathological phenotype validated by aSMA and RUNX2 expression. Conversely, VICs seeded in constructs with increased hyaluran content had lower aSMA and RUNX2. VICs in increased hyaluran constructs showed higher cell

viability compared to VICs seeded in constructs with higher Collagen content[24]. CAVD fibrosis does not stem from a single mechanism but rather a compilation of different processes that intertwined, drive disease progression. In this section, we discussed examples of how fibrosis may be presented in CAVD through cell-to-cell signaling, and cell-ECM interactions whether these are from a biological or mechanical perspective.

1.4 Culture platforms used in CAVD research

A recent review by Cai et al.[25] highlights the traditional and more novel models used to study CAVD. The more traditional models include diet-induced animal models, genetically modified animal models, and 2D culture models, among others. On the more novel spectrum, we have 3D models which include ex-vivo cultures, and 3D scaffold/hydrogels systems. No model is completely perfect. Models such as diet-induced, and genetically modified animals give us the opportunity to study molecular mechanisms, particularly in inflammation, lipid deposition and macrophage infiltration, fibrosis, and calcification all of which occur at diverse stages of CAVD, and which are important for identifying potential therapeutical targets. Mouse and rabbit models are often used due to their relatively low cost and easy maintenance; however, these have limited physiological similarity to the human heart. Pigs, on the other hand, provide us with a more anatomically and physiologically relevant model but their maintenance is costly. Most CAVD research has been done in traditional 2D culture methods where cells (VICs or VECs) are produced from a stem cell line or isolated from an animal or human source and cultured with different pathological stimuli to understand cell responses to disease factors. This approach is widely characterized and relatively involves low cost and maintenance.

Despite being the standard for decades and decades of research, 2D cultures do not entirely replicate the native cells' behaviors that occur within the tissue. This is in part due to the lack of a 3D structure where cells can interact with their extracellular environment and receive biological and mechanical cues from the molecules that surround them. 3D cultures provide an opportunity to bypass some of these constraints. There are two main types of 3D cultures: synthetic and biobased. Synthetic 3D cultures can be used when low reactivity to the environment is essential to isolate variables within the culture. Biobased 3D cultures are used when it is essential to provide cells with cues that they find *in vivo*, hence the use of materials naturally found within the tissue such as ECM molecules (Collagen, FN, GAGs, etc). Although, biomaterials can be used as 2D coatings to study cells-ECM interactions from a topographical perspective, meaning the cells' ability to identify the molecules in their culture substrate and evaluate how the interaction with these triggers the cellular signaling process, using biomaterials in a 3D construct can be exploited to understand how particularly VECs and VICs interact with various pathological features that in a more relevant fashion. For example, 3D cultures can be used to mimic diverse stages of disease. As previously mentioned, our lab and other groups have attempted to build scaffold constructs that mimic the ECM distribution during the early and late stages of CAVD or the ECM composition during these stages. This provides a particularly valuable resource since 2D cultures only allow us to partially understand their responses to pathological signals but not environmental signals that occur during disease. On the other hand, humans' samples only provide us with a snapshot of the end stages of the disease making it challenging to understand what events occur during the early stages of CAVD as most of the diagnoses occur when

intervention is needed. Hence, the need to develop better systems that allow us to study the development of CAVD at different stages of disease while providing cells a more relevant environment for different study applications such as studying the effects of altered ECM molecules from a composition, architecture and mechanical perspectives, cells behavior in response to pathological factors in 3D and open avenues to identify potential therapies. In the next section, we will focus on current research involving the use of biomaterials to study CAVD in the context of inflammation, fibrosis, and calcification.

1.5 Utilization of biomaterials culture platforms to understand the hallmarks of CAVD

The use of biomaterials to study disease progression provides new venues of exploration that cannot be achieved with traditional culture methods. In recent years, biomaterials to study CAVD etiology have been implemented, particularly to study in more detail how cell-ECM and cell-cell interactions contribute to disease progression in the context of AV inflammation, fibrosis, and calcification. Despite the gaps in our understanding of how these hallmarks present in CAVD, we could agree that these processes overlap at different stages of disease. Isolating one specific event would be nearly impossible, but we could puzzle how each of these events comes into play by how they all work in concert. Lipoprotein (a) (LP(a)) has been recognized as a potential driver of inflammation and calcification in CAVD[26,27]. Recent data by Aikawa et al., showed increased calcification of extracellular vehicles (EVs) in acellular 3D Collagen hydrogels treated with EVs collected from conditioned media of VICs exposed to Lp(a). This data suggests that calcification of

the valve ECM by EVs could be mediated through inflammatory mechanisms[28]. In addition to VICs exposure to Lp(a), exposure of VICs to inflammatory cytokines from infiltrating macrophages was suspected to have a role in VICs ability to further CAVD development. Anseth et al., studied specifically how secreted factors from M1 macrophages affected the behavior of VICs cultured in 2D PEG hydrogels and supplemented with M1s conditioned media. Their data showed that tumor necrosis factor-alpha (TNF-α) and interleukin 1 beta (IL-1β) induced derived from M1 macrophages conditioned media had an anti-fibrotic effect noted by down-regulation of (αSMA) expression, reduced stress fiber formation and an increase in cell proliferation. Conversely, it was also found that interleukin 6 (IL6) served as a pro-osteogenic driver noted by the upregulation of RUNX2 and osteopontin. Their results suggest a potential mechanism mediated by these secretory factors to aid VIC transition from a fibrotic to a calcific phenotype[29].

Tintut et al.[30] explored the role of TNF-a, an inflammatory cytokine, in ECM remodeling by VICs cultured in a 3D free-floating and compliant Collagen hydrogel model. TNF-a was found to increase the expression of fibrotic markers of CAVD such as aSMA, Collagen, and fibronectin. In addition, TNF-a promoted hydrogel retraction and stiffening. The formation of calcific nodules within these VIC-laden hydrogels was also observed. Using NF-κB inhibitors blocked TNF-a induced hydrogel retraction. When combined with the inhibition of C-Jun N-terminal kinase, stiffness was also blocked suggesting that the observed TNF-a effects result from stimulation of the cytoskeletal machinery dependent on F-actin assembly and disassembly and actin-myosin interaction.

3D Collagen hydrogels are widely used to study CAVD progression. Combinations of these versatile hydrogel models open avenues to isolate the effects of secretory molecules as previously discussed, as well as the effects of ECM in driving CAVD pathogenesis. A study by Richards et al, highlights the importance of creating 3D models that present with different events as they occur during CAVD progression. Richards found that VICs cultured in 3D Collagen hydrogels containing hydroxy apatite adopted myofibroblastic and osteoblastic behaviors[31]. Dahal et al.[32],cultured VICs in Collagen hydrogels containing CS, HS or Dermatan Sulfate (DS). VICs seeded in the Coll-CS hydrogels exhibited increased myofibroblastic and osteoblastic expression in addition to increased Collagen 1 production and nodule formation. Schroeder et al.[33], created a 3D PEG-Collagen system that allowed for accelerated calcification of VICs when exposed to calcifying media. Traditional calcification studies take longer periods of culture. Schroeders system reduced culture time by 14%-50% providing quicker tools to understand how calcification develops in CAVD as well as providing a system to identify potential therapeutic targets.

The use of biomaterials in research allows us to replicate diverse aspects of tissues that other traditional culture methods cannot. Biomaterials provide tools to recreate tissue mechanics, structure, composition and presentation of biological and biochemical signals in a more physio (patho)logical relevant manner permitting better and more accurate advances toward discovering the mechanisms of disease and prospective disease treatments.

1.6 References

1.Bian W, Wang Z, Sun C, Zhang DM. Pathogenesis and Molecular Immune Mechanism of Calcified Aortic Valve Disease. *Front Cardiovasc Med*. 2021;8:765419. doi:10.3389/fcvm.2021.765419

2.Kraler S, Blaser MC, Aikawa E, Camici GG, Lüscher TF. Calcific aortic valve disease: from molecular and cellular mechanisms to medical therapy. *Eur Heart J*. 2021;43(7):683-697. doi:10.1093/eurheartj/ehab757

3.Nsaibia MJ, Devendran A, Goubaa E, Bouitbir J, Capoulade R, Bouchareb R. Implication of Lipids in Calcified Aortic Valve Pathogenesis: Why Did Statins Fail? *J Clin Med*. 2022;11(12):3331. doi:10.3390/jcm11123331

4.Hulin A, Hego A, Lancellotti P, Oury C. Advances in Pathophysiology of Calcific Aortic Valve Disease Propose Novel Molecular Therapeutic Targets. *Front Cardiovasc Med*. 2018;5:21. doi:10.3389/fcvm.2018.00021

5.Mongkoldhumrongkul N, Yacoub MH, Chester AH. Valve Endothelial Cells - Not Just Any Old Endothelial Cells. *Curr Vasc Pharmacol*. 2016;14(2):146-154. doi:10.2174/1570161114666151202205504

6.El-Hamamsy I, Balachandran K, Yacoub MH, et al. Endothelium-dependent regulation of the mechanical properties of aortic valve cusps. *J Am Coll Cardiol*. 2009;53(16):1448-1455. doi:10.1016/j.jacc.2008.11.056

7.Gee TW, Richards JM, Mahmut A, Butcher JT. Valve endothelial-interstitial interactions drive emergent complex calcific lesion formation in vitro. *Biomaterials*. 2021;269:120669. doi:10.1016/j.biomaterials.2021.120669

8.Ground M, Callon K, Walker R, et al. Perspective Chapter: Valvular Interstitial Cells – Physiology, Isolation, and Culture. In: *Technologies in Cell Culture - A Journey From Basics to Advanced Applications*. IntechOpen; 2023. doi:10.5772/intechopen.112649

9.Grim JC, Aguado BA, Vogt BJ, et al. Secreted factors from pro-inflammatory macrophages promote an osteoblast-like phenotype in valvular interstitial cells. *Arterioscler Thromb Vasc Biol*. 2020;40(11):e296-e308. doi:10.1161/ATVBAHA.120.315261

10.Chen JH, Yip CYY, Sone ED, Simmons CA. Identification and characterization of aortic valve mesenchymal progenitor cells with robust osteogenic calcification potential. *Am J Pathol*. 2009;174(3):1109-1119. doi:10.2353/ajpath.2009.080750

11.Chen JH, Simmons CA. Cell-matrix interactions in the pathobiology of calcific aortic valve disease: critical roles for matricellular, matricrine, and matrix mechanics cues. *Circ Res*. 2011;108(12):1510-1524. doi:10.1161/CIRCRESAHA.110.234237

12.El-Hamamsy I, Chester AH, Yacoub MH. Cellular regulation of the structure and function of aortic valves. *J Adv Res*. 2010;1(1):5-12. doi:10.1016/j.jare.2010.02.007

13.Porras AM, Westlund JA, Evans AD, Masters KS. Creation of disease-inspired biomaterial environments to mimic pathological events in early calcific aortic valve disease. *Proc Natl Acad Sci U S A*. 2018;115(3):E363-E371. doi:10.1073/pnas.1704637115

14.Dahal S, Huang P, Murray BT, Mahler GJ. Endothelial to mesenchymal transformation is induced by altered extracellular matrix in aortic valve endothelial cells. *J Biomed Mater Res A*. 2017;105(10):2729-2741. doi:10.1002/jbm.a.36133

15.Fondard O, Detaint D, Iung B, et al. Extracellular matrix remodelling in human aortic valve disease: the role of matrix metalloproteinases and their tissue inhibitors. *Eur Heart J*. 2005;26(13):1333-1341. doi:10.1093/eurheartj/ehi248

16.Mahler GJ, Farrar EJ, Butcher JT. Inflammatory cytokines promote mesenchymal transformation in embryonic and adult valve endothelial cells. *Arterioscler Thromb Vasc Biol*. 2013;33(1):121-130. doi:10.1161/ATVBAHA.112.300504

17.Alvandi Z, Bischoff J. Endothelial-Mesenchymal Transition in Cardiovascular Disease. *Arterioscler Thromb Vasc Biol*. 2021;41(9):2357-2369. doi:10.1161/ATVBAHA.121.313788

18.Faure E, Bertrand E, Gasté A, Plaindoux E, Deplano V, Zaffran S. Side-dependent effect in the response of valve endothelial cells to bidirectional shear stress. *Int J Cardiol*. 2021;323:220-228. doi:10.1016/j.ijcard.2020.08.074

19.Deb N, Ali MS, Mathews A, Chang YW, Lacerda CM. Shear type and magnitude affect aortic valve endothelial cell morphology, orientation, and differentiation. *Exp Biol Med Maywood NJ*. 2021;246(21):2278-2289. doi:10.1177/15353702211023359

20.Wu S, Li Y, Zhang C, et al. Tri-Layered and Gel-Like Nanofibrous Scaffolds with Anisotropic Features for Engineering Heart Valve Leaflets. *Adv Healthc Mater*. 2022;11(10):e2200053. doi:10.1002/adhm.202200053

21.Kirschner CM, Alge DL, Gould ST, Anseth KS. Clickable, photodegradable hydrogels to dynamically modulate valvular interstitial cell phenotype. *Adv Healthc Mater*. 2014;3(5):649-657. doi:10.1002/adhm.201300288

22.Ali MS, Deb N, Wang X, Rahman M, Christopher GF, Lacerda CMR. Correlation between valvular interstitial cell morphology and phenotypes: A novel way to detect activation. *Tissue Cell*. 2018;54:38-46. doi:10.1016/j.tice.2018.07.004

23.Hjortnaes J, Camci-Unal G, Hutcheson JD, et al. Directing valvular interstitial cell myofibroblast-like differentiation in a hybrid hydrogel platform. *Adv Healthc Mater*. 2015;4(1):121-130. doi:10.1002/adhm.201400029

24.Monroe MN, Nikonowicz RC, Grande-Allen KJ. Heterogeneous multi-laminar tissue constructs as a platform to evaluate aortic valve matrix-dependent pathogenicity. *Acta Biomater*. 2019;97:420-427. doi:10.1016/j.actbio.2019.07.046

25.Zhu Z, Liu Z, Zhang D, Li L, Pei J, Cai L. Models for calcific aortic valve disease in vivo and in vitro. *Cell Regen*. 2024;13:6. doi:10.1186/s13619-024-00189-8

26.Hu J, Lei H, Liu L, Xu D. Lipoprotein(a), a Lethal Player in Calcific Aortic Valve Disease. *Front Cell Dev Biol*. 2022;10:812368. doi:10.3389/fcell.2022.812368

27.Liu Q, Yu Y, Xi R, et al. Association Between Lipoprotein(a) and Calcific Aortic Valve Disease: A Systematic Review and Meta-Analysis. *Front Cardiovasc Med*. 2022;9. doi:10.3389/fcvm.2022.877140

28.Rogers MA, Atkins SK, Zheng KH, et al. Lipoprotein(a) Induces Vesicular Cardiovascular Calcification Revealed With Single-Extracellular Vesicle Analysis. *Front Cardiovasc Med*. 2022;9:778919. doi:10.3389/fcvm.2022.778919

29.Grim JC, Aguado BA, Vogt BJ, et al. Secreted factors from pro-inflammatory macrophages promote an osteoblast-like phenotype in valvular interstitial cells. *Arterioscler Thromb Vasc Biol*. 2020;40(11):e296-e308. doi:10.1161/ATVBAHA.120.315261

30.Lim J, Ehsanipour A, Hsu JJ, et al. Inflammation Drives Retraction, Stiffening, and Nodule Formation via Cytoskeletal Machinery in a Three-Dimensional Culture Model of Aortic Stenosis. *Am J Pathol*. 2016;186(9):2378-2389. doi:10.1016/j.ajpath.2016.05.003

31. Richards JM, Kunitake JAMR, Hunt HB, et al. Crystallinity of hydroxyapatite drives myofibroblastic activation and calcification in aortic valves. *Acta Biomater*. 2018;71:24-36. doi:10.1016/j.actbio.2018.02.024

32. Dahal S, Bramsen JA, Alber BR, et al. Chondroitin Sulfate Promotes Interstitial Cell Activation and Calcification in an In Vitro Model of the Aortic Valve. *Cardiovasc Eng Technol*. 2022;13(3):481-494. doi:10.1007/s13239-021-00586-z

33. Schroeder ME, Gonzalez Rodriguez A, Speckl KF, et al. Collagen networks within 3D PEG hydrogels support valvular interstitial cell matrix mineralization. *Acta Biomater*. 2021;119:197-210. doi:10.1016/j.actbio.2020.11.012

Chapter 2: Objectives

2.1 Motivation

CAVD affects about 10 million individuals of the aging population[1] and this number continues to increase each year posing more challenges to the healthcare system as no effective treatment has been developed to stop the onset of disease progression or halt its development. Lack of understanding of CAVD etiology is one of the main reasons hampering our ability to create effective treatments[2]. It is believed that CAVD pathological processes occur concomitantly, thus a clear path to decipher the underpinnings of how these processes interact with each other during disease development has not been established. In addition, sex as a biological variable has been deemed essential to understand CAVD development as females and males present with different disease pathologies towards the end-stages of the disease[3]. The vast majority of CAVD research (whether in 2D or 3D platforms) has been performed using mixed VIC cultures. For this reason, it is precise that a better understanding of how CAVD develops in females and males through the diverse stages of CAVD is researched. Hence, the need to develop new and improved culture systems/technologies that allows to isolate elements of these processes that occur at diverse stages of disease. In this thesis we will discuss how we developed an improved 3D culture system that allows us to investigate the role ECM (dys)regulation as is observed in through different stages of disease.

2.2 Objective 1: Generate disease-inspired hydrogel models of that mimic the diverse stages of CAVD progression.

3D cultures have revolutionized the way we do research in the present day. Employing 3D culture platforms provides us with the ability to isolate biological, biochemical and mechanical cues that are present in the native and disease tissue in order to explore how these affect cell function and activity. With this in mind, we worked in the development of stage-specific models of CAVD to study how the ECM composition changes observed during CAVD progression affect female and male VICs behavior differently. We built these models based in a GelMA-Collagen interpenetrating network hydrogel model previously designed in our lab which provided the opportunity to obtain a highly mechanically tunable fibrous hydrogel. In chapter 3, we will discuss in detail the creation and characterization of these disease-inspired, stage-specific hydrogel models that mimic early and late-stage hallmarks of CAVD and the biological and architectural role of fibrillar collagen to drive fibrosis in female and male VICs.

2.3 Objective 2: Evaluate the influence of ECM remodeling during CAVD progression in males and females VICs.

In the past decades, much attention has been directed towards understanding how cell-ECM interactions during disease impact further disease progression. It has been well established that ECM (dys)regulation constitutes one of the most notable hallmarks during the development of CAVD. It is known that in diseased aortic valves the valve

trilaminar structure is lost and increased amounts of glycosaminoglycans and fibrillar collagen are found spread across the three main layers of the valve tissue[4]. However, little is understood about how this ECM changes promote disease progression in the context of CAVD. As previously mentioned, sex as a biological variable has been recently considered as an important factor in the understanding of CAVD etiology as females and males exhibit different end-stage pathologies Specifically, for the same degree of valve stenosis, aortic valve from females exhibit high levels of fibrosis while males exhibit high levels of calcification. Therefore, understanding how disease develops in females and males at each stage of disease is essential. In this thesis we explain how we implement the use of stage-specific disease-inspired hydrogel models (as described above) to understand how ECM changes impact female and male VIC behavior. In chapter 4, we explore how increased collagen content affect VIC fibrosis in female and male VICs cultured in disease-inspired systems that mimic collagen enrichment from the early to the late stages of disease. In chapter 5 we explore whether collagen fiber architecture is essential (or not) in driving fibrotic responses in female and male VICs at the late stage of disease.

2.4 Objective 3: Elucidate differential sex response to exposure to TGBFB-1 as a profibrotic pathological stimulus at different stages of CAVD.

TGFB-1 is a well-known pro-fibrotic factor which presence is also known to be part of the ECM fibrocalcific remodeling in CAVD progression. In chapter 4, we explored the combinatorial effects of TGFB-1 as a pathological stimulus and collagen 1 enrichment in

driving female and male VICs fibrotic responses cultured in early and late-stage hydrogel systems. In chapter 5, we explore the combinatorial effects of profibrotic TGFB-1 in female and male VICs cultures in late stages models with varied degrees of fibrillar architecture. Investigating how the ECM in the context of ECM composition and architecture as well as exposure to pathological cues affect VIC pathological behavior provides us with new understanding that inform us on how to better design culture platforms to understand disease etiology and test new therapies.

2.5 References

1.Sylvester CB, Amirkhosravi F, Bortoletto AS, West WJ, Connell JP, Grande-Allen KJ. Dantrolene inhibits lysophosphatidylcholine-induced valve interstitial cell calcific nodule formation via blockade of the ryanodine receptor. *Front Cardiovasc Med*. 2023;10:1112965. doi:10.3389/fcvm.2023.1112965

2.Porras AM, McCoy CM, Masters KS. Calcific Aortic Valve Disease: A Battle of the Sexes. *Circ Res*. 2017;120(4):604-606. doi:10.1161/CIRCRESAHA.117.310440

3.Chen JH, Simmons CA. Cell-matrix interactions in the pathobiology of calcific aortic valve disease: critical roles for matricellular, matricrine, and matrix mechanics cues. *Circ Res*. 2011;108(12):1510-1524. doi:10.1161/CIRCRESAHA.110.234237

4.Hutson HN, Marohl T, Anderson M, Eliceiri K, Campagnola P, Masters KS. Calcific Aortic Valve Disease Is Associated with Layer-Specific Alterations in Collagen Architecture. *PLoS ONE*. 2016;11(9):e0163858. doi:10.1371/journal.pone.0163858

Chapter 3: Engineering of CAVD Disease-Inspired Engineered Scaffolds: A Somewhat Challenging Task

3.1 Abstract

The extracellular matrix (ECM) plays a critical role in maintaining tissue homeostasis and influencing cellular functions such as proliferation, migration, and signaling. Recent research has underscored the significance of ECM in disease progression, particularly in Calcific Aortic Valve Disease (CAVD). In CAVD, ECM components like collagens and glycosaminoglycans (GAGs) are heavily implicated in the disruption of aortic valve structure and the pathological responses of valvular interstitial cells (VICs). GAGs are notably increased in the early stages of CAVD, promoting inflammation through the entrapment of lipoproteins, while collagens, elevated at later stages, contribute to calcific deposits that impair valve mechanics. Despite their pathological roles, these molecules are essential in healthy valves for providing lubricity and mechanical strength. Advancements in tissue engineering now enable the development of more physiologically relevant 3D models to study disease progression, moving beyond traditional 2D cultures. Techniques such as decellularized organ scaffolds, functionalized synthetic molecules, and ECM-integrated hydrogels offer novel platforms to explore cellular interactions with ECM components. In this chapter, we detail the creation of disease-inspired engineered 3D models to investigate sex-specific VIC responses to GAG and collagen elevations in CAVD. We also address the challenges and limitations encountered during the model development and the strategies employed to overcome them.

3.2 Introduction

More attention has been given in the scientific community considers the extracellular matrix (ECM) as a potential regulator of tissue's physiological health or as a contributor to tissue's pathology[1]. The ECM is a complex system - mostly composed of proteins - that sustains the tissue homeostasis and provides the cells with an infrastructure to aid in processes such as cell proliferation, migration and signaling via mechanical or biological stimuli[2]. In light of this, research of pathologies should consider cell-ECM interactions as a potential for disease progression. Research of pathologies such as Calcific Aortic Valve Disease (CAVD) have highlighted the importance of ECM in modulating disease progression as molecules such as Collagens[3–5] and Glycosaminoglycans[6–10] have been found to be heavily involved in disrupting the aortic valve structure and the valve's cells (such as valvular interstitial cells (VICs)) responses. Particularly, Glycosaminoglycans have been found to be highly increased during the early stages of CAVD[7], while collagen have been found to be highly elevated at later stages of disease[4,5]. It is important to note that glycosaminoglycans which have been spotted around calcific nodules[11], are known to entrap and retain lipoproteins which are highly involved in the process of inflammation in CAVD[7]. Collagens on the other hand serve as nucleation sited for calcific deposits which stiffens the valve and impairs its mechanical compliance[5]. However, in healthy valves these two molecules serve important roles such as providing the valve with enough lubricity (GAGs) and strength (Collagens) to withstand the strong mechanical of blood flow.

In the tissue, cells exist within this 3-dimentional ECM structure allowing the cells to interact in many ways with the environment that surrounds them. While many breakthroughs in research of pathological process haven been obtained through culture in 2D platforms, new advances in technologies can now provide us new innovative systems to investigate disease development in more physiological relevant 3D models. Innovations in tissue engineering allows to design and develop disease-inspired models in many ways. For instance, decellularized organs can be used as a tissue scaffold to grow new tissues in an accurate physiological environment, synthetic molecules can be functionalized with specific chemical groups or biological signals to modulate cells behaviors, additionally, isolated ECM molecules could be added to hydrogel constructs allowing us to understand individual cells responses/interactions with a particular ECM molecule. Thus, implementation of new tissue engineering strategies as previously mentioned could help us to better understand the cellular mechanisms that underly disease progression in a more physio(patho)logically relevant manner.

With this in mind, we embarked in our mission to designed and develop disease inspired engineered 3D models to investigate VICs differential sex responses to GAG and Collagen increase as hallmarks of CAVD. In this chapter we will discuss the challenges and limitations we encountered in the creation of disease inspired engineered 3D models and the approaches taken solve these constraints.

3.3 Methods

3.3.1 VIC isolation and expansion

Valvular interstitial cells (VICS) were isolated, expanded and maintained in culture as previously described[12]. Briefly, aortic valve leaflets were excised from 6-month-old pig hearts obtained from our local abattoir (Hoesly's Meats, New Glarus, WI) and incubated for 30 minutes in a collagenase II (Worthington Biochemical Corporation, Lakewood, NJ) solution to remove valvular endothelial cells from the tissue. A second 60-minute incubation followed, in fresh collagenase II solution to release VICS for expansion. VICs were then divided into two subsets, aVICs and qVICs. aVICs were maintained in low glucose Dulbecco's Modified Eagle's Medium (Sigma-Aldrich, St. Louis, MO), supplemented with 2 mM L-glut (Sigma Aldrich), 150 U/mL penicillin/streptomycin (Sigma-Aldrich) and 10% fetal bovine serum (FBS) (Corning, Corning, NY) at 37 °C and 5% CO_2. QVICs where cultured on collagen-1 coated TCPS at 2 μg/cm^2 (Advanced Biomatrix) and maintained in low glucose Dulbecco's Modified Eagle's Medium (Sigma-Aldrich, St. Louis, MO), supplemented with 2 mM L-glut (Sigma Aldrich), 150 U/mL penicillin/streptomycin (Sigma-Aldrich) and 2% fetal bovine serum (FBS) (Corning, Corning, NY), 5.25 μg/mL insulin (Sigma Aldrich), and 10 ng/mL FGF-2 (PeproTech) at 37 °C and 5% CO_2. VICs were not used past passage 3 for any of the experiments.

3.3.2 GelMA Synthesis

Gelatin type A from porcine skin (Sigma Aldrich) was dissolved at 10% w/v in phosphate-buffered saline (1X PBS) (Corning, Corning, NY) at 50 °C. Once the gelatin was

dissolved, methacrylic anhydride (MA) (Sigma Aldrich) was added to the gelatin solution with a syringe in a drop-wise manner and stirred overnight protected from light. The following day, the gelatin-methacrylate (GelMA) reaction solution was centrifuged at 3000 xg for 5 minutes at 37 °C degrees to precipitate unreacted MA. The supernatant was collected and diluted at a 1:4 ratio in pre-warmed 1X PBS at 50 °C and then transferred to 12-14 kDa MWCO dialysis tubing (Spectrum Labs, Rancho Dominguez, CA). The diluted GelMA solution was dialyzed against 1X PBS for 3 days and diH_20 for 3 more days at 50 °C to remove any unreacted MA. PBS and DiH_2O solutions were changed daily through the dialysis process. At the end of the dialysis period, the GelMa solution was filtered, lyophilized and stored at -80 °C until needed for further characterization and use[13].

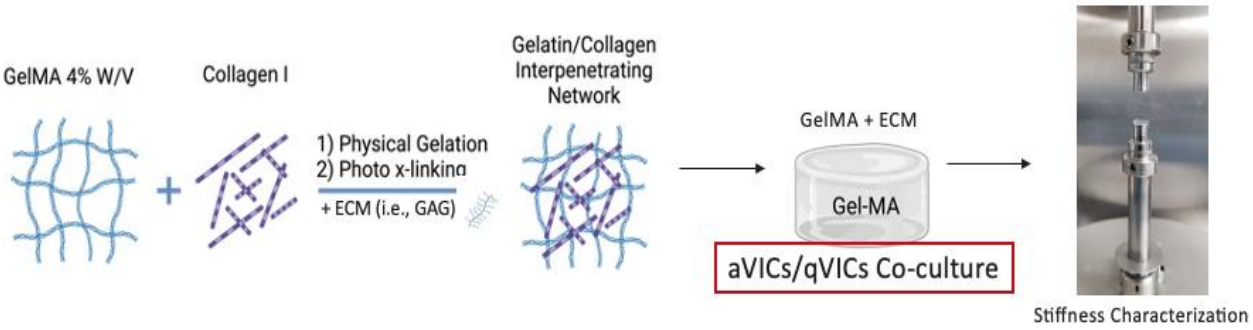

Figure 3.1 Schematic representation of disease inspired models design and stiffness characterization

3.3.3 Creation of healthy, early and late CAVD stage models

3-D disease-inspired scaffolds were developed to mimic gag (healthy to early transition) and collagen enrichment (early to late transition) as a hallmarks of CAVD. All models were created using a GelMA (Gelatin Methacrylate) based hydrogel (4% w/v) with an interpenetrating network of collagen fibers[13]. Scaffolds mimicking healthy valves

contained 0.75 mg/mL collagen I (Col1) (Advanced Biomatrix, San Diego, CA), and 2.5 mg/mL chondroitin sulfate A (CS) from bovine trachea (Sigma Aldrich), early-stage disease contained 0.75 mg/mL Col and 10 mg/mL CS, while late-stage (Late 2X; 2X referred to the increased amount of fibrillar collagen enrichment) disease scaffolds contained 1.5 mg/mL Col1 and 10 mg/mL CS. An additional late model (Late 1X) was created by maintaining the same fibrillar collagen concentration as our early model (0.75 mg/mL Col1) but increasing the total amount of collagen ligand by adding an additional 0.5 mg/mL of GelMa for a total concentration of 1.5 mg/mL of total collagenous protein. This model was created to understand whether expression of fibrotic markers was affected by total collagenous protein enrichment or whether collagen fibrillar structure was the main driver for fibrosis in CAVD.

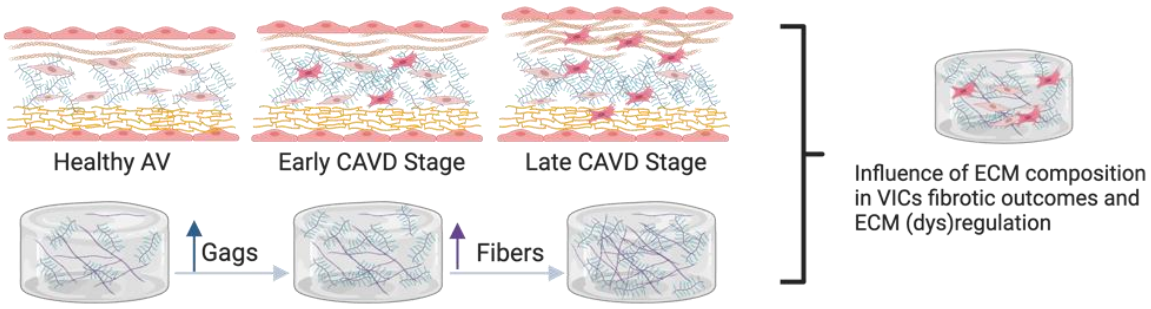

Figure 3.2 Schematic representation designed disease inspired models mimicking early (GAGs enrichment) and late (Collagen enrichment) hallmarks of CAVD and pathological outcomes to measure

Then, to account for over engineering, iterations of these models were created by subtracting CS from the system. To neutralize the collagen added to our GelMa-Coll pre-polymer solutions, 0.1 M NaOH (RPI, Mt. Prospect, IL) and 10x DPBS (Sigma Aldrich) were added at their appropriate ratios. A co-culture of QVIC and aVICs were also added

at a concentration of 2 x 10^6 cells/mL to the pre-polymer solution for a total concentration of of 4 x 10^6 cells/mL, along with photoinitiator lithium-phenyl-2,4,6-trimethylbenzoylphosphinate (LAP) (Sigma Aldrich) at a final concentration of 0.05% w/v. 100 ul of the pre-polymer solution was added to silicone molds (9 mm diameter x 1.7 mm depth) and incubated at 37 °C for 30 minutes to allow for collagen fibrillogenesis. The molds were then incubated at 4 °C for the amount of time previously optimized via dynamic mechanical analysis[13] to reach a Young's modulus of 5-8 kPa and subsequently photocrosslinked under UV light (365 nm) for 6 minutes.

3.3.4 VIC culture in 3D early and late-stage hydrogel models

VICs (qVICS and aVICS co-culture) embedded in this disease-inspired hydrogel models were cultured for a total of 6 days (D0= seeding day, D2 and D4 = media change and collection days, D5 = sample collection for RT-qPCR) in low glucose DMEM, supplemented with 2 mM L-glut, 150 U/mL, penicillin/streptomycin and 10% FBS. Fresh media was provided every other day. Samples for each assay were collected and processed as described in the sections below.

3.3.5 Detection of fibrotic markers via gene expression quantification

Since hallmarks of fibrosis start presenting from the early stages of disease progression, all healthy, early and late-stage (including both Late1x and Late 2X) female and male samples were collected on day 5 and underwent q-PCR screening of known fibrotic markers (listed below). All samples were digested in a collagenase (4.2 mg/mL) digestion solution supplemented with 30% v/v Proteinase K (Qiagen, Hilden, Germany), 50% v/v

10X Trypsin (Gibco, Grand Island, NY) and 20% v/v 1X PBS to facilitate RNA isolation. RNA isolation was performed according to the manufacturer's instruction for Qiagen's RNeasy kit (Qiagen, Germantown, MD). Retrieved RNA was then subjected to reverse transcription using a High-Capacity cDNA Reverse Transcription kit (Applied Biosystems, Foster City, CA). Taqman Gene Expression Assays were used to quantify genetic expression profiles of fibrosis-related genes (*aSMA, COL1A1, FN and TGFB-1*) (Thermo Fisher). All PCR reactions were performed in a Biorad CXF Opus 96 Real Time PCR and analyzed via the delta-delta ct method.

3.3.6 Detection of inflammatory cytokines

Since inflammation is observed in the initial stages of CAVD progression and is likely linked to the effects of GAG enrichment and entrapment of inflammatory molecules, all female and male samples cultured in healthy and early-stage models were collected on days 2 and 4 to evaluate production of inflammatory cytokines, IL6 and IL8 from media in response to GAG enrichment. IL6 and IL8 expression was evaluated via R&D DuoSet ELISA following the manufacturer's instructions. Total cytokine levels were quantified via four-parameter logistic regression.

3.3.7 Statistical Analysis

Each experiment was performed using a n=3 sample. Specifically, VICs isolated from 3 different pigs were pooled for each sex. Data points as seen in each graph represent a sample repeat of this pooled set. Additional experiments performed to validate our results

used a new set of pigs. Statistical analysis was performed via 2-way Anova with Tukey Post-Hoc test. Statistical Significance was considered for all comparisons with $P < 0.05$.

3.4 Results

3.4.1 Inflammation of VICs is sex-dependent

The production of inflammatory cytokines IL6 and IL8 in female and male qVICs and aVICs co-culture, embedded in healthy and early-stage models, was assessed using ELISA at days 2 and 4. Notable sex-specific differences were observed, particularly in IL-6 expression at the early stage (Figure 3.3 a). Female cells exhibited a higher production of IL-6 compared to male cells, a trend that persisted across all conditions and timepoints, although the differences were not always statistically significant. Similarly, sex-specific differences were evident in IL-8 expression, with female cells showing increased IL-8 production in both healthy models at days 2 and 4 and in early-stage models at day 4 (Figure 3.3 b).

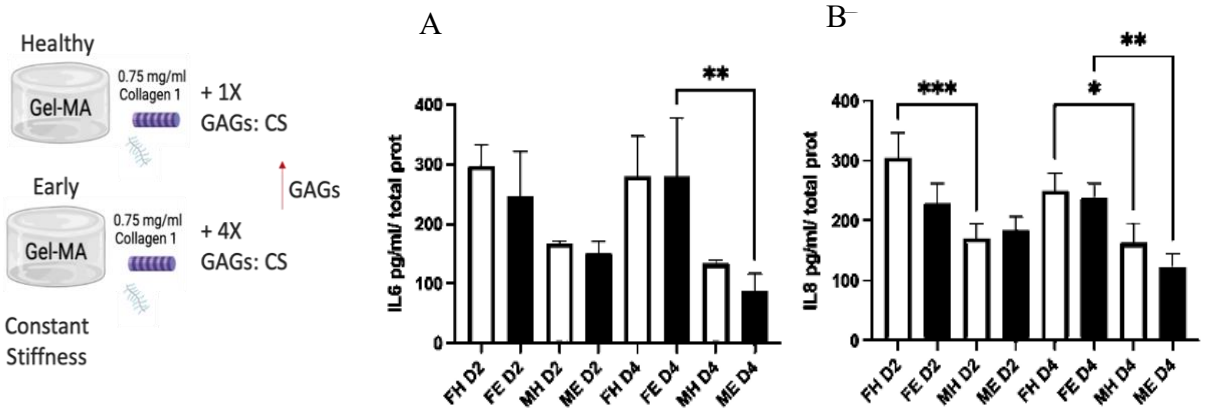

Figure 3.3 Impact of GAG enrichment in a collagen background hydrogel on inflammatory cytokine production by females and male VICs. Cytokine expression of a) IL6 and b) IL8 was measured 2- and 4-days post seeding via ELISA. Results are presented as mean ± standard deviation; *indicates $P < 0.05$ by Tukey Post-hoc test.

3.4.2 Biological sex affects gene expression profiles of CAVD fibrotic markers of VICs cultured in healthy and early-stage models

The expression of fibrotic markers, which are critically involved in the progression of Calcific Aortic Valve Disease (CAVD), was evaluated using RT-qPCR. Gene expression levels were normalized to the female healthy-stage condition to facilitate comparison. The results revealed that males exhibited a more pronounced fibrotic response compared to females. This heightened response was particularly evident in the increased expression of α-Smooth Muscle Actin (aSMA) and Collagen Type I Alpha 1 Chain (COL1A1) genes (Figure 3.4 a and d) across both healthy and early-stage models. Additionally, a similar trend was observed in the expression of Transforming Growth Factor Beta 1 (TGFB-1) (Figure 3.4 c), though this effect was specifically noted in the early-stage model.

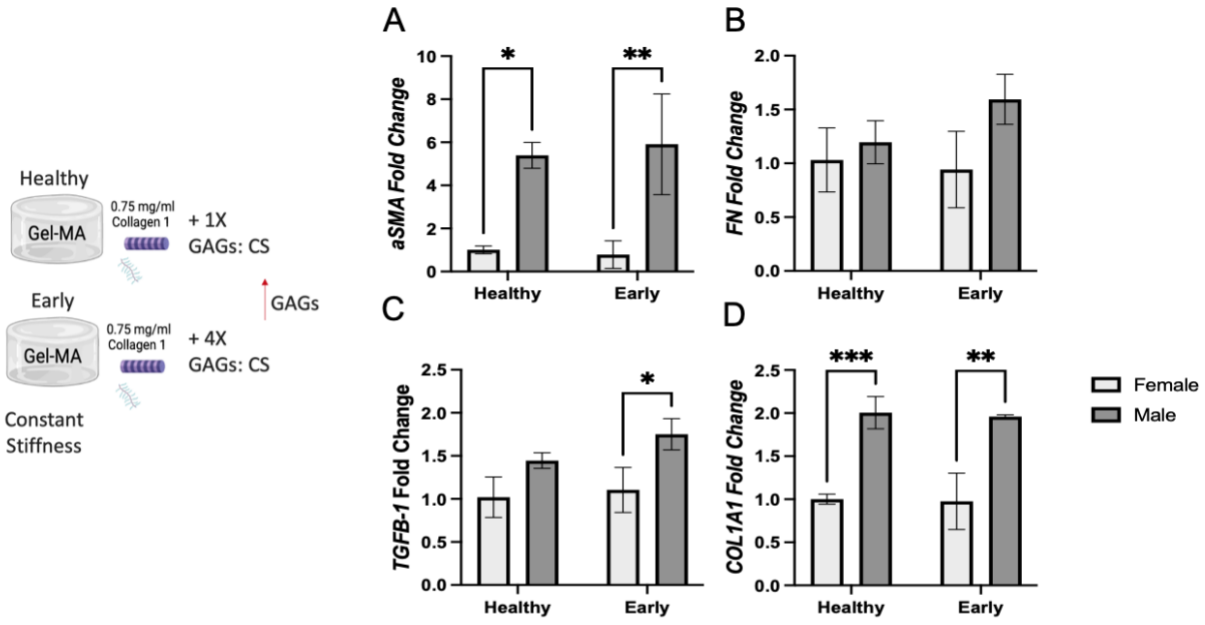

Figure 3.4 Fibrotic gene expression of female and male VICs embedded co-culture in healthy and early-stage models shows a sex-dependent response. Gene expression of fibrotic markers (a) aSMA (ACTA2), b) FN c) TGFB-1, and d) COL1A1 was assessed by RT-qPCR and normalized to female healthy. Results are presented as mean ± standard deviation; *indicates $P < 0.05$ by Tukey Post-hoc test.

3.4.3 Collagen enrichment is sufficient to drive pathological responses regardless of CS presence.

The expression of fibrotic markers involved in the fibrotic progression of Calcific Aortic Valve Disease (CAVD), was assessed through RT-qPCR. Gene expression levels were normalized against the female early-stage condition. Notable sex-specific differences were identified in the expression of key fibrotic markers, including aSMA, FN, TGFB-1, COL1A1. Specifically, males demonstrated a more pronounced fibrotic response compared to females during the early stage of the disease. However, stage-specific differences were predominantly observed in female subjects, where an increase in the expression of all fibrotic markers was noted in the late-stage model (Figure 3.5 a).

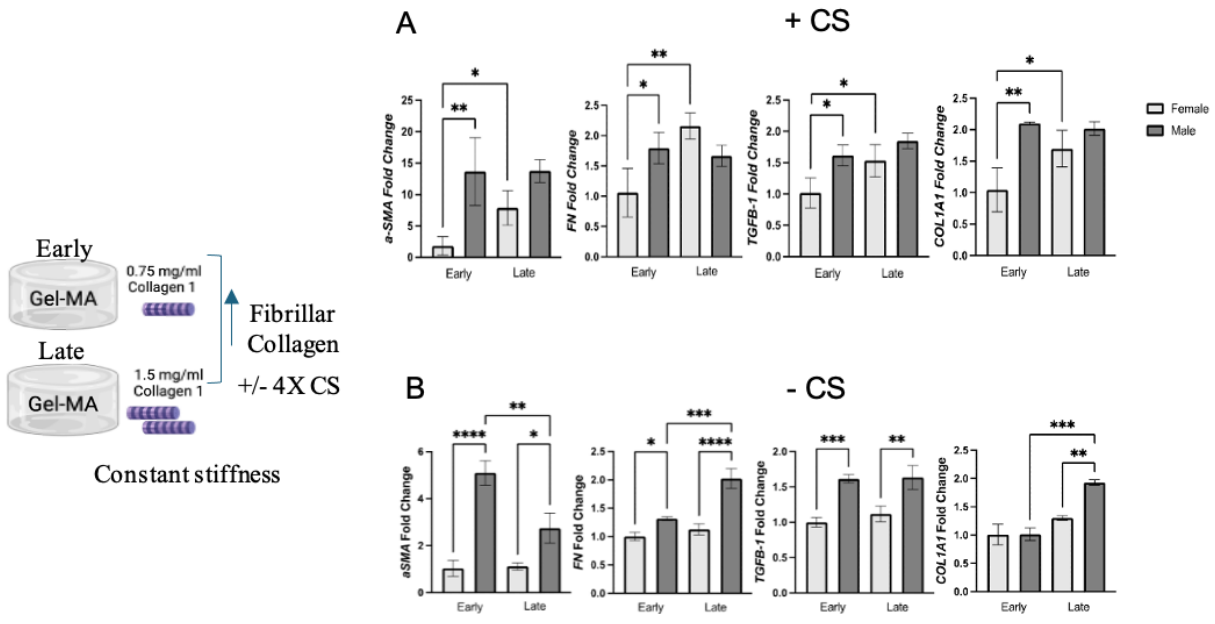

Figure 3.5 Collagen enrichment is sufficient to drive pathological responses regardless of CS presence. Fibrotic gene expression of female and male VICs embedded co-culture in early- and late-stage models shows sex- and stage-dependent responses. Gene expression of fibrotic markers (a) aSMA (ACTA2), b) FN c) TGFB-1, and d) COL1A1 was assessed by RT-qPCR and normalized to female early. Results are presented as mean ± standard deviation; *indicates $P < 0.05$ by Tukey Post-hoc test.

To further evaluate the potential over-engineering of the system, the experiment was replicated in newly generated early and late-stage models that lacked the presence of chondroitin sulfate. Consistent with the initial findings, sex-dependent responses were observed, with males exhibiting a higher fibrotic response than females at both disease stages. Interestingly, when CS was absent, stage-specific differences were observed only in male subjects, indicating that the presence of CS may play a role in modulating the disease progression in a sex-specific manner (Figure 3.5 b).

3.4.4 Total collagen enrichment, but not fiber enrichment, may play a role in driving fibrotic responses regardless of presence or absence of CS

To determine whether the sex- and stage-specific changes observed in the early and late models were driven by the fibrillar architecture of collagen or merely by an overall increase in collagenous protein, we conducted an additional experiment. This involved the creation of a late-stage model referred to as "Late 1X," which maintained the same total collagenous protein content as the standard late-stage model (also referred as "Late 2X") but with the same amount of collagen fibers as seen in the early model.

Our findings revealed that, in the presence of chondroitin sulfate (CS), it was the total enrichment of collagenous protein rather than the enrichment of collagen fibers that primarily drove fibrotic responses, as indicated by the expression of fibrotic markers. Males exhibited a more pronounced fibrotic response than females during the early stage of the disease. However, stage-specific differences were particularly prominent in female subjects, where a notable increase in the expression of all fibrotic markers was observed

in the late-stage model (Figure 3.6 a). Importantly, no significant sex- or stage-specific differences were observed between the Late 1X and Late 2X models in the presence of CS (Figure 3.6 b).

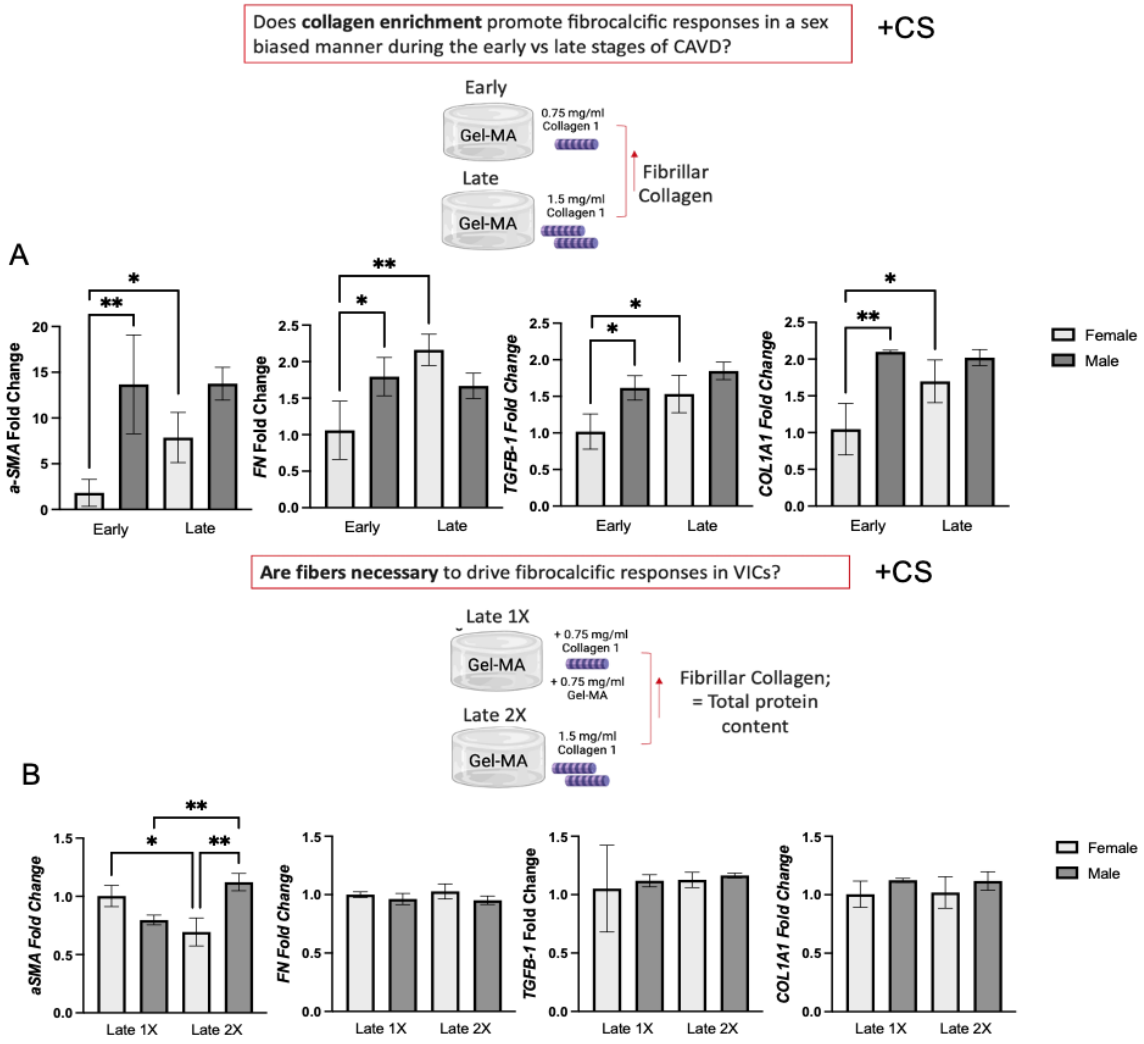

Figure 3.6 Total collagen enrichment, but not fiber enrichment, may play a role in driving fibrotic responses in presence of CS. Collagenous protein enrichment is sufficient to drive pathological responses in presence of CS. Fibrotic gene expression of female and male VICs embedded co-culture in early- and late-stage models shows sex- and stage-dependent responses, while no overall fibrotic expression was observed between the Late 1X and Late 2X models (same amount of total collagenous protein but differing collagen fibers amount). Gene expression of fibrotic markers (a) aSMA (ACTA2), b) FN c) TGFB-1, and d) COL1A1 was assessed by RT-qPCR and normalized to female early or female Late 1X respectively. Results are presented as mean ± standard deviation; *indicates $P < 0.05$ by Tukey Post-hoc test.

In contrast, in the absence of CS, distinct sex-dependent responses were noted, with males showing a higher fibrotic response than females at both disease stages. Interestingly, when CS was lacking, stage-specific differences were apparent only in male subjects, suggesting that CS may influence disease progression in a sex-specific manner (Figure 3.7 a). However, similar to the findings in the presence of CS, no overall sex- or stage-specific differences were observed between the Late 1X and Late 2X models (Figure 3.6 b).

Differences in aSMA expression, as seen in Figures 3.5 b and 3.6 b, may be attributed to the effects of cell imbalance between quiescent valvular interstitial cells (qVICs) and activated valvular interstitial cells (aVICs) within the embedded co-culture. We also examined whether the presence or absence of CS would affect fibrotic responses in female and male VICs in the Late 1X and Late 2X models. Our results indicated that the presence or absence of CS did not significantly impact fibrotic responses in female and male VICs cultured within these systems (Figures 3.8 a and b).

Thus, the primary driver of fibrotic expression across all our models appears to be the total increase in collagenous protein, regardless of other factors such as increased fiber content or the presence of glycosaminoglycans (GAGs) within the system.

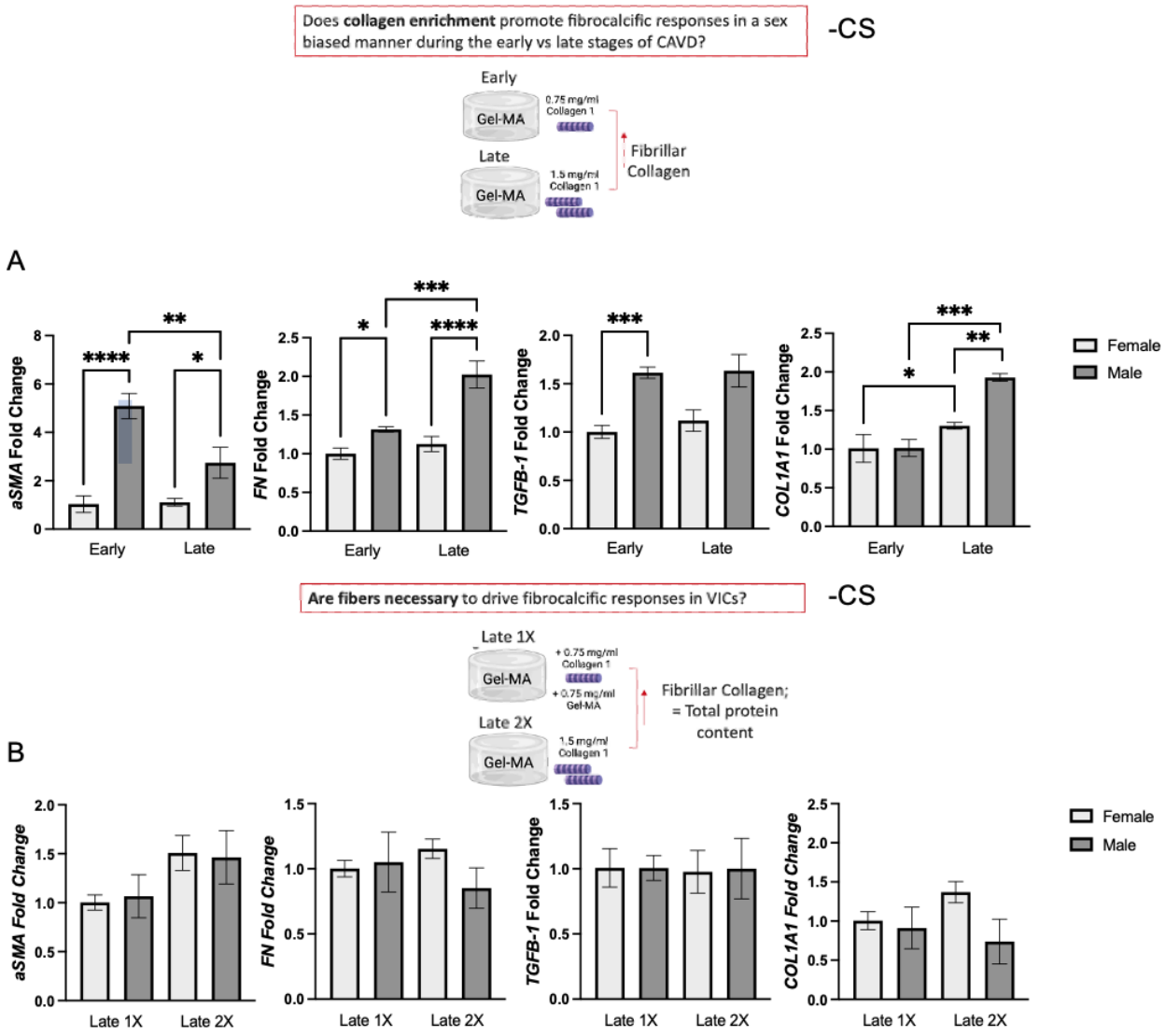

Figure 3.7 Total collagen enrichment, but not fiber enrichment, may play a role in driving fibrotic responses in absence of CS. Collagenous protein enrichment is sufficient to drive pathological responses in presence of CS. Fibrotic gene expression of female and male VICs embedded co-culture in early- and late-stage models shows sex- and stage-dependent responses, while no overall fibrotic expression was observed between the Late 1X and Late 2X models (same amount of total collagenous protein but differing collagen fibers amount). Gene expression of fibrotic markers (a) aSMA (ACTA2), b) FN c) TGFB-1, and d) COL1A1 was assessed by RT-qPCR and normalized to female early or female Late 1X respectively. Results are presented as mean ± standard deviation; *indicates $P < 0.05$ by Tukey Post-hoc test.

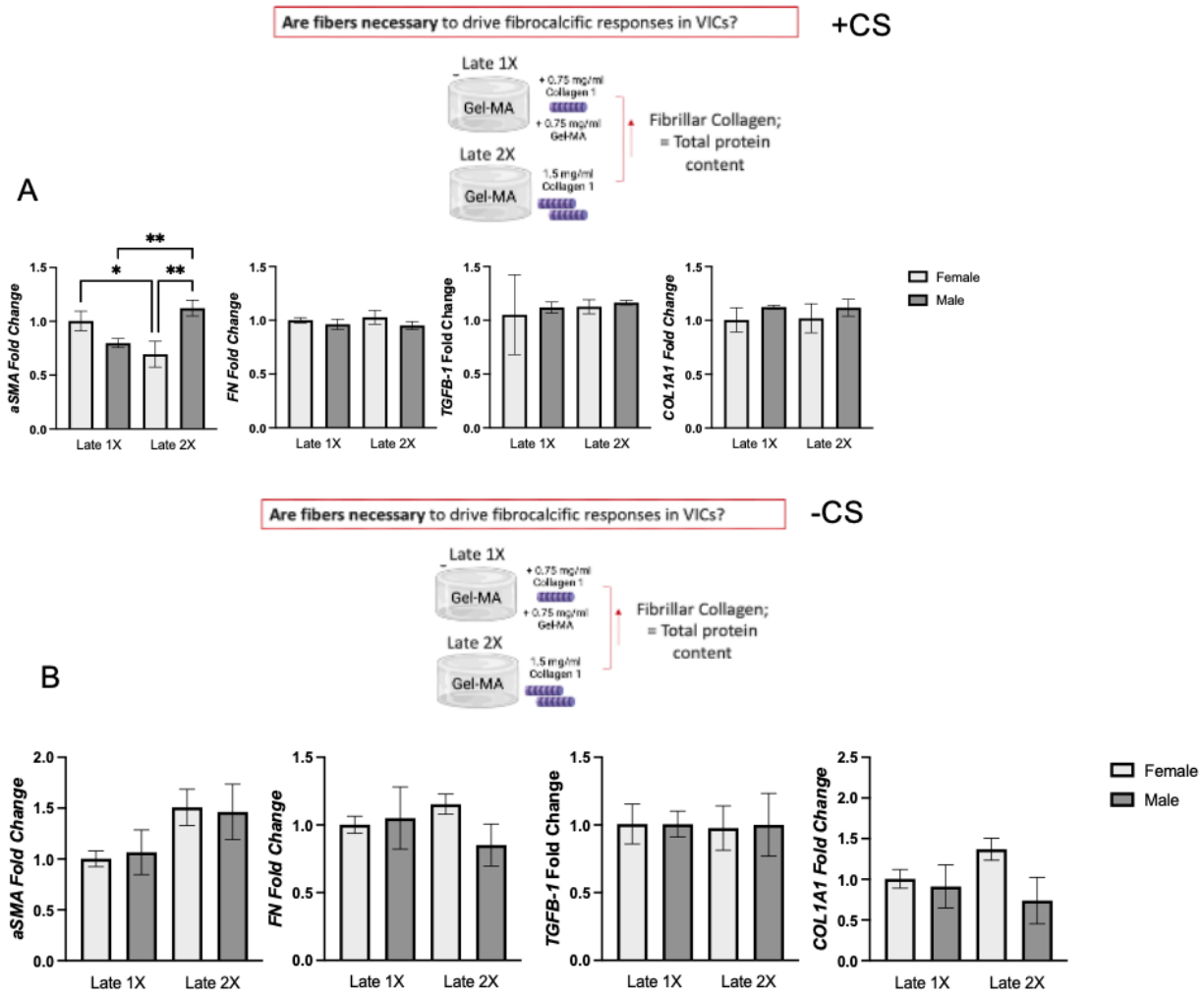

Figure 3.8 Fiber enrichment does not drive fibrotic expression in female and male VICs-coculture in presence or absence of CS. Gene expression of fibrotic markers (a) aSMA (ACTA2), b) FN c) TGFB-1, and d) COL1A1 was assessed by RT-qPCR and normalized to female Late 1X. Results are presented as mean ± standard deviation; *indicates $P < 0.05$ by Tukey Post-hoc test.

3.5 Discussion

In this chapter, we delved into the design and development of various tissue-engineered scaffolds aimed at more accurately replicating the hallmarks of early and late stages of Calcific Aortic Valve Disease (CAVD). Our research primarily focused on two critical areas: the sex-specific responses of valvular interstitial cells (VICs) and the stage-specific responses to changes in the extracellular matrix (ECM) that occur as the disease progresses. By leveraging three-dimensional (3D) models, we were able to overcome some of the limitations inherent in studying CAVD, particularly the scarcity of clinical specimens, which are often available only at advanced stages of the disease.

3D models provide a more physiologically relevant environment, allowing us to better understand the complex interactions between VICs and the ECM as the disease unfolds. This approach is particularly important given the well-established sexual dimorphism in CAVD, where males and females exhibit distinct clinical outcomes despite experiencing the same degree of valve stenosis. Understanding these differences is crucial for unraveling the mechanisms that drive disease progression.

We first investigated the effects on GAG enrichment as observed in the transition from healthy to earlier stages of CAVD. Initiation of inflammation is thought to be a result of lipid infiltration through the epithelial layer of the aortic valve leaflet with chronic inflammation persists across all stages of the disease, with cytokines, chemokines and growth factors, released by inflammatory cells contributing to the activation of VICs[14]. Lipids are known to be retained by GAGs possibly contributing to chronic inflammation in

the valve leaflet during CAVD[7]. Using healthy and early models of CAVD we screened for inflammatory markers (IL6 and IL8) known to influence fibrosis in the aortic valve. Our results suggested that females have a higher inflammatory profile than males, a resulted that often repeated in our 3D models as further described in chapters 4 and 5. We also observed that males have a more pro-fibrotic response compared to females in this enriched GAG models.

We then wanted to explore whether collagen enrichment was a prominent driver of valve fibrosis. For this we created early, and late-stage disease inspired models that mimicked collagen enrichment as observed during CAVD while also keeping our GAG concentration elevated. We observed sex and stage specific differences in regard to fibrotic marker expression with males having a more robust response than females, and stage specific differences observed only in females. To account for the possibility of having an over-engineered system, these experiments were repeated once more by removing CS from our system. While sex-differences trends persisted, stage-specific differences were then reflected only in males. Taken together, these results suggest that males are more sensitive to changes in ECM composition compared to females and, although, GAG presence did not impact sex-differential responses of VICs, they might be needed to better replicate disease pathology as it occurs in females and males.

Because these were the first experiments of its kind during the time these were conducted, no background on potential sex-dependent VIC behavior in a 3D system were known. Other studies had explored the role of GAGs on collagen background hydrogels

in valvular endothelial cells[8], or GAG enrichment in VICs cultured on hydrogel films[7], however these studies lacked insight on sex-depended responses of VICs. However, upon refining our engineered systems we were able to confirm some of these responses in similar engineered tissue engineered models.

Since, fibrotic marker expression was maintained in our early- and late-stage disease models lacking CS, we wondered whether total collagenous enrichment or collagen fiber architecture played a role in driving a robust fibrotic response since it has been well establish that collagen plays an important role in tissue fibrosis and calcification[4,5]. In order to assess for this, we introduced an additional late model that contained the same fibrillar collagen content as our early-stage model but maintained total collagenous protein concentration as our late model. Results from these experiments were obtained in absence and presence of CS as we were able to observe opposing patterns in presence of CS. Results suggested that increased fibrillar content was not the main driver of fibrotic responses in VICs but rather the increase of total collagenous protein content. These results were consistent regardless the presence or absence of CS in the system.

The research presented in this chapter underscores the critical importance of troubleshooting and meticulously designing 3D engineered systems that accurately mimic the various stages of CAVD. The ability to replicate the complex environment of valve tissues in vitro is essential for gaining deeper insights into the disease's progression and the underlying mechanisms that drive it. By refining these models to more closely mirror the physiological conditions of both early and late stages of CAVD, we can better

understand the interactions between VICs and the extracellular matrix, particularly in the context of sex-specific differences.

The development of these engineered disease-inspired models was met with several experimental limitations that posed significant challenges. These limitations included difficulties in the creation and refinement of the engineered scaffolds, the proper selection of cell phenotypes, the timing of sample collection, and obstacles related to sample processing and assay techniques. Each of these issues had the potential to impact the accuracy and relevance of the models, potentially limiting their ability to replicate the complex environment of disease progression effectively.

Despite these challenges, we implemented a series of strategic approaches to address and overcome these hurdles. The following section provides a detailed overview of the specific issues encountered during the development of these models and the solutions we employed to mitigate them. These efforts were crucial in ensuring that the engineered scaffolds more accurately reflected the physiological conditions of CAVD, thereby enhancing the reliability of our findings and contributing to a deeper understanding of the disease.

3.6 Experimental Challenges and Limitations, and Strategies for Resolution

3.6.1 Control of scaffold stiffness

Initially, to control scaffold stiffness, we combined various batches of GelMa with differing levels of methacrylation substitution. However, this approach proved to be time-consuming and often resulted in significant variability in stiffness between different batches and even between repeats of the same batch. Additionally, factors such as exposure to different temperatures or storage conditions, such as in self-thawing freezers, could alter the mechanical properties of the GelMa stocks. Consequently, this variability affected the final stiffness of the hydrogels, despite precise mixing ratios. To mitigate the degradation of mechanical properties, we stored all GelMa batches at -80°C until they were needed.

In 2020, a study by Young et al.[15] investigated the rheological properties of GelMa hydrogels by examining both physical gelation and chemical crosslinking processes. Leveraging gelatin's natural ability to undergo physical gelation, we modified our approach by incubating hydrogel models for varying periods, ranging from 0 to 20 minutes, at 4°C before initiating crosslinking with UV light. This method enabled us to achieve a range of stiffness values from 2 kPa to 50 kPa, depending on the methacrylation substitution levels of the GelMa batch. This revised technique not only significantly reduced the time required for characterization but also enhanced the consistency of stiffness measurements across different experimental repeats.

3.6.2 Selection of proper cell type phenotype

The results presented in this chapter were derived from screening experiments using a mixed co-culture of quiescent valve interstitial cells (qVICs) and activated valve interstitial cells (aVICs) within our stage-specific hydrogel models. This approach was chosen to more accurately replicate physiological conditions and better understand disease progression. However, reproducibility of these findings proved challenging. To address this issue, we isolated qVICs and aVICs and conducted screening experiments separately on our hydrogel models. To further control for variables, we utilized our collagen protein and fiber enrichment models in the absence of chondroitin sulfate.

Experiments with qVIC cultures showed no significant changes in fibrotic markers. This lack of response may be attributed to the culture conditions, as qVICs can remain in a quiescent state when cultured on collagen substrates[16]. In contrast, experiments with aVIC-only cultures demonstrated a greater sensitivity to extracellular matrix (ECM) changes and, as discussed in Chapters 4 and 5, to pathological stimuli. While aVICs provided a more accurate representation of pathological conditions, it is crucial to further characterize qVICs within disease-relevant tissue engineering models. Understanding their responses to various pathological risk factors is essential for elucidating their role in calcific aortic valve disease (CAVD) progression.

Our experiments as previously mentioned uses cells from prepubescent pigs as their hormone levels mimic those of individuals in their old stages of life. However, we must consider that using these young cells to mimic a disease of the elderly could introduce

some limitations as research on cell-aging have shown that cell function, metabolism, biochemical activity and intracellular communication become altered, thus possibly contributing to differential cell responses[17–21]. Future experiments characterizing cell behavior using VICs young and old individuals could provide us with new insights to better mimic the responses clinically observed in patients that suffer from CAVD.

3.6.3 Sample collection timepoints to detect fibrotic markers at a gene and protein level

As we progressed with more advanced models, we quickly recognized the importance of sample collection timepoints in capturing transient expression of inflammatory and fibrotic markers. Our findings indicated that the optimal timepoint for collecting samples to assess inflammatory and fibrotic gene expression was two days post-seeding. For protein expression analysis, as detailed in Chapters 4 and 5, samples were collected five days post-seeding. However, the data on protein expression was inconclusive, suggesting that the timing for protein sample collection should be revisited.

Additionally, there is a need to refine the sample processing techniques, as discussed in the following section. For future experiments, a longitudinal screening of fibrotic (or calcific) marker expression should be implemented to obtain more accurate insights into the activation mechanisms within valve interstitial cells. This approach will help to better understand the dynamic processes involved in disease progression.

3.6.4 Sample processing for protein quantification

Quantifying protein expression from VICs embedded in these models has proven to be the most challenging task in this research. In Chapters 4 and 5, we assessed nascent protein quantification by incorporating a methionine analog that is integrated during protein synthesis. While this method provided semi-quantitative data on overall protein production, it did not allow for the specific quantification of individual extracellular matrix (ECM) proteins.

Attempts to quantify collagen using known staining techniques such as picrosirius red or imaging methods like CNA35 labeling were not appropriate. These techniques measure the total collagen content, but they do not differentiate between collagen synthesized by the VICs and the collagen provided in the system. Consequently, direct quantification of collagen expression from cell lysates was not feasible. Moreover, commercially available kits designed to detect collagen released into the media were either interfered with by media components or lacked sufficient sensitivity. To overcome these challenges, we quantified collagen in Chapters 4 and 5 by analyzing the sample media using Western blotting.

We also aimed to quantify the expression of regulatory ECM molecules such as matrix metalloproteinases (MMPs). Degrading our hydrogel models using collagenases was not an option due to the need to preserve these molecules. Furthermore, commercially available kits that detect MMPs from media or lysates were incompatible with common buffers like RLT and RIPA. To address this, we mechanically homogenized our samples

in RIPA buffer using 0.5 mm stainless steel beads. However, this method was not entirely successful, as the hydrogels were not fully homogenized. Using specific handheld homogenizers might provide a more effective means of processing hydrogel lysates for protein quantification.

Despite these challenges, we obtained results showing detectable levels of MMPs for protein quantification. Initially, a significant constraint was the inability to use standard protein quantification techniques to determine the protein concentration required for loading into a Western blot gel, due to the protein-based nature of our system. We resolved this issue by quantifying DNA in our lysates and establishing a correlation between detectable DNA (representing 100% cell material) and total cell protein. This approach allowed us to load protein in terms of DNA, enabling precise tuning of lysate sample ratios to detect ECM proteins produced by VICs.

Tuning hydrogel models to accurately mimic disease snapshots is crucial for recapitulating the dynamic and complex processes of pathogenesis as they occur in organisms. By refining these models, researchers can gain deeper insights into disease mechanisms, leading to more effective therapeutic strategies.

3.7 Conclusion

The importance of dissecting variables in disease research cannot be overstated, as it allows for the construction of increasingly complex models. A thorough understanding of how cells interact with each component of the extracellular matrix (ECM) and how they respond to various stimuli is crucial for unraveling the sequence of events and the intricate interactions observed in tissue. By gaining a deeper comprehension of these processes, we can develop models that target specific molecules or pathways, ultimately leading to more effective treatments. Such advancements hold the potential to halt or even reverse the progression of diseases like Calcific Aortic Valve Disease (CAVD). This approach not only enhances our knowledge of disease mechanisms but also paves the way for innovative therapeutic strategies tailored to the complexities of individual pathologies.

3.8 References

1.Nerger BA, Jones TM, Rose KWJ, et al. The matrix in focus: new directions in extracellular matrix research from the 2021 ASMB hybrid meeting. *Biol Open*. 2022;11(1):bio059156. doi:10.1242/bio.059156

2.Wight TN, Potter-Perigo S. The extracellular matrix: an active or passive player in fibrosis? *Am J Physiol - Gastrointest Liver Physiol*. 2011;301(6):G950-G955. doi:10.1152/ajpgi.00132.2011

3.Schroeder ME, Gonzalez Rodriguez A, Speckl KF, et al. Collagen networks within 3D PEG hydrogels support valvular interstitial cell matrix mineralization. *Acta Biomater*. 2021;119:197-210. doi:10.1016/j.actbio.2020.11.012

4.Hutson HN, Marohl T, Anderson M, Eliceiri K, Campagnola P, Masters KS. Calcific Aortic Valve Disease Is Associated with Layer-Specific Alterations in Collagen Architecture. *PLoS ONE*. 2016;11(9):e0163858. doi:10.1371/journal.pone.0163858

5.Hutson HN, Kujawa C, Eliceiri K, Campagnola P, Masters KS. Impact of tissue preservation on collagen fiber architecture. *Biotech Histochem*. 2019;94(2):134-144. doi:10.1080/10520295.2018.1530373

6.Dahal S, Bramsen JA, Alber BR, et al. Chondroitin Sulfate Promotes Interstitial Cell Activation and Calcification in an In Vitro Model of the Aortic Valve. *Cardiovasc Eng Technol*. 2022;13(3):481-494. doi:10.1007/s13239-021-00586-z

7.Porras AM, Westlund JA, Evans AD, Masters KS. Creation of disease-inspired biomaterial environments to mimic pathological events in early calcific aortic valve disease. *Proc Natl Acad Sci U S A*. 2018;115(3):E363-E371. doi:10.1073/pnas.1704637115

8.Dahal S, Huang P, Murray BT, Mahler GJ. Endothelial to mesenchymal transformation is induced by altered extracellular matrix in aortic valve endothelial cells. *J Biomed Mater Res A*. 2017;105(10):2729-2741. doi:10.1002/jbm.a.36133

9.Bramsen JA, Alber BR, Mendoza M, et al. Glycosaminoglycans affect endothelial to mesenchymal transformation, proliferation, and calcification in a 3D model of aortic valve disease. *Front Cardiovasc Med*. 2022;9:975732. doi:10.3389/fcvm.2022.975732

10.Wu S, Li Y, Zhang C, et al. Tri-Layered and Gel-Like Nanofibrous Scaffolds with Anisotropic Features for Engineering Heart Valve Leaflets. *Adv Healthc Mater*. 2022;11(10):e2200053. doi:10.1002/adhm.202200053

11.Stephens EH, Saltarrelli JG, Baggett LS, et al. Differential Proteoglycan and Hyaluronan Distribution in Calcified Aortic Valves. *Cardiovasc Pathol Off J Soc Cardiovasc Pathol*. 2011;20(6):334-342. doi:10.1016/j.carpath.2010.10.002

12.Simon LR, Scott AJ, Figueroa Rios L, Zembles J, Masters KS. Cellular-scale sex differences in extracellular matrix remodeling by valvular interstitial cells. *Heart Vessels*. 2023;38(1):122-130. doi:10.1007/s00380-022-02164-2

13.Berger AJ, Linsmeier KM, Kreeger PK, Masters KS. Decoupling the effects of stiffness and fiber density on cellular behaviors via an interpenetrating network of gelatin-methacrylate and collagen. *Biomaterials*. 2017;141:125-135. doi:10.1016/j.biomaterials.2017.06.039

14.Bian W, Wang Z, Sun C, Zhang DM. Pathogenesis and Molecular Immune Mechanism of Calcified Aortic Valve Disease. *Front Cardiovasc Med*. 2021;8:765419. doi:10.3389/fcvm.2021.765419

15.Young AT, White OC, Daniele MA. Rheological Properties of Coordinated Physical Gelation and Chemical Crosslinking in Gelatin Methacryloyl (GelMA) Hydrogels. *Macromol Biosci*. 2020;20(12):2000183. doi:10.1002/mabi.202000183

16.Porras AM, van Engeland NCA, Marchbanks E, et al. Robust Generation of Quiescent Porcine Valvular Interstitial Cell Cultures. *J Am Heart Assoc*. 2017;6(3):e005041. doi:10.1161/JAHA.116.005041

17.Bashey RI, Torii S, Angrist A. Age-related collagen and elastin content of human heart valves. *J Gerontol*. 1967;22(2):203-208. doi:10.1093/geronj/22.2.203

18.Mas-Bargues C, Sanz-Ros J, Huete-Acevedo J, Borrás C. Cell-to-Cell Communication in Aging: Mechanisms, Impact and Therapeutic Prospects. In: Bueno V, ed. *Cellular and Molecular Aspects of Ageing*. Springer Nature Switzerland; 2024:87-122. doi:10.1007/978-3-031-55022-5_8

19.Spadaccio C, Mozetic P, Nappi F, et al. Cells and extracellular matrix interplay in cardiac valve disease: because age matters. *Basic Res Cardiol*. 2016;111(2):16. doi:10.1007/s00395-016-0534-9

20.Flint B, Tadi P. Physiology, Aging. In: *StatPearls*. StatPearls Publishing; 2024. Accessed August 18, 2024. http://www.ncbi.nlm.nih.gov/books/NBK556106/

21.Crane MM, Kaeberlein M. The paths of mortality: How understanding the biology of aging can help explain systems behavior of single cells. *Curr Opin Syst Biol*. 2018;8:25-31. doi:10.1016/j.coisb.2017.11.010

Chapter 4: Creation of stage-specific disease models to elucidate sex differences in aortic valve fibrosis.

4.1 Abstract

Calcific aortic valve disease (CAVD) is characterized by two primary hallmarks: valve fibrosis and calcification[1,2], which result from an imbalance between extracellular matrix (ECM) production and degradation. This study aims to elucidate how ECM composition influences sex- and stage-specific responses in valvular interstitial cells (VICs). To this end, 3D engineered models were developed to mimic collagen enrichment observed during the progression from early to late stages of the disease. Notably, CAVD exhibits sexual dimorphism[3–9], with female patients more frequently presenting with highly fibrotic valves and male patients with highly calcific valves. The mechanisms underlying these distinct clinical outcomes remain poorly understood.

Changes in ECM composition has been highlighted as key drivers of CAVD fibrosis in the literature. By culturing female and male VICs in these 3D scaffolds, the study assessed sex- and stage-related fibrotic responses. Modulation of collagen enrichment resulted in sex-specific responses: females displayed higher inflammatory profiles, while males exhibited stronger fibrotic marker expression. Additionally, stage-specific responses were observed between the early and late stages in males' fibrotic responses, noted by an increase in ECM gene and protein expression.

To understand how pathological responses affect VIC fibrotic responses at different stages of disease, VICs were treated with TGFB-1, a known pro-fibrotic factor. The

responses to TGFB-1 were as follows: in females, exposure to TGFB-1 suppressed the production of inflammatory cytokines, while cytokine expression in males remained unchanged. Both females and males exhibited increased gene expression of fibrotic factors in the late-stage model. However, females appeared more sensitive to TGFB-1 treatment, as indicated by a higher fold increase in gene expression compared to males. TGFB-1 treatment stimulated nascent protein production in females, whereas in males, it decreased nascent protein production towards the late stage. These findings underscore the importance to include sex as a biological variable to study disease progression and highlight the need for the utilization of disease-inspired tissue engineered scaffolds to better understand the relationships between cells and ECM interactions in more physiologically relevant environments.

4.2 Introduction

Calcific aortic valve disease (CAVD) is one of the main causes of morbidity in individuals over the age of 65. It is a progressive disorder characterized by the thickening (sclerosis) and calcification (stenosis) of the aortic valve[5], which leads to impaired valve function and can result in death. Unfortunately, effective treatments have not been developed to date, and valve replacement remains the primary course of treatment.

Several studies have shown that clinical outcomes for the same degree of valve stenosis vary in accordance with biological sex[2,3,5,6,10]. Specifically, females are known to present with highly fibrotic valves, while males tend to have highly calcified valves[1]. To understand the events leading to these clinical presentations, we must delve into the mechanisms of disease etiology and progression and how these differentially affect females and males. One of the main limitations in understanding at which point pathological presentation diverges is the inaccessibility to obtain specimens that provide sequential snapshots of disease progression[11,12]. Additionally, we must recognize that CAVD is a fibrocalcific disorder resulting from complex interactions between valvular interstitial cells (VICs) and their continuous attempts to repair the injured valve.

The healthy aortic valve has three main layers: the fibrosa, spongiosa, and ventricularis, each with its own distinct extracellular matrix (ECM) composition and function. Located on the aortic side, the fibrosa is mainly composed of collagen, which provides mechanical and structural support to the valve[13]. Next to the fibrosa, the spongiosa, mostly composed of proteoglycans, provides the valve with mechanical compliance and lubricity. Lastly,

located on the ventricular side, the ventricularis offers the valve tissue elasticity. VICs populate the valve leaflet and are responsible for maintaining valve homeostasis by regulating cell-to-cell signaling and the extracellular environment.[14]

During disease, quiescent VICs (qVICs) become activated (aVICs) and adopt a myofibroblastic phenotype, leading to maladaptive behaviors that promote fibrosis[14]. Alterations in the ECM related to collagen composition, architecture, and distribution have been identified as significant events in valve fibrosis. Studies by our lab have demonstrated that CAVD progression is accompanied by changes in collagen content and architecture[13]. During disease, collagen has been found to be deposited throughout the valve, with enrichment increasing up to twofold in the spongiosa layer. Collagen deposition in the valve is also known to serve as calcification nucleation sites, thus promoting disease progression[15]. Additionally, several studies have highlighted the role of collagen in modulating cellular behavior.[16–18]

3D tissue-engineered scaffolds provide us with opportunities that traditional culture methods lack. By using 3D tissue-engineered culture platforms, we can develop complex systems that allow cells to interact with their environment as they would in vivo. In this work, we created disease-inspired 3D early- and late-stage models that mimic collagen enrichment observed during disease progression to study sex- and stage-specific responses to changes in ECM composition. We then used these models to understand how exposure to a pathological stimulus altered VICs' fibrotic responses at each stage of the disease.

4.3 Methods

4.3.1 VIC isolation and expansion

Valvular interstitial cells (VICS) were isolated, expanded and maintained in culture as previously described[5]. Briefly, aortic valve leaflets were excised from 6-month-old pig hearts obtained from our local abattoir (Hoesly's Meats, New Glarus, WI) and incubated for 30 minutes in a collagenase II (Worthington Biochemical Corporation, Lakewood, NJ) solution to remove valvular endothelial cells from the tissue. A second 60-minute incubation followed, in fresh collagenase II solution to release VICS for expansion. VICs were then maintained in low glucose Dulbecco's Modified Eagle's Medium (Sigma-Aldrich, St. Louis, MO), supplemented with 2 mM L-glut (Sigma Aldrich), 150 U/mL penicillin/streptomycin (Sigma-Aldrich) and 10% fetal bovine serum (FBS) (Corning, Corning, NY) at 37 °C and 5% CO_2 until they reached passages 2-3. VICs were not used past passage 3 for any of the experiments.

4.3.2 GelMA Synthesis

Gelatin type A from porcine skin (Sigma Aldrich) was dissolved at 10% w/v in phosphate-buffered saline (1X PBS) (Corning, Corning, NY) at 50 °C. Once the gelatin was dissolved, methacrylic anhydride (MA) (Sigma Aldrich) was added to the gelatin solution with a syringe in a drop-wise manner and stirred overnight protected from light. The following day, the gelatin-methacrylate (GelMA) reaction solution was centrifuged at 3000 xg for 5 minutes at 37 °C degrees to precipitate unreacted MA. The supernatant was collected and diluted at a 1:4 ratio in pre-warmed 1X PBS at 50 °C and then transferred

to 12-14 kDa MWCO dialysis tubing (Spectrum Labs, Rancho Dominguez, CA). The diluted GelMA solution was dialyzed against 1X PBS for 3 days and diH_20 for 3 more days at 50 °C to remove any unreacted MA. PBS and DiH_2O solutions were changed daily through the dialysis process. At the end of the dialysis period, the GelMa solution was filtered, lyophilized and stored at -80 °C until needed for further characterization and use[19].

4.3.3 Creating engineered valve models of early and late stages of disease

3-D disease-inspired scaffolds were developed to mimic collagen enrichment as a hallmark of CAVD. All models were created using a GelMA (Gelatin Methacrylate) based hydrogel (4% w/v) with an interpenetrating network of collagen fibers[19]. Scaffolds mimicking early-stage disease contained 0.75 mg/mL collagen I (Col1) (Advanced Biomatrix, San Diego, CA), while late-stage disease scaffolds contained 1.5 mg/mL Col1. To neutralize the collagen added to our GelMa-Coll pre-polymer solutions, 0.1 M NaOH (RPI, Mt. Prospect, IL) and 10x DPBS (Sigma Aldrich) were added at their appropriate ratios. Female and male VICs were also added independently at a concentration of 4 x 10^6 cells/mL to the pre-polymer solution along with photoinitiator lithium-phenyl-2,4,6-trimethylbenzoylphosphinate (LAP) (Sigma Aldrich) at a final concentration of 0.05% w/v. 100 ul of the pre-polymer solution was added to silicone molds (9 mm diameter x 1.7 mm depth) and incubated at 37 °C for 30 minutes to allow for collagen fibrillogenesis. The molds were then incubated at 4 °C for the amount of time previously optimized via dynamic mechanical analysis[19] to reach a Young's modulus of 5-8 kPa and subsequently photocrosslinked under UV light (365 nm) for 6 minutes.

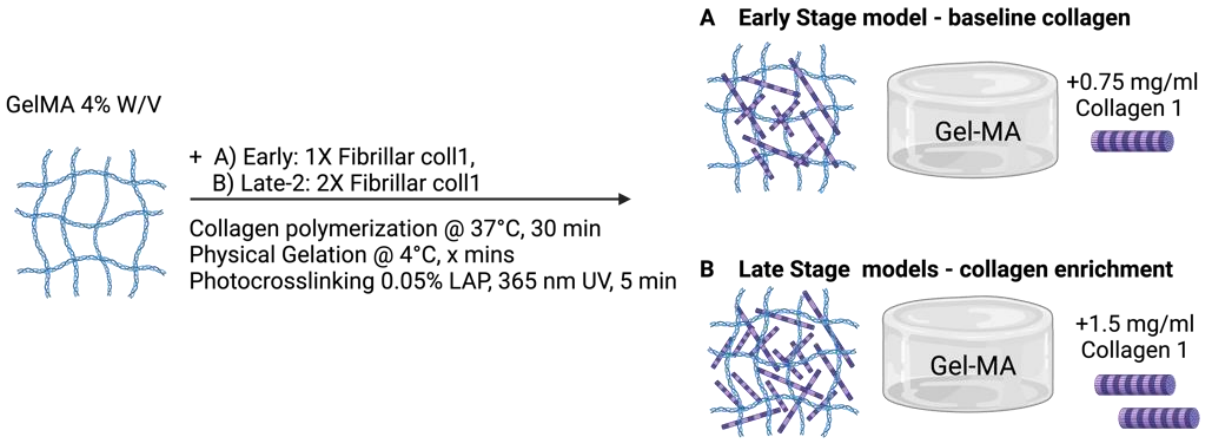

Figure 4.1 Schematic representation of the fabrication of a) early- and b) late-stage specific hydrogel models.

4.3.4 VIC culture in 3D early and late-stage hydrogel models

Early and late-stage models containing female or male VICs as described above (day 0) were cultured for a total of 6 days in low glucose DMEM, supplemented with 2 mM L-glut, 150 U/mL, penicillin/streptomycin and 10% FBS. Fresh media was provided every other day (days 1 and 3; 24 hrs and 72 hours post seeding respectively). In order to determine whether ECM composition affects cellular responsiveness to a pathological stimulus, early- and late-stage disease models were treated with TGFB-1(5 ng/mL) (Peprotech) on days 1 and 3. Media samples were collected on days 3 for inflammatory cytokines (Il-6 and IL-8) and days 3 and 5 for soluble collagen (Collagen-1) quantification. Hydrogel lysates were collected at day 2 for quantification of gene expression (*aSMA, COL1A1, FN, TGFB-1 and CHYSY1*) and at day 5 for protein quantification (FN1, MMP-1 and MMP-9). In addition, a whole hydrogel set was collected on day 5 for nascent protein quantification.

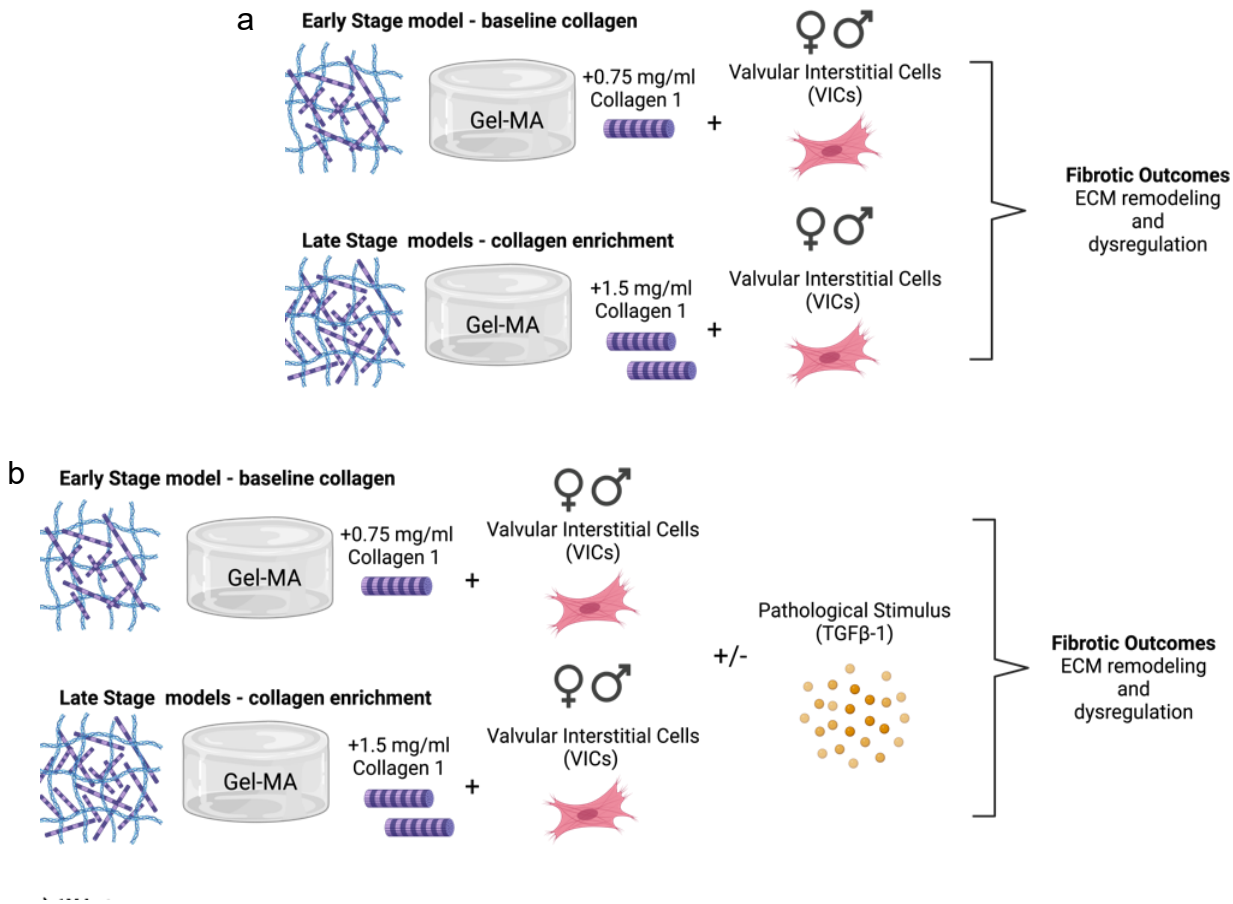

Figure 4.2 Schematic representation of methods. a) Experimental design proposed to understand the effects on VIC fibrotic outcomes stemming from changes in the ECM environment during CAVD progression focused on collagen enrichment as observed during the early and late stages of disease. b) Experimental designed proposed to explore the combinatorial effects of ECM changes in the presence of a pathological stimulus in female and male VICs fibrotic outcomes.

4.3.5 Visualization and quantification of nascent protein produced by VICs

In order to visualize nascent protein deposition by female and male VICs embedded in 3D early- and late- stage models, an adaptation of a previously published technique was followed[20]. Early- and late-stage models were cultured in nascent protein media (high glucose DMEM, no methionine, no cystine) supplemented with 2 mM L-glut, 150 U/mL penicillin/streptomycin, 10% FBS, 100 µg/mL sodium pyruvate, 0.201 mM cystine, 100

μg/mL, 50 μg/mL ascorbate 2-phosphate, and 0.1 mM azidohomoalanine AHA. The media was changed every other day as described above (days 1, 3). On day 5, all hydrogel models were washed in 1% BSA followed by a 40 min incubation in 30 μM DBCO-488[20]. The DBCO-488 undergoes a bio-orthogonal strain-promoted cyclo-addition that allows visualization of all new synthesized protein produced by the VICs. After the incubation period, all hydrogels were washed once again prior to a 30 min incubation in 10% formalin. Once all cells were fixed within the hydrogels, the excess formalin was washed away, and samples were stored in 1X PBS until imaging. All nascent protein imaging was performed on a Nikon AXR Confocal Microscope and image analysis was done on FIJI.

4.3.6 Detection of fibrotic markers via gene expression quantification

All early and late-stage hydrogel models' samples were collected on day 2 (48 hrs post seeding) digested in a collagenase (4.2 mg/mL) digestion solution supplemented with 30% v/v Proteinase K (Qiagen, Hilden, Germany), 50% v/v 10X Trypsin (Gibco, Grand Island, NY) and 20% v/v 1X PBS to facilitate RNA isolation. RNA isolation was performed according to the manufacturer's instruction for Qiagen's RNeasy kit (Qiagen, Germantown, MD). Retrieved RNA was then subjected to reverse transcription using a High-Capacity cDNA Reverse Transcription kit (Applied Biosystems, Foster City, CA). Taqman Gene Expression Assays were used to quantify genetic expression profiles of fibrosis-related genes (*aSMA, COL1A1, FN, TGFB-1 and CHYSY1*) (Thermo Fisher). All PCR reactions were performed in a Biorad CXF Opus 96 Real Time PCR and analyzed via the delta-delta ct method.

4.3.7 Detection of fibrotic markers via protein quantification

For FN1, MMP-1 and MMP-9 protein quantification assays, early- and late-stage hydrogel model samples were collected at day 5. FN1 production in female and male VICs cultured in 3D early- and late-stage models was evaluated via R&D DuoSet ELISA following the manufacturer's instructions. Quantified FN1 levels were normalized to total DNA via picogreen. Quantification of MMP-1 and MMP-9 was determined via Western blot. Lysate samples collected on day 5 were blended in RIPA lysis and extraction buffer (Thermo Fisher) supplemented with 1 mM phenylmethylsulfonyl fluoride (PMSF) and 2 mg/mL protease inhibitor (Thermo Fisher, Rockford, IL) on a tissue homogenizer (Next Advance) with .5 mm stainless steel beads (Next Advance) for 10-15 minutes at medium speed. Due to the protein nature of these hydrogel models, DNA quantification was performed in these lysates to determine how much protein corresponded to the VICs embedded in our models. A DNA-to-protein ratio was calculated to immunoprecipitate our proteins of interest. Immunoprecipitation of MMP-1 and MMP-9 was performed using a Dynabeads Protein g Immunoprecipitation Kit (Thermo Fisher). An MMP-1 and MMP-9 antibody (ab) dilution was used to immunoprecipitate a total of 0.5 ug of protein. Upon immunoprecipitation, samples were incubated at 70 °C for 10 min and followed a standard western blot procedure. Briefly, 0.045 ug of sample was loaded and run in a 15-well Invitrogen wedgewell Tris–Glycine Mini Gels (Thermo Fisher) for 1 h at 120 V. Proteins of interest were then transferred to an Immun-Blot PVDF membrane (Bio-Rad) at 30 V for 1 hr. Once the proteins had been transferred, a 1 hr blot incubation in 5% w/v solution of nonfat dried milk diluted in .1% PBST followed to avoid non-specific binding. A primary MMP-1 or MMP-9 ab (1:1000) solution to the blot and incubated overnight at 4 °C. All

membranes were washed the next day in .1% PBST prior to the addition of the HRP secondary goat-anti Rabbit ab (1:10,000) (Thermo Fisher) and then incubated for 1 h. Subsequently, the blots were washed once again in a .1% PBST solution. Cumulative collagen-1 quantification was also assessed via western blot from pooled media from days 3 and 5. The collagen blot was incubated for 1 hr in collagen-1 primary ab (1:1000) followed by addition of the HRP secondary goat-anti Rabbit ab (1:10,000) and .1% PBST washes as described above. Protein expression levels were detected via ChemiDoc MP Imaging System (Bio-Rad) upon exposure to clarity western ECL substrate (Bio-Rad) and quantified on FIJI.

4.3.8 Detection of inflammatory cytokines

Production of inflammatory cytokines, IL6 and IL8 from media samples was evaluated via R&D DuoSet ELISA following the manufacturer's instructions. Total cytokine levels were quantified via four parameter logistic regression.

4.3.9 Statistical Analysis

Each experiment was performed using a n=3 sample. Specifically, VICs isolated from 3 different pigs were pooled for each sex. Data points as seen in each graph represent a sample repeat of this pooled set. Additional experiments performed to validate our results used a new set of pigs. Statistical analysis was performed via 2-way Anova with Tukey Post-Hoc test. Statistical Significance was considered for all comparisons with $P < 0.05$.

4.4 Results

4.4.1 Inflammation of VICs is sex- and stage- dependent

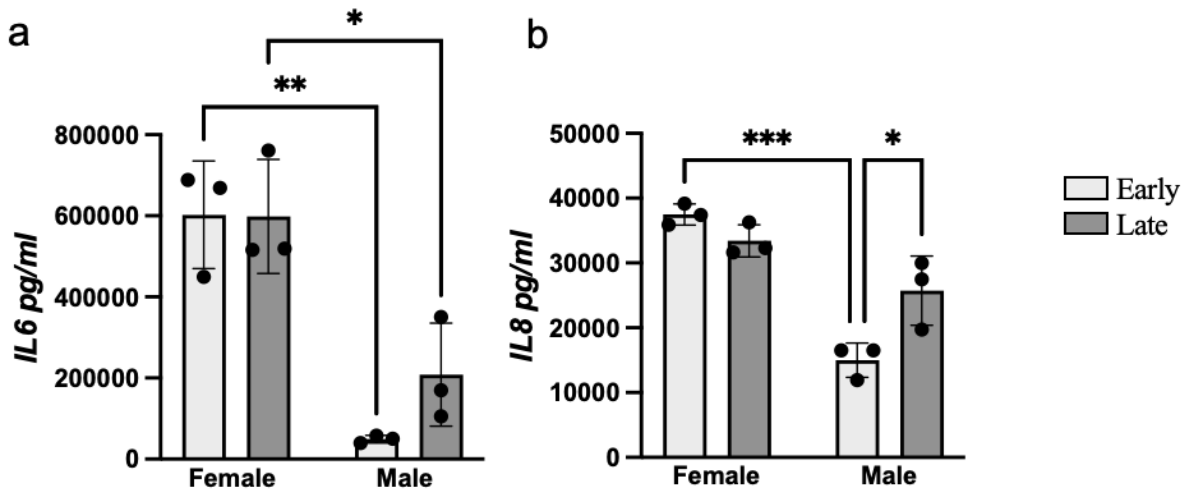

Figure 4.3 Impact of collagen enrichment on inflammatory cytokine production in female and male VICs cultured in early and late-stage disease-inspired models. Cytokine expression of a) IL6 and b) IL8 was measured 2 days post seeding via ELISA. Results are presented as mean ± standard deviation; *indicates $P < 0.05$ by Tukey Post-hoc test.

The production of inflammatory cytokines IL6 and IL8 in female and male VICs, cultured in early- and late-stage models, was assessed using ELISA. Stage-specific responses were observed in IL8 production for males, with those in the late-stage model showing increased IL8 production compared to those in the early-stage model (Figure 4.3, b). Although not statistically significant, a similar trend was noted in IL6 production (Figure 4.3, a). No stage-specific differences in IL6 or IL8 production were found in females. However, sex-dependent responses were observed in IL6 production at both disease stages (Figure 4.3, a) and in IL8 production at the early disease stage (Figure 4.3, b). Notably, females exhibited a higher inflammatory profile, with more than a two-fold increase in IL6 and IL8 production compared to males.

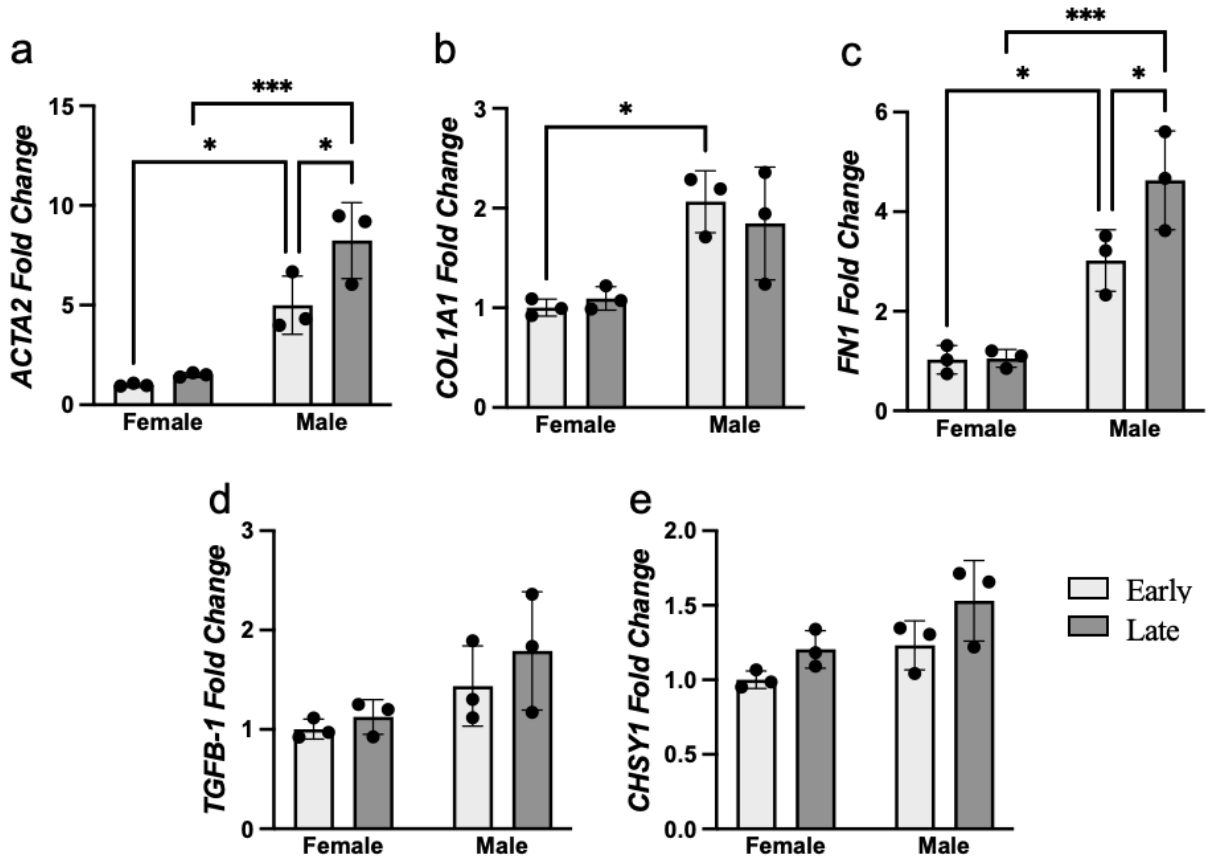

Figure 4.4 Fibrotic gene expression of female and male VICs cultured in early- and late-stage models shows a sex-dependent response. Gene expression of fibrotic markers (a) ACTA2, b) COL1A1, c) FN1, d) TGFB-1, e) CHSY1) was assessed by RT-qPCR and normalized to female early. Results are presented as mean ± standard deviation; *indicates $P < 0.05$ by Tukey Post-hoc test.

4.4.2 Biological sex affects gene expression profiles of CAVD fibrotic markers

Gene expression of known fibrotic markers involved in CAVD development was assessed via RT-qPCR and normalized to our female early-stage condition. The expression of ACTA2 and FN1 (Figure 4.4, a and c) was significantly higher in males compared to females at both stages of the disease. Stage-specific differences were observed only in males at the late stage of the disease, with increased expression of ACTA2 and FN1 (Figure 4.4, a and c). Males also exhibited increased fibrotic expression of COL1A1 (Figure 4.4, b) compared to females, but only in the early-stage models. Although not

statistically significant, a similar trend was observed at the late stage for COL1A1, TGFB-1, and CHSY1 (Figure 4.4, b, d, and e). The expression of these genes remained relatively unchanged between disease stage models for both sexes.

4.4.3 Production of ECM and ECM regulatory proteins

Nascent protein production was measured using fluorescent imaging of DBCO-488 labeled proteins. Briefly, a methionine analog was added to the culture media, allowing nascent proteins to incorporate it during their synthesis. DBCO-488 then undergoes a bio-orthogonal cyclo-addition, enabling imaging of newly synthesized proteins. Stage-specific differences were observed in male VICs, with increased signal intensity at the late-stage model indicating higher protein production at this stage of the disease compared to the early stage (Figure 4.5, a and b). Sex-specific differences were also noted between males and females at the late stage of the disease (Figure 4.5, a and b). FN1 quantification was performed via ELISA, while the expression of Collagen 1 and ECM regulatory proteins such as MMP-1 and MMP-9 was assessed by Western blot (Figure 4.5, c, d, e, and f). No significant trends or differences were observed within or between sexes or disease stages, which may be due to limitations in sample source and the availability of compatible techniques for quantifying these proteins using the current hydrogel model setup.

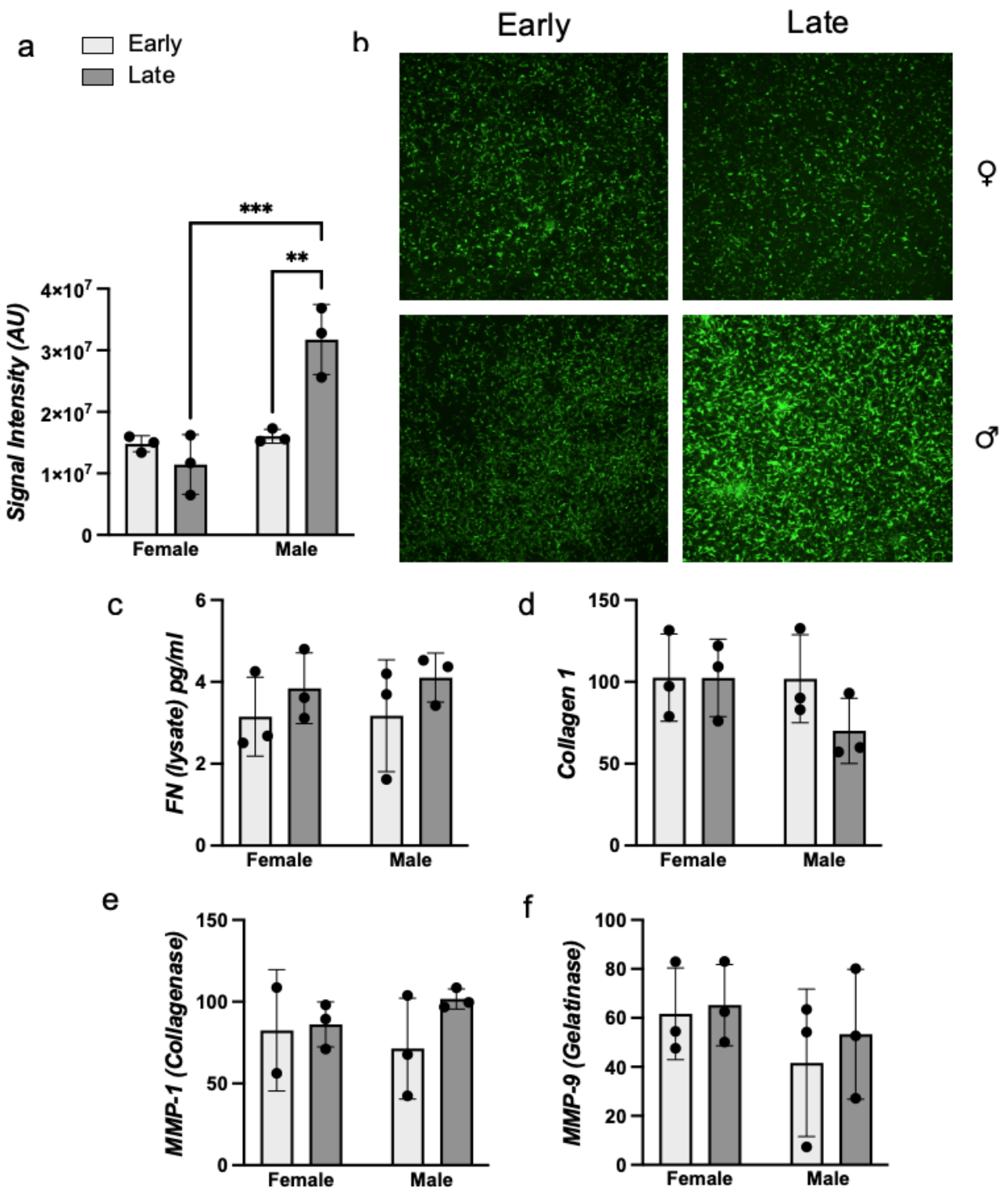

Figure 4.5 ECM- and ECM regulatory proteins expression of female and male VICs cultured in early- and late-stage models. a) Quantification and b) visualization of newly synthesized extracellular proteins. Newly synthesized proteins incorporated AHA, a methionine homolog that allows visualization via DBCO-488 bio-orthogonal cyclo-addition; Quantification of c) Collagen 1 and d) FN1 extracellular matrix production and ECM regulatory proteins e) MMP-1 and f) MMP-9 via Western Blot. Results are presented as mean ± standard deviation; *indicates $P < 0.05$ by Tukey Post-hoc test.

4.4.4 Changes to the ECM composition and pathological stimulus exposure further advances the fibrotic process

To understand how pathological responses affect VIC fibrotic responses at different stages of disease, VICs were treated with TGFB-1, a known pro-fibrotic factor. In the presence of TGFB-1, male VICs showed stage-specific differences at the early stage of disease, particularly in IL8 production (Figure 4.6, d). Interestingly, female VICs cultured in both early- and late-stage models exhibited a significant decrease in IL6 cytokine production (Figure 4.6, a), and although not statistically significant, a similar trend was observed for IL8 (Figure 4.6, b). Cytokine levels in females treated with TGFB-1 were comparable to those in males exposed to the same treatment.

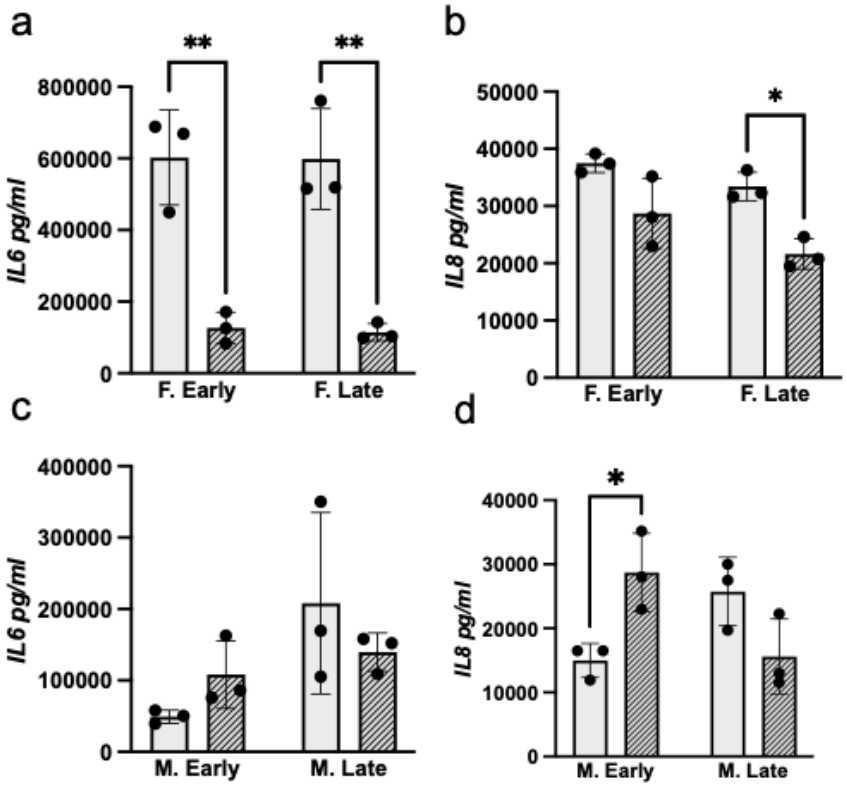

Figure 4.6 Impact of ECM composition and presence of TGFB-1 as a pathological stimulus on inflammatory cytokine production in female and male VICs cultured in early and late-stage disease-inspired models. Cytokine expression of a) IL6 and b) IL8 was measured 2 days post seeding via ELISA. Results are presented as mean ± standard deviation; *indicates $P < 0.05$ by Tukey Post-hoc test.

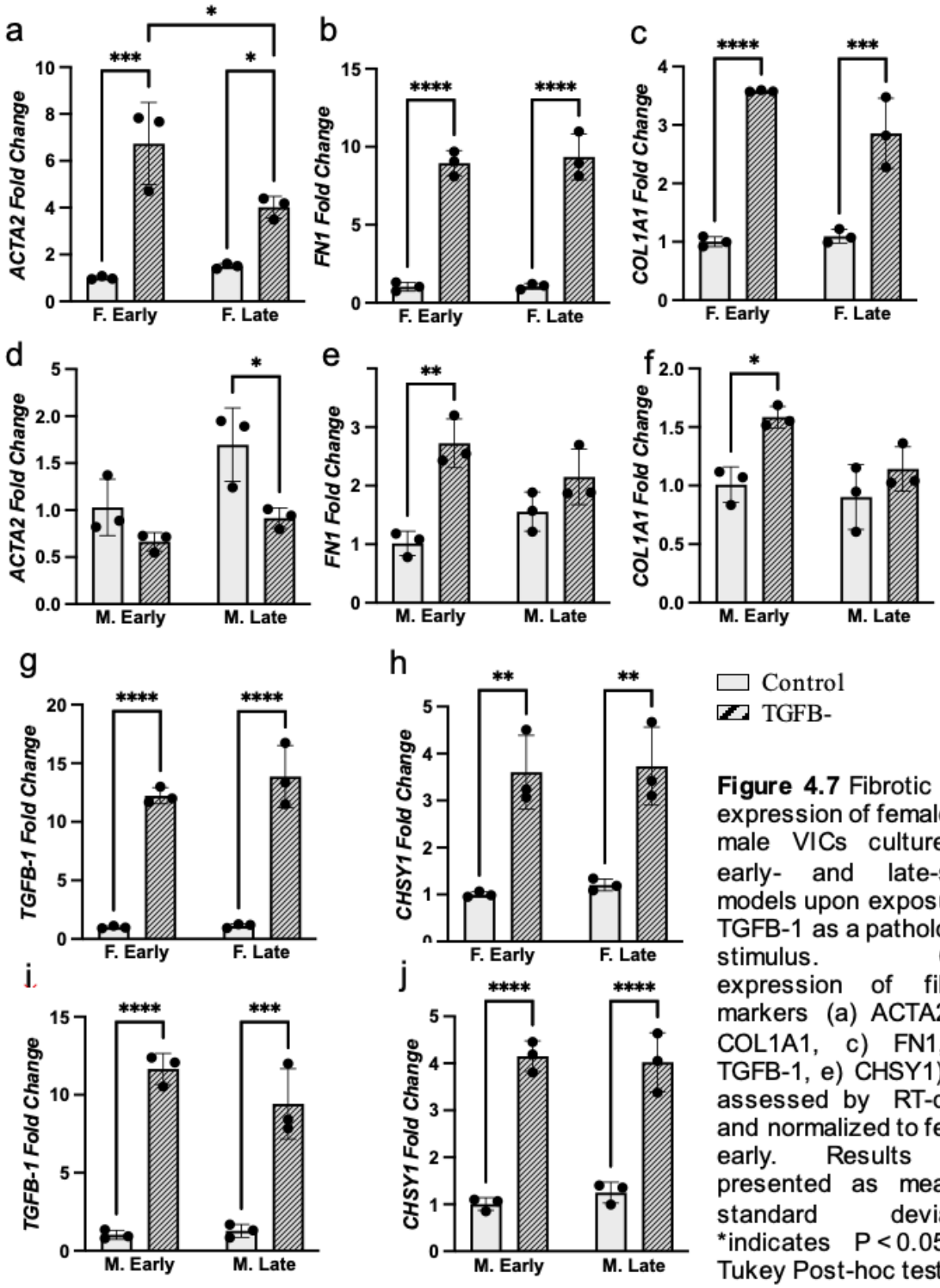

Figure 4.7 Fibrotic gene expression of female and male VICs cultured in early- and late-stage models upon exposure to TGFB-1 as a pathological stimulus. Gene expression of fibrotic markers (a) ACTA2, b) COL1A1, c) FN1, d) TGFB-1, e) CHSY1) was assessed by RT-qPCR and normalized to female early. Results are presented as mean ± standard deviation; *indicates $P < 0.05$ by Tukey Post-hoc test.

Gene expression of fibrosis-related markers was also assessed to understand the effects of ECM changes combined with pathological stimulus exposure. TGFB-1 exposure exacerbated fibrotic responses in females at both disease stages, with increased expression of ACTA2, COL1A1, FN1, TGFB-1, and CHSY1 (Figure 4.7, a-c; g-h). Similarly, males showed an exacerbated fibrotic response for COL1A1 and FN1 (Figure 4.7 e and f), but only at the early stage. Expression of TGFB-1 and CHSY1 (Figure 4.7, i and j) was upregulated only at the late stage. Interestingly, ACTA2 (Figure 4.7, d) expression generally decreased, with statistical significance observed only at the late stage of disease. Additionally, females demonstrated greater sensitivity to TGFB-1 treatment compared to males, with a more pronounced increase in fold expression.

As previously described, ECM and ECM regulatory protein production were assessed using DBCO-488 staining, ELISA, and Western blot. Nascent protein expression increased in females upon exposure to TGFB-1 (Figure 4.8, a, a and b); however, this increase was not statistically significant. ECM proteins (FN1 and Collagen 1) (Figure 4.8, a c and d) and ECM regulatory proteins (MMP1 and MMP9) (Figure 4.8, a e and f) remained unchanged in female VICs at either stage of disease, in both control and treated groups.

In males, nascent protein expression increased in the control group at the late stage. Upon exposure to TGFB-1, nascent protein production also increased in VICs seeded in the early-stage model, but significant protein downregulation was observed at the late stage following treatment (Figure 4.8, b, a and b). ECM proteins (FN1 and Collagen 1)

(Figure 4.8, b, c and d) and ECM regulatory proteins (MMP1 and MMP9) (Figure 4.8, b, e and f) were not altered in male VICs at either stage of disease, in both control and treated groups.

Undetectable differences in female and male VICs cultured in early- and late-stage models exposed to TGFB-1 as a pathological stimulus may be due to limitations in sample source and the availability of compatible techniques for quantifying these proteins using the current hydrogel model setup.

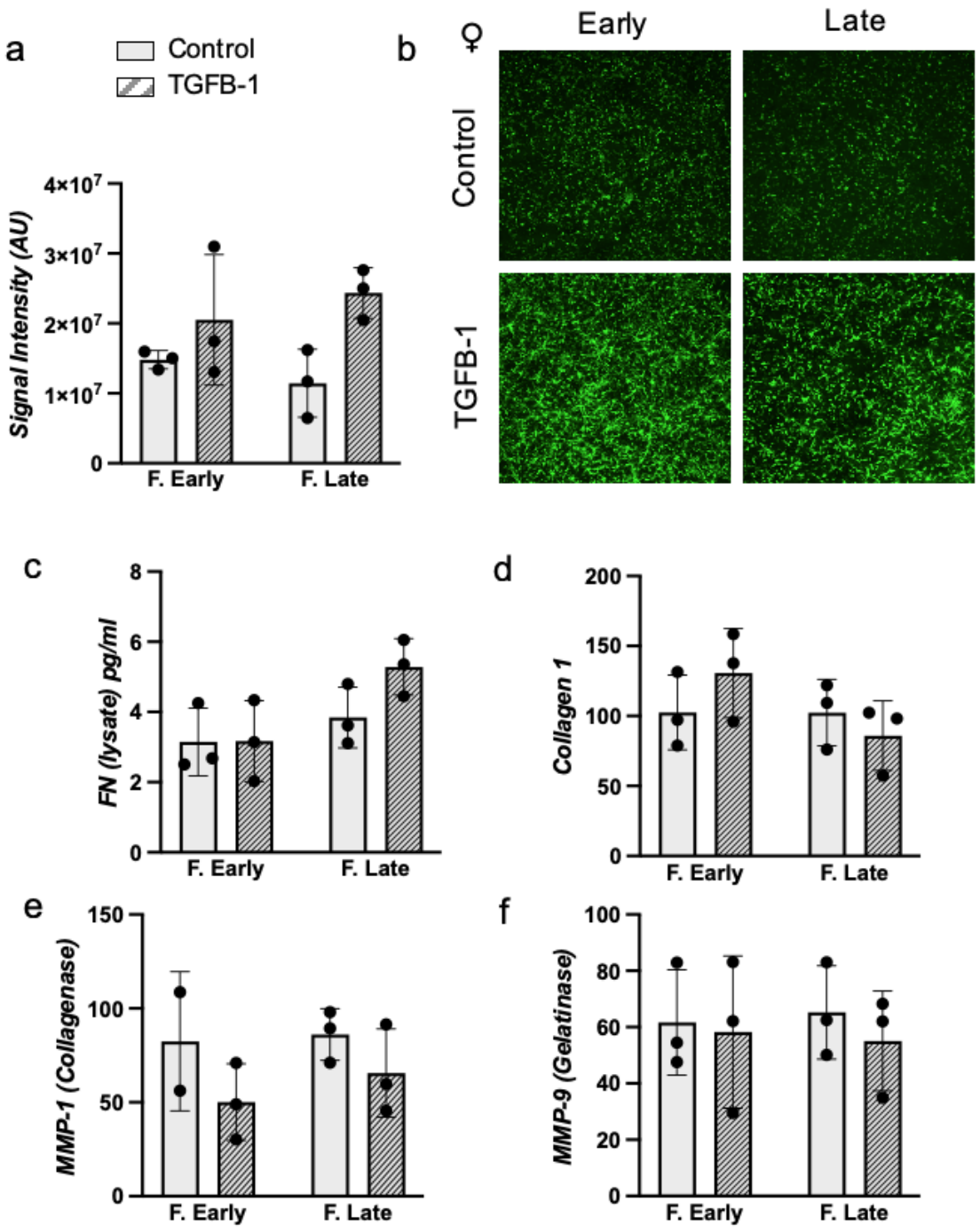

Figure 4.8.a ECM- and ECM regulatory proteins expression of female VICs cultured in early- and late-stage models and upon exposure to TGFB-1. a) Quantification and b) visualization of newly synthesized extracellular proteins via DBCO-488 staining. Quantification of c) Collagen 1 and d) FN1 extracellular matrix production and ECM regulatory proteins e) MMP-1 and f) MMP-9 via Western Blot. Results are presented as mean ± standard deviation; *indicates $P < 0.05$ by Tukey Post-hoc test.

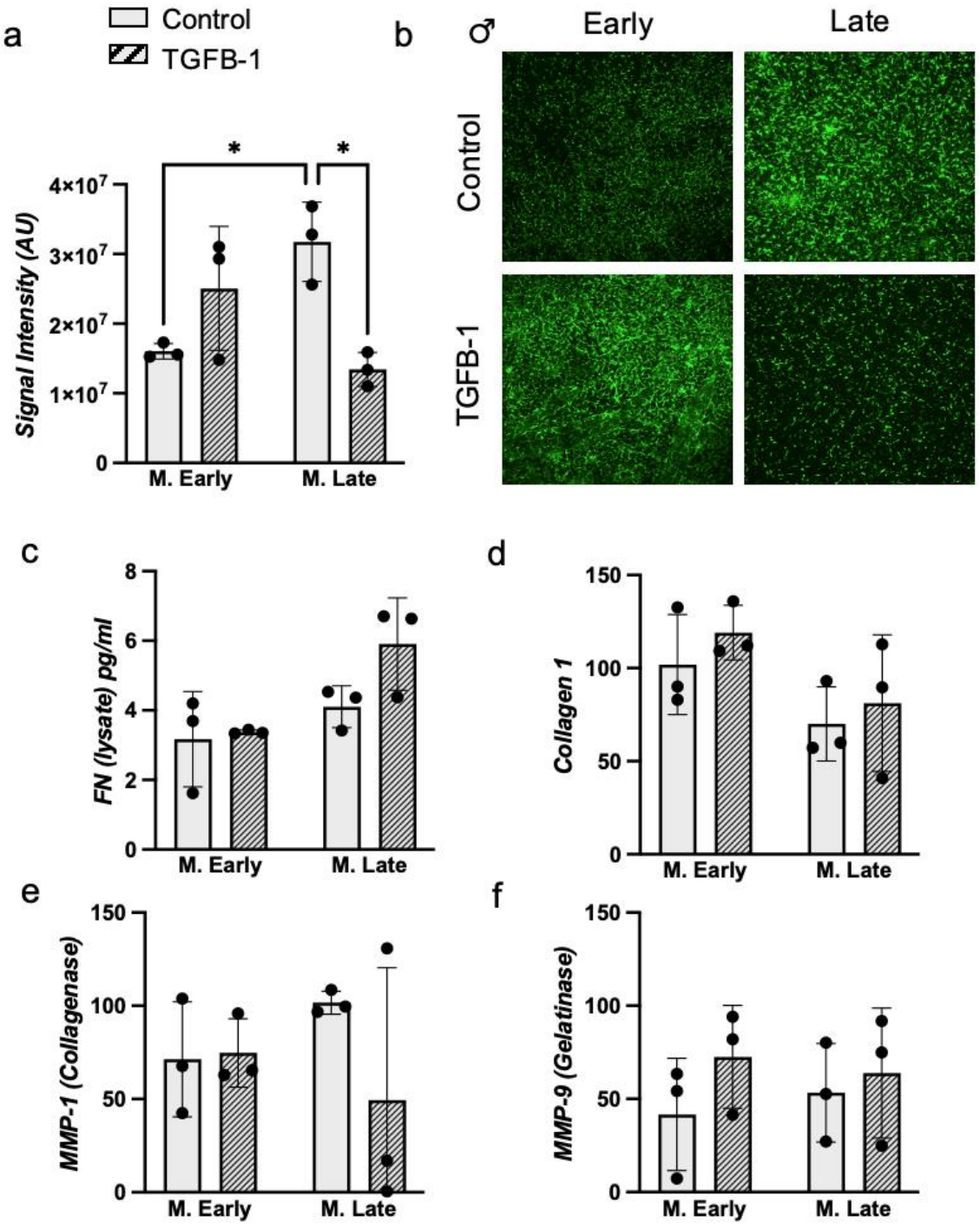

Figure 4.8.b ECM- and ECM regulatory proteins expression of male VICs cultured in early- and late-stage models and upon exposure to TGFB-1. a) Quantification and b) visualization of newly synthesized extracellular proteins via DBCO-488 staining. Quantification of c) Collagen 1 and d) FN1 extracellular matrix production and ECM regulatory proteins e) MMP-1 and f) MMP-9 via Western Blot. Results are presented as mean ± standard deviation; *indicates $P < 0.05$ by Tukey Post-hoc test.

4.5 Discussion

In this chapter, we investigated the effects of collagen enrichment in driving sex- and stage-dependent fibrotic responses in VICs. Sexual dimorphism in CAVD has been identified, with females and males presenting different clinical outcomes for the same degree of valve stenosis[1]. As mentioned frequently throughout this text, CAVD is a complex pathology involving many mechanisms that collectively contribute to valvular degeneration. Chronic inflammation is present during all stages of the disease. Cytokines, chemokines, growth factors, and cathepsins released by inflammatory cells contribute to VIC activation[21].Activated VICs adopt a myofibroblast phenotype, continuously attempting to correct perceived valve injury by producing and remodeling the valve ECM, a process known as fibrosis. This maladaptive remodeling results in disorganized deposition of ECM molecules, which destroys the valve's trilaminar structure and affects valvular function. In this chapter, we examined inflammatory markers linked to valve fibrosis and calcification[22,23].

A 2D study by our lab investigated cellular-scale differences in porcine VICs gene expression profiles of pathological markers associated with specific events in CAVD. Gene expression of IL6 was found to be upregulated in males compared to females, suggesting that males are more likely to undergo an interleukin-mediated inflammatory process impacting other cellular functions affected during the disease[24]. However, research directed towards understanding the differential inflammation profiles in females and males, and how these differences affect other processes of disease progression at a protein level, has not been addressed.

Our study looked at IL6 and IL8 expression in female and male VICs cultured in 3D systems that mimicked changes in ECM composition observed during disease progression. We found that IL6 and IL8 cytokine levels were significantly increased in females compared to males at both stages (early and late for IL6; early for IL8)(Figure 4.3, a and b). In this work, cytokine upregulation in females compared to males could result from VIC-ECM interactions in a model that more accurately replicates in vivo architecture and/or the fact that females experience changes inflammatory profiles at different timepoints of their lives. It is well known that females undergoing menopause have a raise in the expression of inflammatory cytokines[25]. In this study we used pre-pubescent pigs which levels of estrogen mimic those of females undergoing menopause as they have not reached puberty. This could explain our observed increase in IL6 and IL8 in females compared to males. Additionally, this response could be a result of an interplay between the lack of cardio protective hormones and the cell-ECM interactions in these disease models. 3D biomimetic systems provide opportunities to better understand cell behavior and responses.

As previously mentioned, fibrosis occurs as a consequence of chronic inflammation and VIC activation. Given the difference in clinical outcomes observed, it is crucial to examine fibrotic markers to understand at which point in disease progression females and males diverge. Sex- and stage-specific VIC responses regarding fibrosis were examined via RT-qPCR (ACTA2, COL1A1, FN1, TGFB-1, CHSY1), ELISA (FN1), nascent protein production, and Western Blot (MMP1 and MMP9). RT-qPCR results showed that male VICs produce a stronger fibrotic response than females at both stages of disease. The observed increased expression of ACTA2, TGFB-1, and FN1 (Figure 4.4, a, c and d) in

males compared with females coincides with previous findings by our group[26], where expression of fibrotic markers was assessed in 2D cultures of female and male VICs. However, this study contrasts our results regarding COL1A1 and CHSY1 (Figure 4.4, b and d) expression, where we observed increased expression of COL1A1 and CHSY1 in males compared to females. Nonetheless, our results coincide with those of Ferdous, Z. et al.[27] in which VICs from rat or porcine origin were cultured in 2D and primed with osteogenic media. A possible reason for the discrepancies regarding COL1A1 and CHSY1 expression could be the effects of culture conditions, such as the presence of fibrillar collagen in our system and the presence of ascorbic acid in osteogenic media, which is essential for collagen biosynthesis.

ECM and ECM regulatory molecules were also assessed in the previously mentioned study by our group[26]. Protein expression of soluble collagen 1 and MMP9 was also elevated in female. No differences were found between females and males for MMP1 expression. Although, we measured ECM and ECM regulatory molecules (Figure 4.5) in our study, differential protein expression of ECM and ECM regulatory proteins were non observed for either sex/stage. The results from these experiments could be affected by several sample processing and availability of technique limitations encountered during this investigation leading to disparate sample distribution. Therefore, at this moment, no conclusions could be drawn from current data.

Production of newly synthesized proteins was increased in males compared to females. Additionally, increased protein production levels are also observed to increase from early to late stages of disease for male VICs. Non-observable changes nascent protein

production was observed in females at either stage of disease. A possible reason for this could be that female VICs may need additional stimulus to promote sufficient VIC activation to reach a fibrotic state and ECM remodeling state.

We discussed the fibrotic responses from VICs to changes observed in diseased valve. However, since CAVD is a complex process in which several events occur simultaneously, we wanted to use this opportunity to explore VICs responsiveness to a pathological stimulus when experiencing disease related changes in ECM composition. In order to achieve this, female and male VICs cultured in early and late-stage models were treated with 5 ng/mL of TGFB-1. Although, TGFB-1 is a known profibrotic factor, it is also known to serve as a regulatory molecule in the expression of inflammatory molecules[28,29]. TGFB-1 has pro- and anti-inflammatory properties. TGFB-1 interaction with other cells, ECM and signaling molecules can trigger either of these roles. Some studies have linked TGFB-1 suppression of inflammatory molecules to be SMAD2/3 dependent[30,31] however, the mechanisms on how this occurs is not fully understood[30]. We assessed the inflammatory of female and male VICs in at the early and late stages upon exposure to TGFB-1. A marked reduction of IL6 and IL8 expression was observed in female at both stages of disease (Figure 4.6, a and b). TGFB-1 did not appear to alter IL6 expression at either stage for males (Figure 4.6, c) however, it increased IL8 expression but only at the early stage (Figure 4.6, d). TGFB-1 is often associated with its ability to promote inflammatory responses, and because of this we must consider that it is also known to regulate many pathways related to inflammation such as NF-kB, SMAD2/3, JAK-STAT, among others[32]. A plausible explanation for decrease cytokine

production of IL6 in females treated with TGFB-1 could be related to regulatory effects with any of these pathways. A study by Davidson, B. et al.[33] found that TGFB-1 can in fact decrease expression of IL6 receptors thus dampening IL6 signaling in chondrocytes through regulation of JAK-STAT, signaling. A study by Manning, A,M. and Chen, C.C. have found that there is a complex interplay between cytokines and other signaling molecules which impact their expression. TGFB-1 was found to downregulate IL8 expression by regulating IL4 expression[34].

Gene fibrotic expression of TGFB-1 treated VICs cultured in early and late-stage models was assessed to understand the combinatorial effects of VIC responses to changes in the ECM in presence of a pathological stimulus. As previously discussed, both female and male fibrotic markers expression was upregulated at both stages upon TGFB-1 treatment (Figure 4.7, a-j). This was an expected response, due to the known pro-fibrotic effects of TGFB-1, except, for ACTA2 (Figure 4.7, d) decreased expression in male VICs at both stages. No studies, showing down regulation of ACTA2 by TGFB-1 treatment is not known. The reasons for this behavior are unknown; but it could be an effect of cell-ECM-pathological stimuli interactions in our collagen enriched hydrogel models. Nonetheless, the observed increased expression of fibrotic markers to TGFB-1 (Figure 4.7, a-j) exposure coincides with many studies in CAVD research[35–37]. Interestingly, females appear to be more susceptible to TGFB-1 treatment as fold of gene expression was more prominent than that of males (Figure 4.7, a, b, c, g, and h). This coincided with the results from James, M. in which sex-specific differences were found in regard to TGFB-1 expression in which TGFB-1 ligand was highly expressed in hearts from healthy

males compared to healthy female hearts, but this trend changed, upon measuring TGFB-1 ligand expression in diseased hearts[38].

Lastly, we looked at the expression of ECM and ECM regulatory molecules (Figure 4.8.a and 4.8.b) in VICS cultured in early and late-stage disease models primed with TGFB-1 as a pathological stimulus. No stage specific differences were observed in females or males. Some However, results from this data must be revised as limitation in sample processing and available techniques to measure expression of these molecules were present. Because of this, no definitive conclusions or comparisons can be established. Differences in nascent protein production in males were observed at both stages with an expected increase in TGFB-1 treated VICs at the early condition. Unexpectedly, nascent protein production decreased at the late-stage model. Further, studies must be done to corroborate if this effect is due to increased MMP production/activity.

4.6 Conclusion

In conclusion, our findings demonstrate that inflammation of VICs is both sex- and stage-dependent, with females exhibiting higher baseline levels of inflammatory cytokines than males in both early and late-stage models of CAVD. In contrast, inflammatory expression in males increases significantly at the later stage model of disease. TGFB-1 plays a critical role in regulating cytokine expression in females during both early and late-stage disease-inspired models. Additionally, collagen enrichment influences markers of myofibroblastic activation and ECM molecules, particularly FN1 in males during late-stage models. Notably, males display higher fibrotic expression than females in both early and late conditions. TGFB-1 exacerbates fibrotic responses in both female and male VICs across early and late stages of disease. The expression of nascent protein production is also sex- and stage-dependent, with TGFB-1 increasing the production of newly synthesized proteins at early stages in females and males but decreasing this effect in males at late stages, potentially due to regulation via ECM-regulating proteins. These results underscore the importance of considering sex as a biological variable in CAVD research to understand the mechanisms underlying disease progression better. Furthermore, implementing 3D disease-inspired systems that model stages of disease progression enhance our understanding of the complex interplay between cells and their microenvironment.

4.7 References

1.Chen JH, Simmons CA. Cell-matrix interactions in the pathobiology of calcific aortic valve disease: critical roles for matricellular, matricrine, and matrix mechanics cues. *Circ Res*. 2011;108(12):1510-1524. doi:10.1161/CIRCRESAHA.110.234237

2.Büttner P, Feistner L, Lurz P, Thiele H, Hutcheson JD, Schlotter F. Dissecting Calcific Aortic Valve Disease-The Role, Etiology, and Drivers of Valvular Fibrosis. *Front Cardiovasc Med*. 2021;8:660797. doi:10.3389/fcvm.2021.660797

3.Voisine M, Hervault M, Shen M, et al. Age, Sex, and Valve Phenotype Differences in Fibro-Calcific Remodeling of Calcified Aortic Valve. *J Am Heart Assoc Cardiovasc Cerebrovasc Dis*. 2020;9(10):e015610. doi:10.1161/JAHA.119.015610

4.Porras AM, McCoy CM, Masters KS. Calcific Aortic Valve Disease: A Battle of the Sexes. *Circ Res*. 2017;120(4):604-606. doi:10.1161/CIRCRESAHA.117.310440

5.Simon LR, Scott AJ, Figueroa Rios L, Zembles J, Masters KS. Cellular-scale sex differences in extracellular matrix remodeling by valvular interstitial cells. *Heart Vessels*. 2023;38(1):122-130. doi:10.1007/s00380-022-02164-2

6.Walker CJ, Schroeder ME, Aguado BA, Anseth KS, Leinwand LA. Matters of the heart: Cellular sex differences. *J Mol Cell Cardiol*. 2021;160:42-55. doi:10.1016/j.yjmcc.2021.04.010

7.Saeed S, Dweck MR, Chambers J. Sex differences in aortic stenosis: from pathophysiology to treatment. *Expert Rev Cardiovasc Ther*. 2020;18(2):65-76. doi:10.1080/14779072.2020.1732209

8.Masjedi S, Lei Y, Patel J, Ferdous Z. Sex-related differences in matrix remodeling and early osteogenic markers in aortic valvular interstitial cells. *Heart Vessels*. 2017;32(2):217-228. doi:10.1007/s00380-016-0909-8

9.Summerhill VI, Moschetta D, Orekhov AN, Poggio P, Myasoedova VA. Sex-Specific Features of Calcific Aortic Valve Disease. *Int J Mol Sci*. 2020;21(16):5620. doi:10.3390/ijms21165620

10.McCoy CM, Nicholas DQ, Masters KS. Sex-Related Differences in Gene Expression by Porcine Aortic Valvular Interstitial Cells. *PLOS ONE*. 2012;7(7):e39980. doi:10.1371/journal.pone.0039980

11.Scott AJ, Simon LR, Hutson HN, Porras AM, Masters KS. Engineering the Aortic Valve Extracellular Matrix Through Stages of Development, Aging, and Disease. *J Mol Cell Cardiol*. 2021;161:1-8. doi:10.1016/j.yjmcc.2021.07.009

12.Porras AM, Westlund JA, Evans AD, Masters KS. Creation of disease-inspired biomaterial environments to mimic pathological events in early calcific aortic valve disease. *Proc Natl Acad Sci U S A*. 2018;115(3):E363-E371. doi:10.1073/pnas.1704637115

13.Hutson HN, Marohl T, Anderson M, Eliceiri K, Campagnola P, Masters KS. Calcific Aortic Valve Disease Is Associated with Layer-Specific Alterations in Collagen Architecture. *PLoS ONE*. 2016;11(9):e0163858. doi:10.1371/journal.pone.0163858

14.Liu AC, Joag VR, Gotlieb AI. The Emerging Role of Valve Interstitial Cell Phenotypes in Regulating Heart Valve Pathobiology. *Am J Pathol*. 2007;171(5):1407-1418. doi:10.2353/ajpath.2007.070251

15.Kirsch T, Ishikawa Y, Mwale F, Wuthier RE. Roles of the nucleational core complex and collagens (types II and X) in calcification of growth plate cartilage matrix vesicles. *J Biol Chem*. 1994;269(31):20103-20109.

16.Sapudom J, Mohamed WKE, Garcia-Sabaté A, et al. Collagen Fibril Density Modulates Macrophage Activation and Cellular Functions during Tissue Repair. *Bioeng Basel Switz*. 2020;7(2):33. doi:10.3390/bioengineering7020033

17.Schroeder ME, Gonzalez Rodriguez A, Speckl KF, et al. Collagen networks within 3D PEG hydrogels support valvular interstitial cell matrix mineralization. *Acta Biomater*. 2021;119:197-210. doi:10.1016/j.actbio.2020.11.012

18.Agarwal M, Goheen M, Jia S, Ling S, White ES, Kim KK. Type I Collagen Signaling Regulates Opposing Fibrotic Pathways through α2β1 Integrin. *Am J Respir Cell Mol Biol*. 2020;63(5):613-622. doi:10.1165/rcmb.2020-0150OC

19.Berger AJ, Linsmeier KM, Kreeger PK, Masters KS. Decoupling the effects of stiffness and fiber density on cellular behaviors via an interpenetrating network of gelatin-methacrylate and collagen. *Biomaterials*. 2017;141:125-135. doi:10.1016/j.biomaterials.2017.06.039

20.Loebel C, Mauck RL, Burdick JA. Local nascent protein deposition and remodelling guide mesenchymal stromal cell mechanosensing and fate in three-dimensional hydrogels. *Nat Mater*. 2019;18(8):883-891. doi:10.1038/s41563-019-0307-6

21.Bian W, Wang Z, Sun C, Zhang DM. Pathogenesis and Molecular Immune Mechanism of Calcified Aortic Valve Disease. *Front Cardiovasc Med*. 2021;8:765419. doi:10.3389/fcvm.2021.765419

22.Dhayni K, Chabry Y, Hénaut L, et al. Aortic valve calcification is promoted by interleukin-8 and restricted through antagonizing CXC motif chemokine receptor 2. *Cardiovasc Res*. 2023;119(13):2355-2367. doi:10.1093/cvr/cvad117

23.Li Y, Zhao J, Yin Y, Li K, Zhang C, Zheng Y. The Role of IL-6 in Fibrotic Diseases: Molecular and Cellular Mechanisms. *Int J Biol Sci*. 2022;18(14):5405-5414. doi:10.7150/ijbs.75876

24.McCoy CM, Nicholas DQ, Masters KS. Sex-related differences in gene expression by porcine aortic valvular interstitial cells. *PloS One*. 2012;7(7):e39980. doi:10.1371/journal.pone.0039980

25.Malutan AM, Dan M, Nicolae C, Carmen M. Proinflammatory and anti-inflammatory cytokine changes related to menopause. *Przeglad Menopauzalny Menopause Rev*. 2014;13(3):162-168. doi:10.5114/pm.2014.43818

26.Simon LR, Scott AJ, Figueroa Rios L, Zembles J, Masters KS. Cellular-scale sex differences in extracellular matrix remodeling by valvular interstitial cells. *Heart Vessels*. 2023;38(1):122-130. doi:10.1007/s00380-022-02164-2

27.Masjedi S, Lei Y, Patel J, Ferdous Z. Sex-related differences in matrix remodeling and early osteogenic markers in aortic valvular interstitial cells. *Heart Vessels*. 2017;32(2):217-228. doi:10.1007/s00380-016-0909-8

28.Sanjabi S, Oh SA, Li MO. Regulation of the Immune Response by TGF-β: From Conception to Autoimmunity and Infection. *Cold Spring Harb Perspect Biol*. 2017;9(6):a022236. doi:10.1101/cshperspect.a022236

29.Hatamzade Esfahani N, Day AS. The Role of TGF-β, Activin and Follistatin in Inflammatory Bowel Disease. *Gastrointest Disord*. 2023;5(2):167-186. doi:10.3390/gidisord5020015

30.Takimoto T, Wakabayashi Y, Sekiya T, et al. Smad2 and Smad3 are redundantly essential for the TGF-beta-mediated regulation of regulatory T plasticity and Th1 development. *J Immunol Baltim Md 1950*. 2010;185(2):842-855. doi:10.4049/jimmunol.0904100

31.McKarns SC, Schwartz RH, Kaminski NE. Smad3 is essential for TGF-beta 1 to suppress IL-2 production and TCR-induced proliferation, but not IL-2-induced proliferation. *J Immunol Baltim Md 1950*. 2004;172(7):4275-4284. doi:10.4049/jimmunol.172.7.4275

32.Deng Z, Fan T, Xiao C, et al. TGF-β signaling in health, disease, and therapeutics. *Signal Transduct Target Ther*. 2024;9(1):61. doi:10.1038/s41392-024-01764-w

33.Wiegertjes R, van Caam A, van Beuningen H, et al. TGF-β dampens IL-6 signaling in articular chondrocytes by decreasing IL-6 receptor expression. *Osteoarthritis Cartilage*. 2019;27(8):1197-1207. doi:10.1016/j.joca.2019.04.014

34.Chen CC, Manning AM. TGF-beta 1, IL-10 and IL-4 differentially modulate the cytokine-induced expression of IL-6 and IL-8 in human endothelial cells. *Cytokine*. 1996;8(1):58-65. doi:10.1006/cyto.1995.0008

35.Cloyd KL, El-Hamamsy I, Boonrungsiman S, et al. Characterization of porcine aortic valvular interstitial cell “calcified” nodules. *PloS One*. 2012;7(10):e48154. doi:10.1371/journal.pone.0048154

36.Walker GA, Masters KS, Shah DN, Anseth KS, Leinwand LA. Valvular myofibroblast activation by transforming growth factor-beta: implications for pathological extracellular matrix remodeling in heart valve disease. *Circ Res*. 2004;95(3):253-260. doi:10.1161/01.RES.0000136520.07995.aa

37.Jenke A, Kistner J, Saradar S, et al. Transforming growth factor-β1 promotes fibrosis but attenuates calcification of valvular tissue applied as a three-dimensional calcific aortic valve disease model. *Am J Physiol Heart Circ Physiol*. 2020;319(5):H1123-H1141. doi:10.1152/ajpheart.00651.2019

38.Sex-Specific Differences of Transforming Growth Factor β Expression in Cardiac Hypertrophy and Heart Failure - James - 2016 - The FASEB Journal - Wiley Online Library. Accessed July 27, 2024. https://faseb.onlinelibrary.wiley.com/doi/10.1096/fasebj.30.1_supplement.1119.19

Chapter 5: Collagen Enrichment and Fiber Architecture: Unraveling the biological and architectural roles of Collagen in CAVD Fibrosis

5.1 Abstract

Calcific aortic valve disease (CAVD) is characterized by changes in collagen content and architecture within the valve. In healthy aortic valves, collagen type I predominantly constitutes the fibrosa and is oriented circumferentially, providing mechanical stability against the constant blood flow through the heart. In CAVD, increased production of collagen type I and altered microarchitecture contribute to disease progression by promoting fibrosis and calcification, which further stiffen the valve[1].

Collagen type I is versatile, offering both biological and biochemical cues through its specific adhesion sequences that interact with cells, while its fibrillar architecture impacts tissue mechanics and cellular behavior. This study aims to understand how collagen's biological and architectural properties influence fibrosis in CAVD. We developed a novel 3D disease-inspired scaffold that maintains the total collagenous protein content as in our previously designed late-stage model, while varying fibrillar content (1X vs. 2X). These scaffold models were used to examine the expression of fibrotic markers to better understand sex-dependent responses to collagen's structural and biological properties. Our results reveal no differences in VICs' fibrotic expression in response to increased fiber content, however sex-dependent responses were maintained.

Valvular interstitial cells (VICs) were then primed with TGF-β1 to determine whether total collagenous protein or collagen fiber architecture affects cellular responsiveness to a pathological stimulus. We found that exposure to a pathological stimulus maybe ne necessary to perceive VICs differential responses to changes to its extracellular environment. These findings underscore the importance of collagen in CAVD and provide insights into the complex interplay between collagen architecture, pathological stimuli, and fibrotic responses.

5.2 Introduction

Collagen 1, the most common type of fibrillar collagen, comprises about 50% of the AV dry weight[2]. In healthy valves, collagen can be found as densely packed bundles in the fibrosa layer[3,4], providing the valve with the ability to withstand the continuous mechanical forces exerted by blood flow throughout the heart. In addition to providing mechanical support in tissues, collagen 1 has been found to modulate cell behavior by promoting cell activation, cell migration, and serving as a nucleation site for calcium deposition[5].

Various studies have demonstrated the importance of collagen in maintaining valve homeostasis. Dysregulation of the valve ECM has been linked to critical changes in collagen content and architecture. During disease, collagen production is upregulated, and its deposition is spread out across the valve. Increased amounts, up to twofold, of fibrillar collagen are found in the spongiosa layer, where collagen fibers have increased width and density. Conversely, collagen fibers from the fibrosa layer become shortened[1,6].

Although collagen is often associated as a fibrocalcific contributor, it can also help cells maintain a quiescent state. When naïve VICs are cultured on collagen-coated substrates, markers of myofibroblast expression and fibrosis decrease[7]. Because of collagen's key role in fibrocalcific processes, many studies have incorporated this ECM in their culture platforms. For instance, Mahler et al. used a collagen-based platform to understand the effect of GAGs in EndMT, while Butcher et al. used collagen hydrogels to explore VEC EndMT. Both were able to replicate EndMT by VECs; Mahler without incorporating

osteogenic media, and Butcher without the presence of GAGs. Mahler has also exploited the properties of collagen 1 hydrogels to generate disease-on-a-chip models to study the effects of shear stress on VECs.

Other groups focus on the architectural aspects of collagen fibers and have created synthetic fibers that mimic specific features of healthy ECM. Various studies by Baker et al. have shown that cells cultured on soft but fibrous networks show increased spreading, proliferation, and biomechanical cell signaling[8,9]. Myofibroblasts cultured in similar conditions become activated in low stiffness matrices[10].

Given the pivotal role of collagen in fibrosis, understanding how this molecule contributes to fibrosis in CAVD is crucial. Based on the findings from Chapter 4, which identified increased expression of fibrotic markers associated with collagen enrichment, we aimed to investigate the impact of collagen's biological and architectural properties on fibrosis. To this end, we developed a novel 3D disease-inspired scaffold, maintaining the total collagenous protein content of our late-stage model but with varying fiber concentrations. These scaffolds were used to assess the expression of fibrotic markers and evaluate sex-dependent responses to collagen's biological and architectural features. Additionally, we explored the combinatorial effects of enriched fibrillar collagen and pathological stimuli, specifically TGFB, on fibrotic marker expression.

5.3 Methods

5.3.1 VIC isolation and expansion

Valvular interstitial cells (VICS) were isolated, expanded and maintained in culture as previously described[11]. Briefly, aortic valve leaflets were excised from 6-month-old pig hearts obtained from our local abattoir (Hoesly's Meats, New Glarus, WI) and incubated for 30 minutes in a collagenase II (Worthington Biochemical Corporation, Lakewood, NJ) solution to remove valvular endothelial cells from the tissue. A second 60-minute incubation followed, in fresh collagenase II solution to release VICS for expansion. VICs were then maintained in low glucose Dulbecco's Modified Eagle's Medium (Sigma-Aldrich, St. Louis, MO), supplemented with 2 mM L-glut (Sigma Aldrich), 150 U/mL penicillin/streptomycin (Sigma-Aldrich) and 10% fetal bovine serum (FBS) (Corning, Corning, NY) at 37 °C and 5% CO_2 until they reached passages 2-3. VICs were not used past passage 3 for any of the experiments.

5.3.2 GelMA Synthesis

Gelatin type A from porcine skin (Sigma Aldrich) was dissolved at 10% w/v in phosphate-buffered saline (1X PBS) (Corning, Corning, NY) at 50 °C. Once the gelatin was dissolved, methacrylic anhydride (MA) (Sigma Aldrich) was added to the gelatin solution with a syringe in a drop-wise manner and stirred overnight protected from light. The following day, the gelatin-methacrylate (GelMA) reaction solution was centrifuged at 3000 xg for 5 minutes at 37 °C degrees to precipitate unreacted MA. The supernatant was collected and diluted at a 1:4 ratio in pre-warmed 1X PBS at 50 °C and then transferred

to 12-14 kDa MWCO dialysis tubing (Spectrum Labs, Rancho Dominguez, CA). The diluted GelMA solution was dialyzed against 1X PBS for 3 days and diH_20 for 3 more days at 50 °C to remove any unreacted MA. PBS and DiH_2O solutions were changed daily through the dialysis process. At the end of the dialysis period, the GelMa solution was filtered, lyophilized and stored at -80 °C until needed for further characterization and use[12].

5.3.3 Creation of disease inspired late-stage models with varied collagen fiber content

In order to understand whether expression of fibrosis markers as observed in chapter 4 was driven by collagen's biological or architectural properties a new 3-D disease-inspired scaffold was developed to maintain total collagenous protein as our late-stage model but containing half the amount of collagen fibers. All models were created using a GelMA (Gelatin Methacrylate) based hydrogel (4% w/v) with an interpenetrating network of collagen fibers[12]. Our traditional late-stage condition contained 1.5 mg/mL collagen 1 (Advanced Biomatrix, San Diego, CA) while a modified late condition contained 0.75 mg/mL collagen I and 0.75 mg/ml collagen ligand in the form of GelMa to maintain equal amounts of total collagenous protein while differing in the amount of total collagen fibers (Figure 5.1). To avoid confusion, we will refer to our modified late condition as late-1X (or 1X) and late-2X (or 2X) to our traditional late scaffold. To neutralize the collagen added to our GelMa-Coll pre-polymer solutions, 0.1 M NaOH (RPI, Mt. Prospect, IL) and 10x DPBS (Sigma Aldrich) were added at their appropriate ratios. Female and male VICs were also added independently at a concentration of 4 x 10^6 cells/mL to the pre-polymer

solution along with photoinitiator lithium-phenyl-2,4,6-trimethylbenzoylphosphinate (LAP) (Sigma Aldrich) at a final concentration of 0.05% w/v. 100 ul of the pre-polymer solution was added to silicone molds (9 mm diameter x 1.7mm depth) and incubated at 37 °C for 30 minutes to allow for collagen fibrillogenesis. The molds were then incubated at 4 °C for the amount of time previously optimized via dynamic mechanical analysis[12] to reach a Young's modulus of 5-8 kPa and subsequently photocrosslinked under UV light (365 nm) for 6 minutes.

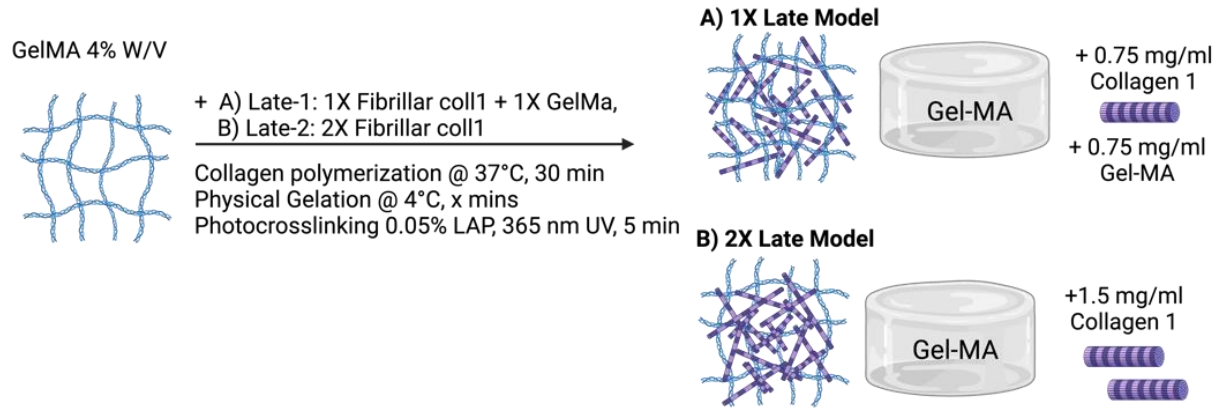

Figure 5.1 Schematic representation of the fabrication of late-stage hydrogel models containing equal amounts of total collagenous protein but varying amounts of fibers. Late-1X (a) contains 0.75 mg/mL fibrillar collagen 1, whereas as late-2X (b) contains 1.5 mg/mL.

5.3.4 VICs culture in 3D late-stage models with varied fibrillar collagen content

Late-1X and 2X models containing female or male VICs as described above (day 0) were cultured for a total of 6 days in low glucose DMEM, supplemented with 2 mM L-glut, 150 U/mL, penicillin/streptomycin and 10% FBS. Fresh media was provided every other day (days 1 and 3; 24 hrs and 72 hours post seeding respectively) (Figure 5.2 a). In order to determine whether total collagenous protein, or collagen fiber architecture affects cellular

responsiveness to a pathological stimulus, late-1X and 2X disease models were treated with TGF-β1 (5 ng/mL) (Peprotech) on days 1 and 3 (Figure 5.2 b). Media samples were collected on days 3 for inflammatory cytokines (IL-6 and IL-8) and days 3 and 5 for cumulative soluble collagen (Collagen 1) quantification. Hydrogel lysates were collected at day 2 for quantification of gene expression (*aSMA, COL1A1, FN, TGFB-1 and CHYSY1*) and at day 5 for protein quantification (FN1, MMP-1 and MMP-9). In addition, a whole hydrogel set was collected on day 5 for nascent protein quantification.

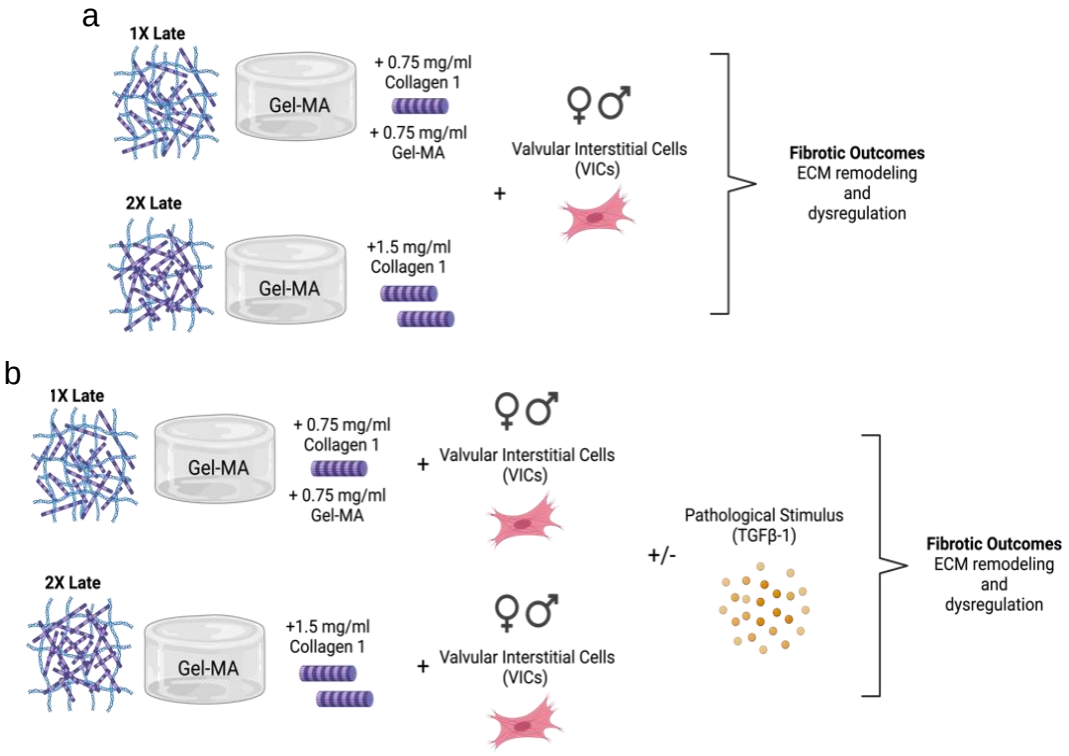

Figure 5.2 Schematic representation of methods. a) Experimental design proposed to understand the effects on VIC fibrotic outcomes stemming from changes in fiber enrichment. b) Experimental designed proposed to explore the combinatorial effects of changes in fibers concentration in the presence of a pathological stimulus in female and male VICs fibrotic outcomes.

5.3.5 Visualization and quantification of nascent protein produced by VICs

In order to visualize nascent protein deposition by female and male VICs embedded in 3D late-1X and 2X models, an adaptation of a previously published technique was followed[13]. Late-1X and 2X models were cultured in nascent protein media (high glucose DMEM, no methionine, no cystine) supplemented with 2 mM L-glut, 150 U/mL penicillin/streptomycin, 10% FBS, 100 µg/mL sodium pyruvate, 0.201 mM cystine, 100 µg/mL, 50 µg/mL ascorbate 2-phosphate, and 0.1 mM azidohomoalanine AHA. The media was changed every other day as described above (days 1, 3). On day 5, all hydrogel models were washed in 1% BSA followed by a 40 min incubation in 30 µM DBCO-488 (). The DBCO-488 undergoes a bio-orthogonal strain-promoted cyclo-addition that allows visualization of all new synthesized protein produced by the VICs. After the incubation period, all hydrogels were washed once again prior to a 30 min incubation in 10% formalin. Once all cells were fixed within the hydrogels, the excess formalin was washed away, and samples were stored in 1X PBS until imaging. All nascent protein imaging was performed on a Nikon AXR Confocal Microscope and image analysis was done on FIJI.

5.3.6 Detection of fibrotic markers via gene expression quantification

All late-1X and 2X hydrogel models' samples were collected on day 2 (48 hrs post seeding) digested in a collagenase (4.2 mg/mL) digestion solution supplemented with 30% v/v Proteinase K (Qiagen, Hilden, Germany), 50% v/v 10X Trypsin (Gibco, Grand Island, NY) and 20% v/v 1X PBS to facilitate RNA isolation. RNA isolation was performed according to the manufacturer's instruction for Qiagen's RNeasy kit (Qiagen,

Germantown, MD). Retrieved RNA was then subjected to reverse transcription using a High-Capacity cDNA Reverse Transcription kit (Applied Biosystems, Foster City, CA). Taqman Gene Expression Assays were used to quantify genetic expression profiles of fibrosis-related genes (*aSMA, COL1A1, FN, TGFB-1 and CHYSY1*) (Thermo Fisher). All PCR reactions were performed in a Biorad CXF Opus 96 Real Time PCR and analyzed via the delta-delta ct method.

5.3.7 Detection of fibrotic markers via protein quantification

For FN1, MMP-1 and MMP-9 protein quantification assays, late-1X and 2X hydrogel models samples were collected at day 5. FN1 production in female and male VICs cultured in 3D late-1X and 2X models was evaluated via R&D DuoSet ELISA following the manufacturer's instructions. Quantified FN1 levels were normalized to total DNA via picogreen. Quantification of MMP-1 and MMP-9 was determined via Western blot. Lysate samples collected on day 5 were blended in RIPA lysis and extraction buffer (Thermo Fisher) supplemented with 1 mM phenylmethylsulfonyl fluoride (PMSF) and 2 mg/mL protease inhibitor (Thermo Fisher, Rockford, IL) on a tissue homogenizer (Next Advance) with .5mm stainless steel beads (Next Advance) for 10-15 minutes at medium speed. Due to the protein nature of these hydrogel models, DNA quantification was performed in these lysates to determine how much protein corresponded to the VICs embedded in our models. A DNA-to-protein ratio was calculated to immunoprecipitate our proteins of interest. Immunoprecipitation of MMP-1 and MMP-9 was performed using a Dynabeads Protein g Immunoprecipitation Kit (Thermo Fisher). An MMP-1 and MMP-9 antibody (ab) dilution was used to immunoprecipitate a total of 0.5 ug of protein. Upon

immunoprecipitation, samples were incubated at 70 °C for 10 min and followed a standard western blot procedure. Briefly, 0.045 ug of sample was loaded and run in a 15-well Invitrogen wedgewell Tris–Glycine Mini Gels (Thermo Fisher) for 1 h at 120 V. Proteins of interest were then transferred to an Immun-Blot PVDF membrane (Bio-Rad) at 30 V for 1 hr. Once the proteins had been transferred, a 1 hr blot incubation in 5% w/v solution of nonfat dried milk diluted in .1% PBST followed to avoid non-specific binding. A primary MMP-1 or MMP-9 ab (1:1000) solution to the blot and incubated overnight at 4 °C. All membranes were washed the next day in .1% PBST prior to the addition of the HRP secondary goat-anti Rabbit ab (1:10,000) (Thermo Fisher) and then incubated for 1 h. Subsequently, the blots were washed once again in a .1% PBST solution. Cumulative collagen-1 quantification was also assessed via western blot from pooled media from days 3 and 5. The collagen blot was incubated for 1 hr in collagen-1 primary ab (1:1000) followed by the addition of the HRP secondary goat-anti Rabbit ab (1:10,000) and .1% PBST washes as described above. Protein expression levels were detected via ChemiDoc MP Imaging System (Bio-Rad) upon exposure to clarity western ECL substrate (Bio-Rad) and quantified on FIJI.

5.3.8 Detection of inflammatory cytokines

Production of inflammatory cytokines, IL6 and IL8 from media samples was evaluated via R&D DuoSet ELISA following the manufacturer's instructions. Total cytokine levels were quantified via four-parameter logistic regression.

5.3.9 Statistical Analysis

Each experiment was performed using a n=3 sample. Specifically, VICs isolated from 3 different pigs were pooled for each sex. Data points as seen in each graph represent a sample repeat of this pooled set. Additional experiments performed to validate our results used a new set of pigs. Statistical analysis was performed via 2-way Anova with Tukey Post-Hoc test. Statistical Significance was considered for all comparisons with $P < 0.05$.

5.4 Results

5.4.1 Sex-Dependent Inflammatory Responses are Independent of Total Fiber Amount

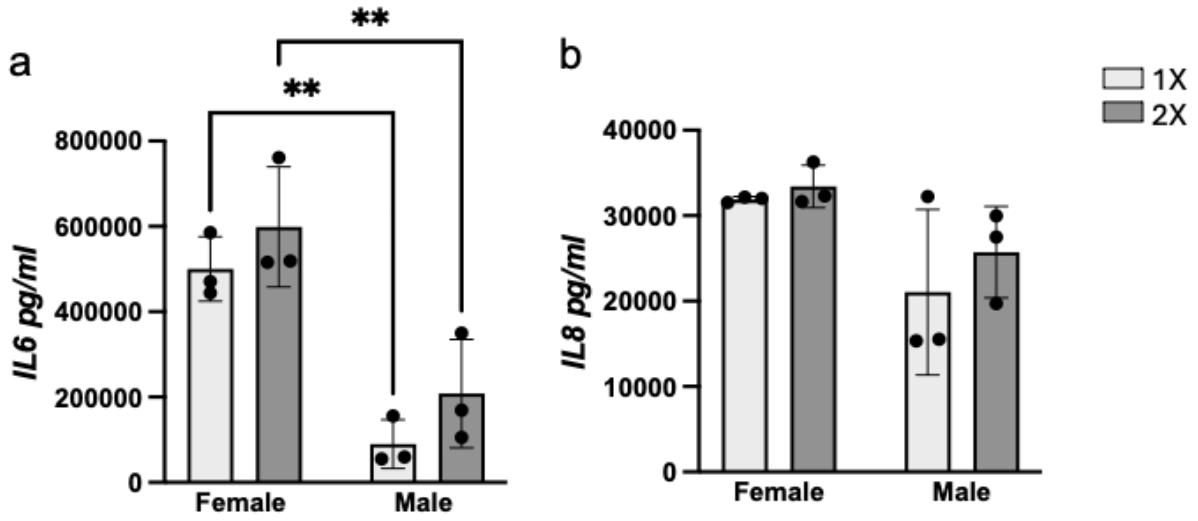

Figure 5.3 Impact of increased fiber content from 1X to 2X fibrillar collagen concentration with equal amounts of total collagenous protein on inflammatory cytokine production in female and male VICs. Cytokine expression of a) IL6 and b) IL8 was measured 2 days post seeding via ELISA. Results are presented as mean ± standard deviation; *indicates $P < 0.05$ by Tukey Post-hoc test.

Inflammatory cytokine production of IL6 and IL8 in female and male VICs cultured in late-stage models with equal collagenous protein content but varying amounts of collagen fibers (late-1X = 0.75 mg/mL Collagen 1 + 0.75 mg/mL Gelatin vs late-2X = 1.5 mg/mL Collagen 1) was assessed via ELISA. Sex-dependent responses were observed in both late-1X and late-2X conditions, with females exhibiting higher IL6 production compared to males (Figure 5.3, a). Differences between/within sexes were not observed for IL8 production in either group (Figure 5.3, b).

5.4.2 Collagen Architecture Alone Does Not Drive Fibrosis in Female and Male VICs

Gene expression of CAVD fibrotic markers was assessed in female and male VICs cultured in models with 1X or 2X total collagen fiber content via RT-qPCR. Male VICs showed significantly increased gene expression of ACTA2 and FN1 (Figure 5.4, a and c) in both 1X and 2X conditions compared to female VICs. Although not significant, a similar trend was observed for TGFB-1 expression (Figure 5.4, d). Males also exhibited increased expression of COL1A1 and CHSY1 (Figure 5.4, b and e) compared to females, but only in the late-1X condition. Increased fiber content did not affect the expression of fibrotic markers within each sex.

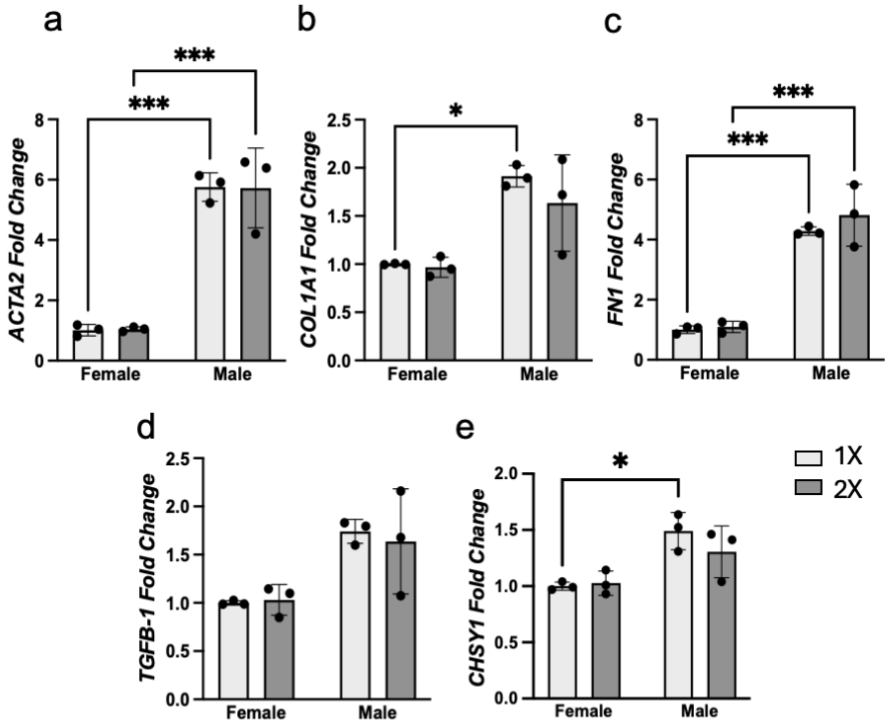

Figure 5.4 Fibrotic gene expression of female and male VICs cultured in 1X and 2X late-models shows a sex-dependent response. Gene expression of fibrotic markers (a) ACTA2, b) COL1A1, c) FN1, d) TGFB-1, e) CHSY1) was assessed by RT-qPCR and normalized to 1X female. Results are presented as mean ± standard deviation; *indicates $P < 0.05$ by Tukey Post-hoc test.

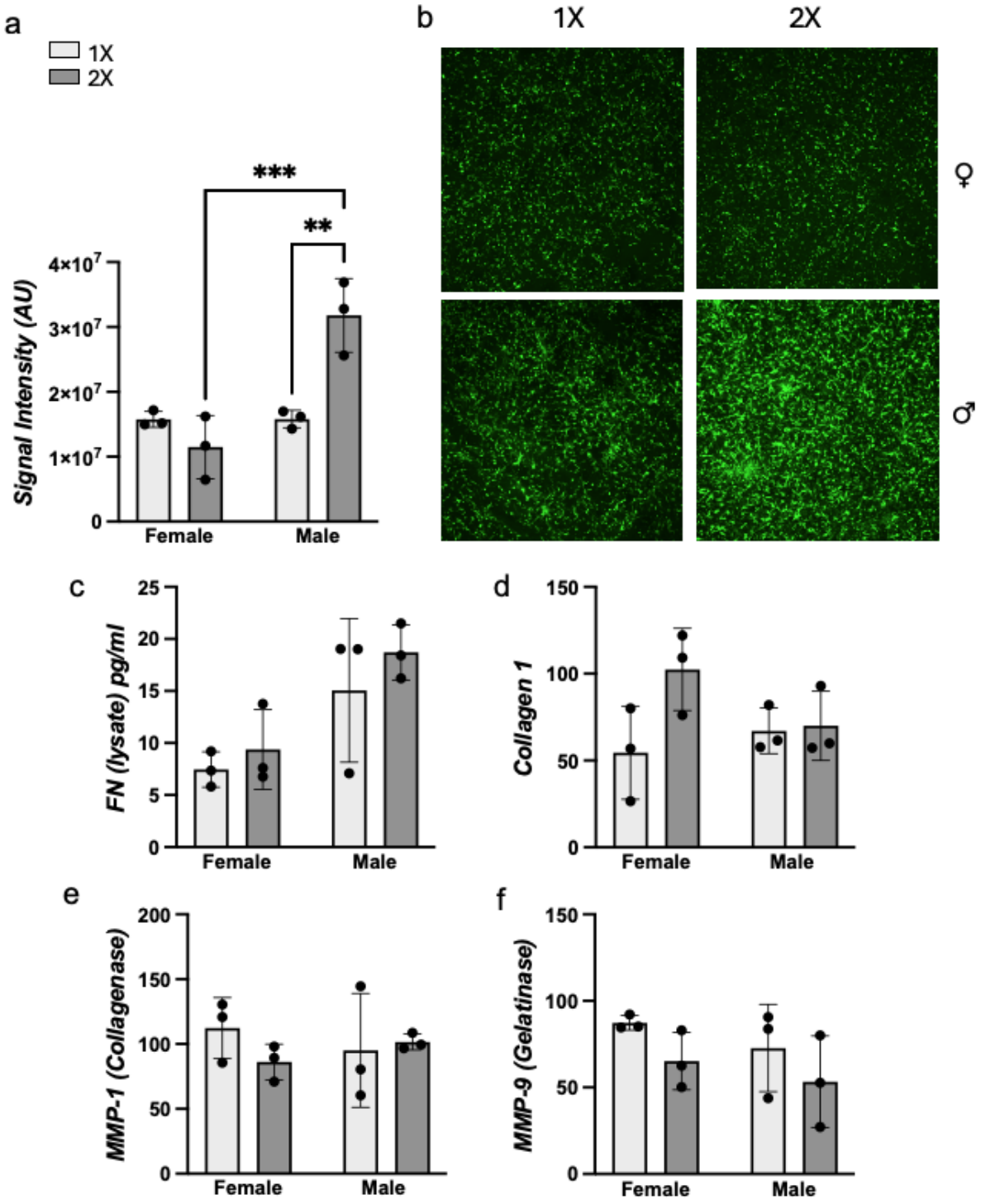

Figure 5.5 ECM- and ECM regulatory proteins expression of female and male VICs cultured in 1X and 2X late-stage models. a) Quantification and b) visualization of newly synthesized extracellular proteins. Newly synthesized proteins incorporated AHA, a methionine homolog that allows visualization via DBCO-488 bio-orthogonal cyclo-addition; Quantification of c) Collagen 1 and d) FN1 extracellular matrix production and ECM regulatory proteins e) MMP-1 and f) MMP-9 via Western Blot. Results are presented as mean ± standard deviation; *indicates $P < 0.05$ by Tukey Post-hoc test.

5.4.3 Impact of Increased Fiber Content on ECM and ECM Regulatory Protein Production

To understand the impact of collagen's biological or architectural role in fibrotic progression, nascent protein expression was visualized using DBCO-488 labeling of a methionine analog incorporated during protein synthesis. Quantification of specific ECM and ECM regulatory proteins was performed via ELISA (FN1) and Western blot (Collagen 1, MMP1, and MMP9). Increased protein production was observed in males only in the late-2X condition compared to late-1X. Sex differences in nascent protein production was also evident in late-2X (Figure 5.3, a and b). However, increased expression of ECM and ECM regulatory proteins was not observed in females or males in either late-1X or late-2X conditions (Figure 5.3, c-f).

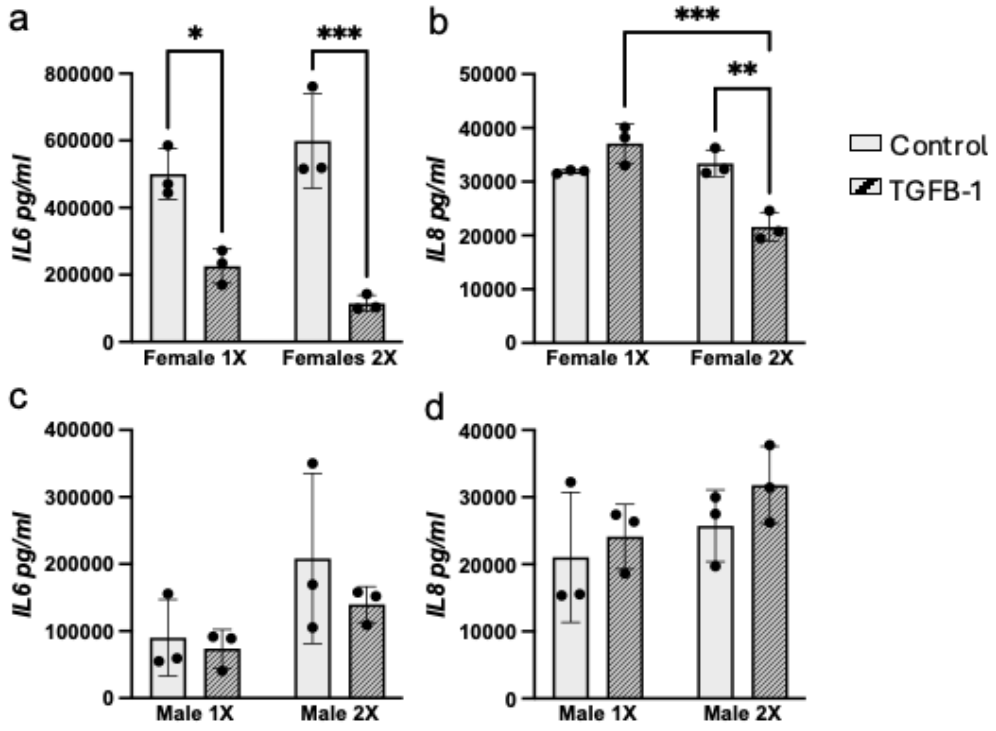

Figure 5.6 Impact of increased fiber content and presence of TGFB-1 as a pathological stimulus on inflammatory cytokine production in female and male VICs. Cytokine expression of a) IL6 and b) IL8 was measured 2 days post seeding via ELISA. Results are presented as mean ± standard deviation; *indicates $P < 0.05$ by Tukey Post-hoc test.

5.4.4 Effects of Collagen Fiber Enrichment and Pathological Stimulus in VIC Fibrotic Responses

To explore cellular responsiveness to a pathological stimulus, female and male VICs cultured in late-1X and late-2X systems were treated with TGFB-1 at 5 ng/mL. Female VICs showed a significant decrease in IL6 production for both late-1X and late-2X conditions. Reduced IL8 production was observed only in the late-2X condition. IL6 or IL8 cytokine production was not affected in males between late-1X and late-2X conditions or between control and treated groups.

Gene expression of fibrosis-related markers was assessed via RT-qPCR. TGFB-1 exposure exacerbated fibrotic responses in females for ACTA2, FN1, TGFB-1, and CHSY1 in both 1X and 2X conditions between control and treated groups. Additionally, TGFB-1 primed females VICs cultured in the late-2X condition were more susceptible to TGFB-1 treatment noted by increased expression of these genes compared to treated females in the late-1X condition. COL1A1 expression in females increased only in the late-2X condition; primed VICs in the 2X groups were also more susceptible to TGFB-1 treatment in comparison to treated VIC in the 1X group (Figure 5.7, a-c; g-h). Males also exhibited an exacerbated fibrotic response for ACTA2, FN1, and COL1A1 (Figure 5.7, d-f), but only in the late-1X condition. TGFB-1 expression increased in both 1X and 2X conditions, while CHSY1 expression increased only in the late-2X condition (Figure 5.7, i and j). In contrast to females, males treated with TGFB-1 experienced a decrease in ACTA2 and COL1A1 expression – and an increase in CHSY1 expression – between males treated in the 1X versus 2X condition. Interestingly, fold change between the

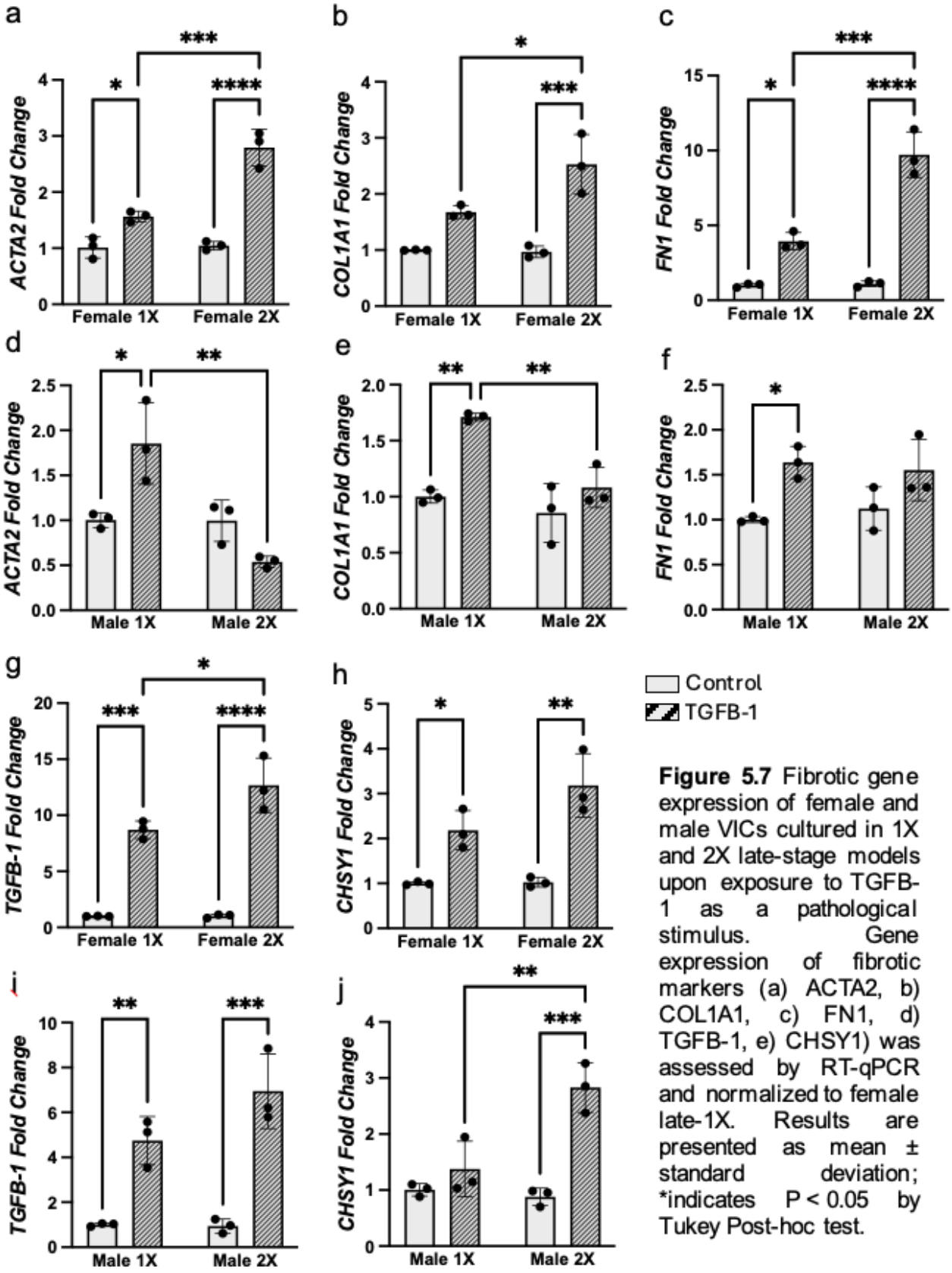

Figure 5.7 Fibrotic gene expression of female and male VICs cultured in 1X and 2X late-stage models upon exposure to TGFB-1 as a pathological stimulus. Gene expression of fibrotic markers (a) ACTA2, b) COL1A1, c) FN1, d) TGFB-1, e) CHSY1) was assessed by RT-qPCR and normalized to female late-1X. Results are presented as mean ± standard deviation; *indicates $P < 0.05$ by Tukey Post-hoc test.

control and treated groups was higher in females compared to males; suggesting that female VICs are more susceptible to TGFB-1.

As previously described, ECM and ECM regulatory protein production was assessed via DBCO-488 staining, ELISA, and Western blot. Nascent protein expression increased in females upon TGFB-1 exposure (Figure 5.8, a, a and b) in both late-1X and late-2X conditions. FN1 expression was also upregulated in females in both late-1X and late-2X conditions. ECM (Collagen 1) and ECM regulatory proteins (MMP1 and MMP9) (Figure 5.8, a e and f) were not altered in female VICs in either late-1X or late-2X conditions, nor in control or treated groups.

Nascent protein expression increased in males in the control group but only in the elate-2X condition. Nascent protein production also increased upon TGFB-1 exposure but only in VICs seeded in the late-1X model; significant protein downregulation was observed in the late-2X condition upon treatment (Figure 5.8, a and b), and between 1X and 2X primed VICs. ECM proteins (FN1 and Collagen 1) (Figure 5.8, b, c and d) and ECM regulatory proteins (MMP1 and MMP9) (Figure 5.8, b, e and f) were not altered in male VICs in control or treated groups for 1X and 2X conditions.

Undetectable protein differences in female and male VICs cultured in 1X and 2X models exposed to TGFB-1 as a pathological stimulus may be due to limitations in sample source/processing and the availability of compatible techniques for quantifying these proteins using the current hydrogel model setup.

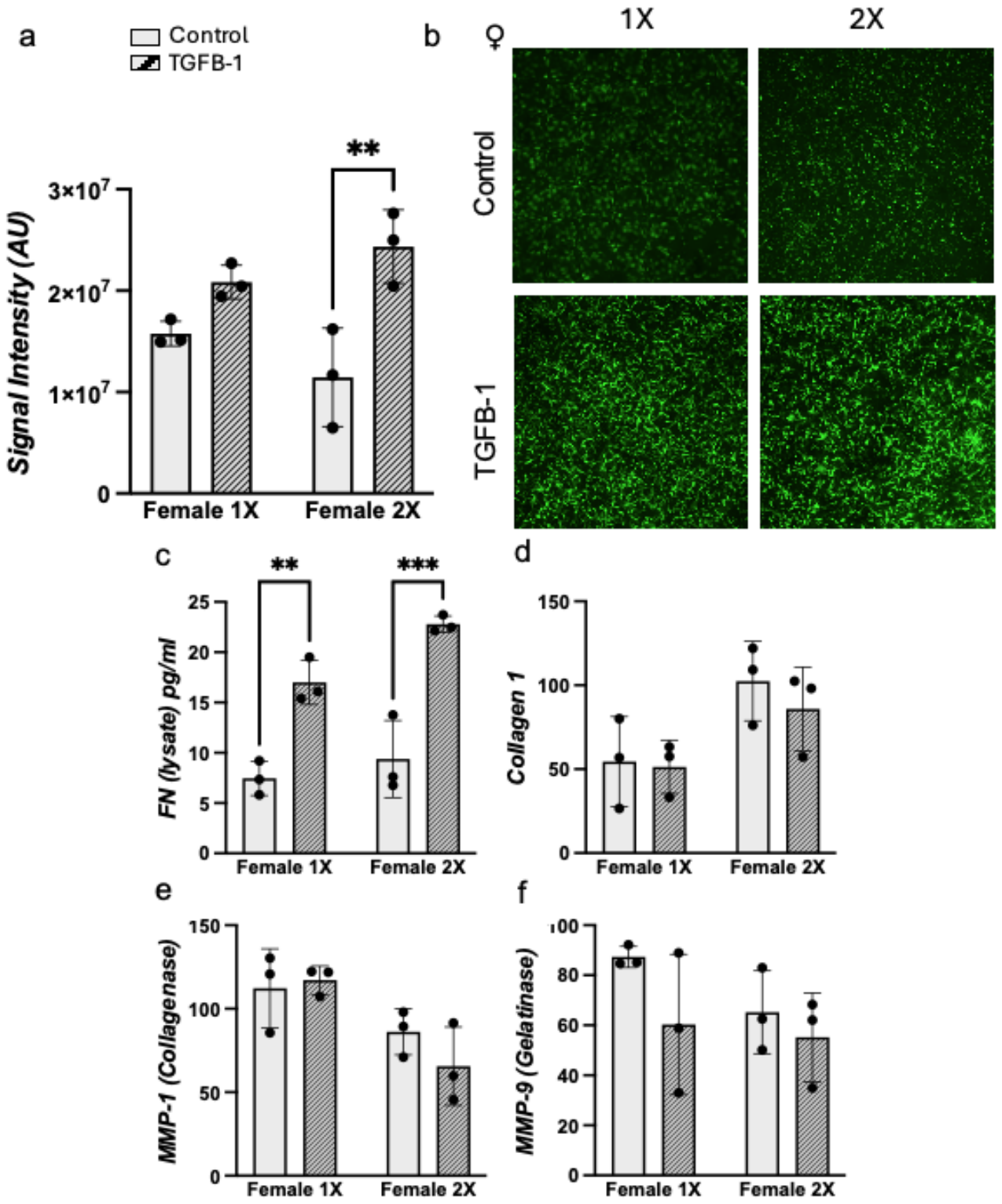

Figure 5.8.a ECM- and ECM regulatory proteins expression of female VICs cultured in 1X and 2X late-stage models and upon exposure to TGFB-1. a) Quantification and b) visualization of newly synthesized extracellular proteins via DBCO-488 staining. Quantification of c) Collagen 1 and d) FN1 extracellular matrix production and ECM regulatory proteins e) MMP-1 and f) MMP-9 via Western Blot. Results are presented as mean ± standard deviation; *indicates $P < 0.05$ by Tukey Post-hoc test.

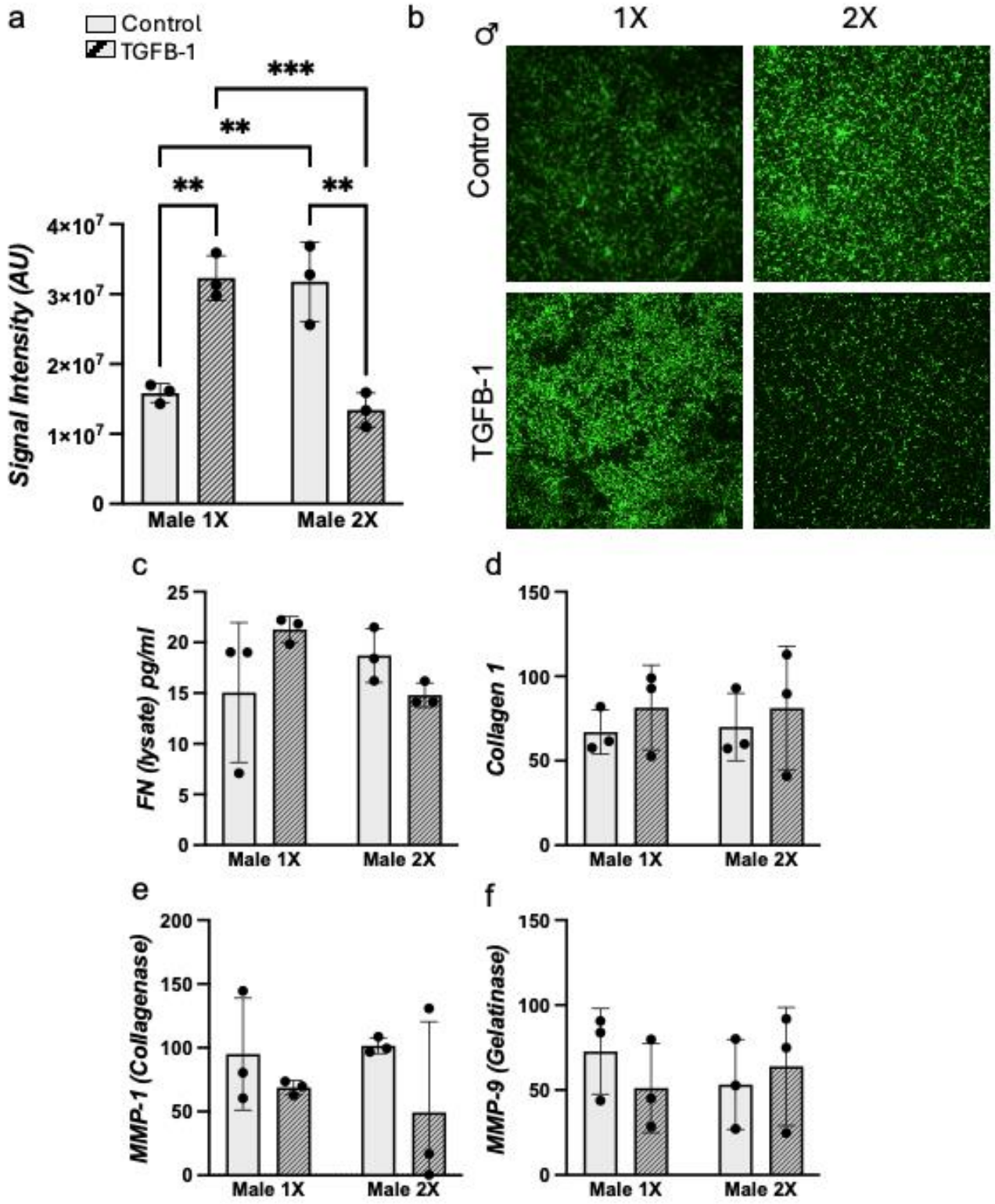

Figure 5.8.b ECM- and ECM regulatory proteins expression of male VICs cultured in 1X and 2X late-stage models and upon exposure to TGFB-1. a) Quantification and b) visualization of newly synthesized extracellular proteins via DBCO-488 staining. Quantification of c) Collagen 1 and d) FN1 extracellular matrix production and ECM regulatory proteins e) MMP-1 and f) MMP-9 via Western Blot. Results are presented as mean ± standard deviation; *indicates $P < 0.05$ by Tukey Post-hoc test.

5.5 Discussion

In this chapter, we aimed to understand the biological and architectural roles of collagen in CAVD fibrosis. Two hydrogel models were developed containing the same amount of total collagenous protein but varying amounts of collagen fibers, 1X and 2X. VIC fibrotic responses were evaluated by examining the change in the production of cytokines associated with CAVD progression and the gene and protein expression of fibrotic markers.

We first looked at IL6 and IL8 expression in female and male VICs cultured in our 1X and 2X fiber models. Sex differences were observed between females and males for both 1X and 2X conditions (Figure 5.3, a and b) but only for IL6 expression. IL8 expression remained unchanged for females and males in both models. These results coincide with our previous findings in Chapter 4, where females were observed to have a higher inflammatory profile than males. Studies often portray males as having higher inflammation profiles than females[14,15]. However, it is widely recognized that menopausal women exhibit increased levels of inflammatory cytokines[16]. In this work, we used pre-pubescent pigs' hearts, which have estrogen levels comparable to those found in females undergoing menopause. The observed increase in inflammatory cytokine expression in females versus males could thus be attributed to the similarities in hormone levels. Collagen fiber enrichment did not affect IL6 and IL8 expression in female or male VICs. Research linking direct correlation between collagen and increased inflammation has not been extensively pursued. However, some studies claim that collagen could be used as a potential therapy to decrease inflammation[17,18], but the mechanism for the anti-

inflammatory effects of collagen remains elusive. We could speculate that providing VICs with a collagenous fiber environment may be beneficial in maintaining baseline levels of inflammation in both females and males.

We evaluated the expression of fibrosis-related markers in female and male VICs experiencing increased fiber availability in their environment on an equally enriched collagen matrix. Genetic expression of fibrotic markers showed that, generally, males have stronger fibrotic responses compared to females (Figure 5.4, a-e). These results coincide with current CAVD literature, which indicates that males have higher expression levels of fibrotic markers than females[15,19,20]. Increased amounts of fibrillar collagen do not promote or enhance fibrotic responses in female and male VICs. This contrasts with many studies in which the presence of fibers has been noted as key in driving fibrotic differentiation[10,21]. However, we must consider that in healthy tissues, collagen forms part of the matrix composition and contributes to tissue homeostasis. Previous research by our lab has demonstrated that collagen is needed to maintain VIC quiescence and prevent expression of calcification markers[7]. Fiber increase alone in our models may not be sufficient to drive a more robust fibrotic response in female and male VICs.

Fibrosis is characterized by the continuous remodeling of the ECM, where protein production surpasses the rate of protein degradation. To better understand the biological and architectural roles of collagen in contributing to CAVD, we examined the production of nascent proteins and ECM and ECM regulatory proteins (Figure 5.5). For this purpose, we looked at the production of newly synthesized proteins and ECM and ECM regulatory proteins such as FN1, COL1A1, MMP-1, and MMP-9. Increased amounts of protein

production were observed in males in the 2X condition compared to males in 1X and females in 2X (Figure 5.5, a and b). Increased fibrillar collagen appears to impact the biosynthesis of new proteins. However, protein expression of ECM and ECM regulatory proteins appeared to be unaffected. This could be due in part to disparate sample distribution, which could be impacted by sample processing and the availability of techniques to quantify these proteins. At this moment, further experimentation is necessary to accurately describe the effects of fiber enrichment and sex-dependent behaviors.

As previously mentioned, hallmarks of CAVD such as inflammation, fibrosis, and collagen overlap lead to a variety of complex interactions that drive disease progression. Thus, we wanted to explore how VIC responsiveness to a pathological stimulus was affected by changes in total collagen fiber enrichment on an equally collagen-enriched background. To achieve this, female and male VICs cultured in 1X and 2X models were treated with 5 ng/mL of TGFB-1. Although TGFB-1 is a known profibrotic factor, it also functions as a regulatory molecule in the expression of inflammatory molecules[22,23]. As mentioned in Chapter 4, TGFB-1 has pro- and anti-inflammatory properties. TGFB-1 interaction with other cells, the ECM, and signaling molecules can result in either of these roles. Some studies have linked TGFB-1 inhibition of inflammatory markers to SMAD2/3 signaling[24,25] Nonetheless, the mechanisms of how this occurs remain elusive.

We assessed the inflammatory response of female and male VICs in 1X and 2X models upon exposure to TGFB-1. Significant reduction of IL6 was observed in females in both

1X and 2X (Figure 5.6, a) models and IL8 at 2X (Figure 5.6, b). TGFB-1 did not affect IL8 expression in either 1X or 2X conditions (Figure 5.6 c and d). TGF-β1 is frequently linked to its capacity to enhance inflammatory responses by regulating several inflammatory mechanisms. NF-kB, SMAD2/3, JAK-STAT, among others, are some of the inflammatory pathways regulated by TGFB-1[26]. Similar to our observations in Chapter 4, cytokine production of IL6 and IL8 in females treated with TGFB-1 could be related to regulatory effects within any of these pathways. Previous studies have found that TGFB-1 dampens IL6 expression through the regulation of IL6 receptors via JAK-STAT signaling[27]. Other studies have found that TGFB-1 can modulate the expression of other cytokines which, in turn, alter IL6 expression[28].

Gene expression of fibrotic markers in TGFB-1 treated VIC cultures in 1X and 2X fiber models was assessed to better understand the impact of the biological and architectural roles of collagen combined with exposure to a pathological stimulus in driving CAVD fibrosis. TGFB-1 increased the expression of fibrotic markers in females cultured in 1X and 2X for ACTA2, FN1, TGFB-1, CHSY1, and COL1A1 (Figure 5.7, a,b,c,g, and h). Increased expression of TGFB-1 and CHSY1 (Figure 5.7, I and j) in TGFB-1 treated male VICs was observed in both 1X and 2X models. Increased expression for ACTA2, COL1A1, and FN1 was observed only in the 1X model (Figure 5.7, d-f). Overall, these results coincide with other studies in which fibrotic responses have been shown to be elevated upon treatment with TGFB-1[29–31]. Interestingly, increased fiber enrichment, as modeled in our 2X condition, appeared to further enhance fibrotic expression in VICs upon exposure to TGFB-1 treatment. This suggests that increasing fiber concentration

may prime VICs to be more sensitive to pathological stimuli, leading to poorer fibrotic outcomes. This novel approach to understanding the biological and architectural roles of collagen in VICs exposed to pathological stimuli provides us with new insights into how the necessity of fibers to modulate VIC pathological responses. New study directions could be further explored to understand other ECM-cell, bio-signaling interactions in CAVD.

Regarding the quantification of ECM and ECM regulatory proteins, increased nascent protein production and FN1 expression were observed in TGFB-1 treated females in both 1X and 2X conditions, which validates our previous observation regarding the upregulation of gene fibrotic expression for FN1 (Figure 5.8.a, a and b).

Nascent ECM production in males was observed to be highly elevated in the VICs treated with TGFB-1 in 1X and between the 1X and 2X control groups (Figure 5.8.b, a). A significant decrease in nascent protein production was observed between TGFB-1 treated 1X and 2X conditions and between the 2X control and treated groups. The reason for such a decrease in the 2X treated condition could be explained by a possible upregulation of MMP proteins. However, current data for ECM and ECM regulatory proteins in females and males is being revised as sample distribution could have affected the identification of differences between all tested groups.

It is important to note that while our system offers cells an increase in fiber enrichment, it lacks other properties such as fiber orientation and alignment. In healthy valves, collagen

is typically oriented in the circumferential direction[1,32] and aligned parallel with the valvular endothelium[33]. However, the aortic valve leaflets are known to be more mechanically compliant in the radial direction than in the circumferential direction[34]. Several studies have been conducted to assess how fiber alignment and orientation are affected during disease. A study by Chung-Hao, L. (2022) showed that collagen fibers reorient towards the direction of the greatest applied load and incrementally realign with increasing applied stress[32]. This property allows the valve to better withstand the mechanical load exerted by constant blood flow[32,35,36]. While many studies have examined the effects and roles of fibers in impacting the valve's mechanics, no studies have focused on understanding how fiber alignment and orientation affect VIC behavior during CAVD,

Fiber alignment and orientation have been proven to affect many cellular properties, including cell morphology, migration, and metabolism. A study by Shi, Y. et al. (2022) found that ST2 cells (bone marrow mesenchymal cells) cultured on a random fiber pattern exhibited an increase in markers that upregulate glycolysis, while cells cultured on aligned fibers exhibited a decrease in these markers[37]. Other studies show that cells tend to migrate faster on aligned fibers[38], which is a behavior commonly observed during the metastasis of cancerous cells[39,40].

Given this, we should point out that the lack of fiber alignment and orientation within our disease-inspired models limits our understanding of potential critical behaviors that could impact VIC responses to ECM pathological changes during disease progression. Further studies may need to consider these properties.

5.6 Conclusions

In conclusion, females VICs exhibit inherently higher inflammatory expression compared to males in collagen-enriched matrices, regardless of fiber concentration. TGF-β1 expression plays a crucial role in regulating this inflammatory response in female VICs. Males, on the other hand, demonstrate a more pronounced fibrotic profile than females within these collagen matrices. It is evident that collagen fiber architecture alone is insufficient to induce a fibrotic response; rather, it is the combination with pathological stimuli that drives fibrotic expression in both female and male VICs. Notably, female VICs are more sensitive to these pathological stimuli than their male counterparts, highlighting the importance of considering sex-specific responses and the implementation of novel disease-inspired tissue engineered models to better understand the processes involved in CAVD progression.

5.7 References

1.Hutson HN, Marohl T, Anderson M, Eliceiri K, Campagnola P, Masters KS. Calcific Aortic Valve Disease Is Associated with Layer-Specific Alterations in Collagen Architecture. *PLoS ONE*. 2016;11(9):e0163858. doi:10.1371/journal.pone.0163858

2.Bashey RI, Torii S, Angrist A. Age-related collagen and elastin content of human heart valves. *J Gerontol*. 1967;22(2):203-208. doi:10.1093/geronj/22.2.203

3.Latif N, Sarathchandra P, Taylor PM, Antoniw J, Yacoub MH. Localization and pattern of expression of extracellular matrix components in human heart valves. *J Heart Valve Dis*. 2005;14(2):218-227.

4.Scott M, Vesely I. Aortic valve cusp microstructure: the role of elastin. *Ann Thorac Surg*. 1995;60(2 Suppl):S391-394. doi:10.1016/0003-4975(95)00263-k

5.Kirsch T, Ishikawa Y, Mwale F, Wuthier RE. Roles of the nucleational core complex and collagens (types II and X) in calcification of growth plate cartilage matrix vesicles. *J Biol Chem*. 1994;269(31):20103-20109.

6.Hutson HN, Kujawa C, Eliceiri K, Campagnola P, Masters KS. Impact of tissue preservation on collagen fiber architecture. *Biotech Histochem*. 2019;94(2):134-144. doi:10.1080/10520295.2018.1530373

7.Porras AM, van Engeland NCA, Marchbanks E, et al. Robust Generation of Quiescent Porcine Valvular Interstitial Cell Cultures. *J Am Heart Assoc*. 2017;6(3):e005041. doi:10.1161/JAHA.116.005041

8.Hiraki HL, Matera DL, Wang WY, et al. Fiber density and matrix stiffness modulate distinct cell migration modes in a 3D stroma mimetic composite hydrogel. *Acta Biomater*. 2023;163:378-391. doi:10.1016/j.actbio.2022.09.043

9.Baker BM, Trappmann B, Wang WY, et al. Cell-mediated fibre recruitment drives extracellular matrix mechanosensing in engineered fibrillar microenvironments. *Nat Mater*. 2015;14(12):1262-1268. doi:10.1038/nmat4444

10.Davidson CD, Jayco DKP, Matera DL, et al. Myofibroblast activation in synthetic fibrous matrices composed of dextran vinyl sulfone. *Acta Biomater*. 2020;105:78-86. doi:10.1016/j.actbio.2020.01.009

11.Simon LR, Scott AJ, Figueroa Rios L, Zembles J, Masters KS. Cellular-scale sex differences in extracellular matrix remodeling by valvular interstitial cells. *Heart Vessels*. 2023;38(1):122-130. doi:10.1007/s00380-022-02164-2

12.Berger AJ, Linsmeier KM, Kreeger PK, Masters KS. Decoupling the effects of stiffness and fiber density on cellular behaviors via an interpenetrating network of gelatin-

methacrylate and collagen. *Biomaterials*. 2017;141:125-135. doi:10.1016/j.biomaterials.2017.06.039

13.Loebel C, Mauck RL, Burdick JA. Local nascent protein deposition and remodelling guide mesenchymal stromal cell mechanosensing and fate in three-dimensional hydrogels. *Nat Mater*. 2019;18(8):883-891. doi:10.1038/s41563-019-0307-6

14.Man JJ, Beckman JA, Jaffe IZ. Sex as a Biological Variable in Atherosclerosis. *Circ Res*. 2020;126(9):1297-1319. doi:10.1161/CIRCRESAHA.120.315930

15.McCoy CM, Nicholas DQ, Masters KS. Sex-related differences in gene expression by porcine aortic valvular interstitial cells. *PloS One*. 2012;7(7):e39980. doi:10.1371/journal.pone.0039980

16.Malutan AM, Dan M, Nicolae C, Carmen M. Proinflammatory and anti-inflammatory cytokine changes related to menopause. *Przeglad Menopauzalny Menopause Rev*. 2014;13(3):162-168. doi:10.5114/pm.2014.43818

17.Schwarz D, Lipoldová M, Reinecke H, Sohrabi Y. Targeting inflammation with collagen. *Clin Transl Med*. 2022;12(5):e831. doi:10.1002/ctm2.831

18.Katsumata K, Ishihara J, Mansurov A, et al. Targeting inflammatory sites through collagen affinity enhances the therapeutic efficacy of anti-inflammatory antibodies. *Sci Adv*. 2019;5(11):eaay1971. doi:10.1126/sciadv.aay1971

19.Simon LR, Scott AJ, Figueroa Rios L, Zembles J, Masters KS. Cellular-scale sex differences in extracellular matrix remodeling by valvular interstitial cells. *Heart Vessels*. 2023;38(1):122-130. doi:10.1007/s00380-022-02164-2

20.Masjedi S, Lei Y, Patel J, Ferdous Z. Sex-related differences in matrix remodeling and early osteogenic markers in aortic valvular interstitial cells. *Heart Vessels*. 2017;32(2):217-228. doi:10.1007/s00380-016-0909-8

21.Davidson MD, Song KH, Lee MH, et al. Engineered Fibrous Networks To Investigate the Influence of Fiber Mechanics on Myofibroblast Differentiation. *ACS Biomater Sci Eng*. 2019;5(8):3899-3908. doi:10.1021/acsbiomaterials.8b01276

22.Sanjabi S, Oh SA, Li MO. Regulation of the Immune Response by TGF-β: From Conception to Autoimmunity and Infection. *Cold Spring Harb Perspect Biol*. 2017;9(6):a022236. doi:10.1101/cshperspect.a022236

23.Hatamzade Esfahani N, Day AS. The Role of TGF-β, Activin and Follistatin in Inflammatory Bowel Disease. *Gastrointest Disord*. 2023;5(2):167-186. doi:10.3390/gidisord5020015

24.Takimoto T, Wakabayashi Y, Sekiya T, et al. Smad2 and Smad3 are redundantly essential for the TGF-beta-mediated regulation of regulatory T plasticity and Th1

development. *J Immunol Baltim Md 1950*. 2010;185(2):842-855. doi:10.4049/jimmunol.0904100

25.McKarns SC, Schwartz RH, Kaminski NE. Smad3 is essential for TGF-beta 1 to suppress IL-2 production and TCR-induced proliferation, but not IL-2-induced proliferation. *J Immunol Baltim Md 1950*. 2004;172(7):4275-4284. doi:10.4049/jimmunol.172.7.4275

26.Deng Z, Fan T, Xiao C, et al. TGF-β signaling in health, disease, and therapeutics. *Signal Transduct Target Ther*. 2024;9(1):61. doi:10.1038/s41392-024-01764-w

27.Wiegertjes R, van Caam A, van Beuningen H, et al. TGF-β dampens IL-6 signaling in articular chondrocytes by decreasing IL-6 receptor expression. *Osteoarthritis Cartilage*. 2019;27(8):1197-1207. doi:10.1016/j.joca.2019.04.014

28.Chen CC, Manning AM. TGF-beta 1, IL-10 and IL-4 differentially modulate the cytokine-induced expression of IL-6 and IL-8 in human endothelial cells. *Cytokine*. 1996;8(1):58-65. doi:10.1006/cyto.1995.0008

29.Jenke A, Kistner J, Saradar S, et al. Transforming growth factor-β1 promotes fibrosis but attenuates calcification of valvular tissue applied as a three-dimensional calcific aortic valve disease model. *Am J Physiol Heart Circ Physiol*. 2020;319(5):H1123-H1141. doi:10.1152/ajpheart.00651.2019

30.Walker GA, Masters KS, Shah DN, Anseth KS, Leinwand LA. Valvular myofibroblast activation by transforming growth factor-beta: implications for pathological extracellular matrix remodeling in heart valve disease. *Circ Res*. 2004;95(3):253-260. doi:10.1161/01.RES.0000136520.07995.aa

31.Cloyd KL, El-Hamamsy I, Boonrungsiman S, et al. Characterization of porcine aortic valvular interstitial cell “calcified” nodules. *PloS One*. 2012;7(10):e48154. doi:10.1371/journal.pone.0048154

32.Hudson LT, Laurence DW, Lau HM, Mullins BT, Doan DD, Lee CH. Linking collagen fiber architecture to tissue-level biaxial mechanical behaviors of porcine semilunar heart valve cusps. *J Mech Behav Biomed Mater*. 2022;125:104907. doi:10.1016/j.jmbbm.2021.104907

33.Clift CL, Su YR, Bichell D, et al. Collagen fiber regulation in human pediatric aortic valve development and disease. *Sci Rep*. 2021;11(1):9751. doi:10.1038/s41598-021-89164-w

34.Chen JH, Simmons CA. Cell-matrix interactions in the pathobiology of calcific aortic valve disease: critical roles for matricellular, matricrine, and matrix mechanics cues. *Circ Res*. 2011;108(12):1510-1524. doi:10.1161/CIRCRESAHA.110.234237

35.Joyce EM, Liao J, Schoen FJ, Mayer JE, Sacks MS. FUNCTIONAL COLLAGEN FIBER ARCHITECTURE OF THE PULMONARY HEART VALVE CUSP. *Ann Thorac Surg*. 2009;87(4):1240-1249. doi:10.1016/j.athoracsur.2008.12.049

36.Goth W, Potter S, Allen AC, Zoldan J, Sacks MS, Tunnell JW. Non-destructive reflectance mapping of collagen fiber alignment in heart valve leaflets. *Ann Biomed Eng*. 2019;47(5):1250-1264. doi:10.1007/s10439-019-02233-0

37.You C, Sun Q, Zhang M, Wei Q, Shi Y. The alignment of the substrate nanofibers directing cellular energy metabolism. *Colloid Interface Sci Commun*. 2022;50:100665. doi:10.1016/j.colcom.2022.100665

38.Jenkins TL, Little D. Synthetic scaffolds for musculoskeletal tissue engineering: cellular responses to fiber parameters. *NPJ Regen Med*. 2019;4:15. doi:10.1038/s41536-019-0076-5

39.Pathak A, Kumar S. Independent regulation of tumor cell migration by matrix stiffness and confinement. *Proc Natl Acad Sci*. 2012;109(26):10334-10339. doi:10.1073/pnas.1118073109

40.Zanotelli MR, Miller JP, Wang W, et al. Tension directs cancer cell migration over fiber alignment through energy minimization. *Biomaterials*. 2024;311:122682. doi:10.1016/j.biomaterials.2024.122682

Chapter 6: Conclusions and Recommendations

6.1 Conclusions

The efforts in this work emphasize the importance of using 3D culture systems to create platforms that more accurately reflect the complexities of naïve and diseased tissues. This approach elevates our research by providing a more realistic model of biological processes. Equally important is raising awareness about the significant gap in knowledge resulting from the failure to consider sex as a biological variable. Differences between sexes have always been evident in clinical settings, yet they have often been overlooked. Recognizing that biological sex impacts how diseases manifest in our bodies offers new opportunities to understand and combat these diseases more effectively.

The work in the preceding chapters describes the development of disease-inspired engineered models that mimic pathological ECM changes in early and late stages of CAVD to understand how these events affect female and male VIC fibrosis, and the pathological expression of fibrillar collagen enrichment to understand the roles of collagen's biological and architectural features.

We found that 3D biomimetics of diseased ECM influence fibrosis in various ways. Early and late-stage models, as well as our fiber enrichment models, provided insights into the inflammatory profiles of VICs, with females showing an increased production of inflammatory cytokines compared to males. We also observed that TGFB-1 plays a key

role in regulating cytokine expressions but only in female VICs. In both chapters, fibrosis expression in males is significantly higher than in females. However, Chapter 4 described these findings as stage-dependent, while in Chapter 5, collagen fiber enrichment was not key to driving this fibrotic response. The introduction of TGFB-1 exacerbated fibrotic responses in both females and males across both engineered setups. Female VICs in early and late stages, as well as in 1X and 2X models, appeared to be more susceptible to TGFB-1 treatment than males. Interestingly, TGFB-1 treatment modulated a higher fibrotic response for both female and male VICs in our fibrillar collagen-enriched model. Mixed results and conclusions were observed regarding nascent protein production and expression of ECM and ECM regulatory proteins for both engineered platforms. These discrepancies are due to limitations in sample processing and the limited availability of current techniques to quantify the expression of these molecules. The data pertaining to these experiments is currently under revision and in progress.

Sex differences are consistently observed across all the experiments conducted in this thesis. However, the underlying mechanisms driving these differences remain largely unexplored and require further investigation. Given that the experiments utilize cells from prepubescent pigs, it is plausible to argue that hormones are not the primary contributors to the observed sex differences in this experimental context. This is because the hormone levels in prepubescent pigs are relatively similar between sexes, thereby reducing the likelihood that hormonal fluctuations are the key drivers of these variations.

Consequently, alternative explanations for the observed sex differences must be considered. One possibility could involve the influence of chromosomal sex, where the

inherent differences between XX and XY chromosomes contribute to cellular behavior in a sex-specific manner. Another potential factor could be X-chromosome inactivation, which might differ between male and female cells, leading to distinct cellular responses. Additionally, epigenetic modifications could play a crucial role, as they are known to regulate gene expression in a sex-dependent manner, potentially driving the differences observed in the experimental outcomes.

Wiese, C. and Reue, K. discuss that because sexual chromosomes dictate the development of sex-hormones producing organs, investigating the isolated effects of genetic sex in cardiovascular diseases has proven to be a challenging task. However, a different approach can be taken by study the association between the likelihood or severity of cardiovascular disease in patients that possess a different genetic sex composition[1]. One study found that men who suffer from Klinefelter syndrome which genetic composition consist of an additional X chromosome (XXY) exhibited an increase in cardiovascular mortality compared to males with a standard genetic makeup (XY)[2]. Similarly, cardiovascular disease susceptibility is also present in patients who suffer from Turner syndrome (XO)[2] yet the exact reasons on how sex chromosomes affect these outcomes remain unknown.

These leads us to our next point of consideration which is the escaping of X inactivation. Naturally, individuals with two copies of the X (XX) chromosome have one of these copies transcriptionally silenced[1,3]. Because of this, no significant sex differences in the level of expression between XX and XY cells are observed. However, there are certain instances

in which one of the extra X chromosomes escape its inactivation. In these cases, it has been found that failure in x-linked inactivation have detrimental effects for cell function and signaling, therefore offering a plausible explanation for observed differences in cardiovascular diseases. Recently, a study by Anseth, K. et al, (2022) found that genes that escape X chromosome inactivation such as *BMX and STS* modulate sex-dependent myofibroblast activation via the Rho-associated kinase signaling[4]**.**

Lastly, these factors could significantly influence the epigenetic regulation of gene expression, contributing to sex differences in cardiovascular diseases. Epigenetics involves changes in gene activity through mechanisms like DNA methylation and histone modification, without altering the DNA sequence[5]. For instance, gonadal hormones may affect DNA methylation and histone modifications, while genes escaping X-linked inactivation, such as those encoding histone demethylases, can alter histone modifications leading to differential susceptibility for cardiovascular disease in females and males. Epigenetic regulation is dynamic and is influenced by many factors complicating the study of sex differences.

Understanding how all these processes lead to divergent sex-dependent outcomes in cardiovascular disease progression is vital for developing targeted therapies to reduce cardiovascular disease risks in both sexes.

Throughout this thesis, were able to point out sex-dependent responses in regard to TFGB treatment. We tried to explain these differences based on known roles of TGFB in regulating ECM production and regulation of inflammatory factors (BMP and SMAD signaling). It is noteworthy to point that the pathways involved in the observed differences

also affect other cellular processes such as cell development and growth (via SMADs) and cell lineage commitment, differentiation, proliferation and apoptosis (via BMPs)[6].

Although not often mentioned, TGFB is also known for its role in regulating sex related hormones and sexual genes. However, the ways in which TGFB signaling and sex-differences are linked need yet to be uncovered. Previous studies have shown that in 72 out of 114 species is sex-determination genes are regulated by TGFB[7,8]. For instance, in fish sex-determination occurs by BMP signaling regulation by TGFB[8]. Other studies have linked TGFB pathway inactivation via SMADs in response to estrogen (SOURCE) and testosterone[9]. Responses to TGFB can be sex and cell dependent. Mammary gland epithelia cells, for example, are known to be very sensitive to TGF-B Induced cell cycle arrest and apoptosis[10].A study by Laiho, M. and Band, A. (2011) found that estrogen receptor alpha in these cells, blocks TGFB signaling via SMADs. In contrast, other studies have shown, inhibition of sex hormones by TGFB in Leydig cells by downregulation of CYP19[11].

Despite the amount of research conducted exploring the link between sex differences and TGFB, a clear understanding is halted by the ways in which diverse cells, tissue and species are differentially affects TGFB and its interaction with many other signaling pathways. Furthermore, the link between TGFB in regard to sex differences in cardiovascular diseases is largely unexplored. Research exploring the effects of TGFB regulation of sex hormones and sex related genes in regard to cardiovascular diseases could thus be a promising venue to the development better treatments options for CAVD.

Taken together, the findings of this thesis hope to underscore the necessity of integrating 3D-engineered platforms to gain deeper insights into the progression of CAVD. Furthermore, it highlights the importance of employing sex-specific cultures to develop more precise and effective therapeutic strategies.

6.2 Future Recommendations

6.2.1 Application of 3D Disease-Inspired Scaffolds to Study Cell-ECM Interactions in CAVD Progression

3D disease-inspired systems offer valuable platforms for investigating the independent effects of VICs and specific ECM components, as well as the complex interactions between VICs, ECM, and tissue mechanics. Our previous work involved creating a sophisticated system by incorporating GAGs into a collagen-based matrix to study the effects of CS + Collagen 1 enrichment. Using this system, we can explore various factors that influence CAVD progression, such as the impact of GAG molecules on inflammatory and fibrocalcific responses in VICs cultured in a collagen matrix. Previous studies have highlighted the role of different GAG molecules in contributing to CAVD pathology[12,13].

6.2.2 Application of 3D Disease-Inspired Scaffolds to Study ECM Mechanics Interactions

Tissue stiffness significantly influences cell behavior. Various tissues exhibit different stiffness levels that drive specific cellular functions. Increased stiffness in VICs promotes

myofibroblastic differentiation, fibrosis, and calcification, effects that can be reversed by modulating scaffold stiffness[14–16]. The combinatorial effects of ECM enrichment can be coupled with changes in matrix stiffness, adding complexity to these systems. Our highly tunable hydrogel models offer the opportunity to incorporate essential ECM ligands while controlling hydrogel bulk stiffness. This approach is particularly useful for exploring how ECM composition combined with varying stiffness can modulate cell behavior. Continued research can decode the role of each ECM component, allowing for various combinations to be studied for potential interactions tied to specific disease progression events.

6.2.3 Disease-Engineered Scaffolds to Explore Targeted Therapeutic Targets

Understanding the differential sex-dependent responses of VICs during disease progression is particularly important for developing targeted treatments that can efficiently improve patient prognosis. This is further supported by research highlighting how females and males can respond differently to pharmacological treatments. Hajjar, I. et al. (2022)[17] found that hypertension drugs such as Candesartan and Enalapril affect women and men differently, with Enalapril lowering arterial stiffness more effectively in females than in males. Another study by Fortes, Z. et al. (2006)[18] demonstrated that Losartan was more effective at correcting endothelial dysfunction in female rats compared to males. A thorough review by Nicolaou, P. et al. (2021)[19] describes in more detail the sex differences found in heart failure medications targeting the renin-angiotensin-aldosterone system. In this review, Losartan was found to have similar effects in women and men.

The great tunability of the scaffolds used in this work, can be leveraged to create diverse ECM-risk factor/pathological stimuli platforms to better understand how potential therapeutic targets can affect females and male. Opposed to 2D culture platforms, 3D platforms can be used to better mimic the cells physiological environment thus, serving as better tools to identify therapeutic targets, advancing the potential for discovering improved treatments[20].

6.2.4 Longitudinal Studies

Studies like ours typically consider specific time points that are traditionally tested repeatedly. However, CAVD develops over a long period, which cannot be equally replicated in vitro. Tissue-engineered disease models can mimic various aspects or stages of disease progression, allowing for longitudinal studies to understand transient gene and protein expression in VICs in response to a myriad of conditions.

6.3 References

1.Reue K, Wiese CB. Illuminating the Mechanisms Underlying Sex Differences in Cardiovascular Disease. *Circ Res*. 2022;130(12):1747-1762. doi:10.1161/CIRCRESAHA.122.320259

2.Silberbach M, Roos-Hesselink JW, Andersen NH, et al. Cardiovascular Health in Turner Syndrome: A Scientific Statement From the American Heart Association. *Circ Genomic Precis Med*. 2018;11(10):e000048. doi:10.1161/HCG.0000000000000048

3.Arnold AP, Cassis LA, Eghbali M, Reue K, Sandberg K. Sex Hormones and Sex Chromosomes Cause Sex Differences in the Development of Cardiovascular Diseases. *Arterioscler Thromb Vasc Biol*. 2017;37(5):746-756. doi:10.1161/ATVBAHA.116.307301

4.Aguado BA, Walker CJ, Grim JC, et al. Genes That Escape X Chromosome Inactivation Modulate Sex Differences in Valve Myofibroblasts. *Circulation*. 2022;145(7):513-530. doi:10.1161/CIRCULATIONAHA.121.054108

5.Thej C, Kishore R. Epigenetic regulation of sex dimorphism in cardiovascular health. *Can J Physiol Pharmacol*. Published online March 1, 2024. doi:10.1139/cjpp-2023-0406

6.Katagiri T, Watabe T. Bone Morphogenetic Proteins. *Cold Spring Harb Perspect Biol*. 2016;8(6):a021899. doi:10.1101/cshperspect.a021899

7.Yu H, Du X, Chen X, Liu L, Wang X. Transforming growth factor-β (TGF-β): A master signal pathway in teleost sex determination. *Gen Comp Endocrinol*. 2024;355:114561. doi:10.1016/j.ygcen.2024.114561

8.Pan Q, Kay T, Depincé A, et al. Evolution of master sex determiners: TGF-β signalling pathways at regulatory crossroads. *Philos Trans R Soc Lond B Biol Sci*. 2021;376(1832):20200091. doi:10.1098/rstb.2020.0091

9.Braga M, Bhasin S, Jasuja R, Pervin S, Singh R. Testosterone inhibits transforming growth factor-β signaling during myogenic differentiation and proliferation of mouse satellite cells: potential role of follistatin in mediating testosterone action. *Mol Cell Endocrinol*. 2012;350(1):39-52. doi:10.1016/j.mce.2011.11.019

10.Band AM, Laiho M. Crosstalk of TGF-β and Estrogen Receptor Signaling in Breast Cancer. *J Mammary Gland Biol Neoplasia*. 2011;16(2):109-115. doi:10.1007/s10911-011-9203-7

11.Yang Q, Ma B, Qiao H, et al. TGFB1 represses the expression of SF1 and LRH1 to inhibit E2 production in rat LCs. *Reprod Camb Engl*. 2017;153(5):621-629. doi:10.1530/REP-16-0044

12.Porras AM, Westlund JA, Evans AD, Masters KS. Creation of disease-inspired biomaterial environments to mimic pathological events in early calcific aortic valve disease. *Proc Natl Acad Sci U S A*. 2018;115(3):E363-E371. doi:10.1073/pnas.1704637115

13.Dahal S, Huang P, Murray BT, Mahler GJ. Endothelial to mesenchymal transformation is induced by altered extracellular matrix in aortic valve endothelial cells. *J Biomed Mater Res A*. 2017;105(10):2729-2741. doi:10.1002/jbm.a.36133

14.Wu S, Li Y, Zhang C, et al. Tri-Layered and Gel-Like Nanofibrous Scaffolds with Anisotropic Features for Engineering Heart Valve Leaflets. *Adv Healthc Mater*. 2022;11(10):e2200053. doi:10.1002/adhm.202200053

15.Kirschner CM, Alge DL, Gould ST, Anseth KS. Clickable, photodegradable hydrogels to dynamically modulate valvular interstitial cell phenotype. *Adv Healthc Mater*. 2014;3(5):649-657. doi:10.1002/adhm.201300288

16.Ali MS, Deb N, Wang X, Rahman M, Christopher GF, Lacerda CMR. Correlation between valvular interstitial cell morphology and phenotypes: A novel way to detect activation. *Tissue Cell*. 2018;54:38-46. doi:10.1016/j.tice.2018.07.004

17.Rogers SC, Ko YA, Quyyumi AA, Hajjar I. Differential Sex-Specific Effects of Angiotensin-Converting Enzyme Inhibition and Angiotensin Receptor Blocker Therapy on Arterial Function in Hypertension: CALIBREX Trial. *Hypertension*. 2022;79(10):2316-2327. doi:10.1161/HYPERTENSIONAHA.122.19105

18.Rodrigues SF de P, dos Santos RA, Silva-Antonialli MM, et al. Differential effect of losartan in female and male spontaneously hypertensive rats. *Life Sci*. 2006;78(19):2280-2285. doi:10.1016/j.lfs.2005.09.049

19.Nicolaou PA. Sex differences in heart failure medications targeting the renin-angiotensin-aldosterone system. *Eur J Pharmacol*. 2021;897:173961. doi:10.1016/j.ejphar.2021.173961

20.Marei I, Abu Samaan T, Al-Quradaghi MA, et al. 3D Tissue-Engineered Vascular Drug Screening Platforms: Promise and Considerations. *Front Cardiovasc Med*. 2022;9:847554. doi:10.3389/fcvm.2022.847554